# **Springer Theses**Recognizing Outstanding Ph.D. Research

Nozomi Saito

# Hierarchical Bottom-Up Methodology for Integrating Dynamic Ethynylhelicene Oligomers

Synthesis, Double-Helix
Formation, and the HigherAssembly Formation



### **Springer Theses**

Recognizing Outstanding Ph.D. Research

For further volumes: http://www.springer.com/series/8790

#### Aims and Scope

The series "Springer Theses" brings together a selection of the very best Ph.D. theses from around the world and across the physical sciences. Nominated and endorsed by two recognized specialists, each published volume has been selected for its scientific excellence and the high impact of its contents for the pertinent field of research. For greater accessibility to non-specialists, the published versions include an extended introduction, as well as a foreword by the student's supervisor explaining the special relevance of the work for the field. As a whole, the series will provide a valuable resource both for newcomers to the research fields described, and for other scientists seeking detailed background information on special questions. Finally, it provides an accredited documentation of the valuable contributions made by today's younger generation of scientists.

#### Theses are accepted into the series by invited nomination only and must fulfill all of the following criteria

- They must be written in good English.
- The topic should fall within the confines of Chemistry, Physics, Earth Sciences, Engineering and related interdisciplinary fields such as Materials, Nanoscience, Chemical Engineering, Complex Systems and Biophysics.
- The work reported in the thesis must represent a significant scientific advance.
- If the thesis includes previously published material, permission to reproduce this must be gained from the respective copyright holder.
- They must have been examined and passed during the 12 months prior to nomination.
- Each thesis should include a foreword by the supervisor outlining the significance of its content.
- The theses should have a clearly defined structure including an introduction accessible to scientists not expert in that particular field.

#### Nozomi Saito

# Hierarchical Bottom-Up Methodology for Integrating Dynamic Ethynylhelicene Oligomers

Synthesis, Double-Helix Formation, and the Higher-Assembly Formation

Doctoral Thesis accepted by Tohoku University, Sendai, Japan



Author Dr. Nozomi Saito Tohoku University Sendai Japan Supervisor Prof. Masahiko Yamaguchi Tohoku University Sendai Japan

ISSN 2190-5053 ISSN 2190-5061 (electronic) ISBN 978-4-431-54513-2 ISBN 978-4-431-54514-9 (eBook) DOI 10.1007/978-4-431-54514-9

Springer Tokyo Heidelberg New York Dordrecht London

Library of Congress Control Number: 2013943979

#### © Springer Japan 2013

This work is subject to copyright. All rights are reserved by the Publisher, whether the whole or part of the material is concerned, specifically the rights of translation, reprinting, reuse of illustrations, recitation, broadcasting, reproduction on microfilms or in any other physical way, and transmission or information storage and retrieval, electronic adaptation, computer software, or by similar or dissimilar methodology now known or hereafter developed. Exempted from this legal reservation are brief excerpts in connection with reviews or scholarly analysis or material supplied specifically for the purpose of being entered and executed on a computer system, for exclusive use by the purchaser of the work. Duplication of this publication or parts thereof is permitted only under the provisions of the Copyright Law of the Publisher's location, in its current version, and permission for use must always be obtained from Springer. Permissions for use may be obtained through RightsLink at the Copyright Clearance Center. Violations are liable to prosecution under the respective Copyright Law. The use of general descriptive names, registered names, trademarks, service marks, etc. in this publication does not imply, even in the absence of a specific statement, that such names are exempt from the relevant protective laws and regulations and therefore free for general use.

While the advice and information in this book are believed to be true and accurate at the date of publication, neither the authors nor the editors nor the publisher can accept any legal responsibility for any errors or omissions that may be made. The publisher makes no warranty, express or implied, with respect to the material contained herein.

Printed on acid-free paper

Springer is part of Springer Science+Business Media (www.springer.com)

#### Parts of this thesis have been published in the following journal articles:

- 1. "Hetero-Double-Helix Formation by an Ethynylhelicene Oligomer Possessing Pefluorooctyl Side Chains" Ryo Amemiya, Nozomi Saito, Masahiko Yamaguchi. *J. Org. Chem.* **2008**, *73*, 7137–7144. *Reproduces with permission*
- 2. "Side Chain Effect on the Double Helix Formation of Ethynylhelicene Oligomers" Nozomi Saito, Ryo Terakawa, Masanori Shigeno, Ryo Amemiya, Masahiko Yamaguchi. *J. Org. Chem.* **2011**, *76*, 4841–4858. *Reproduces with permission*
- 3. "Two-component Fibers/Gels and Vesicle Formed from Hetero-double-Helices of Pseudoenantiomeric Ethynylhelicene Oligomers with Branched Side-chains" Nozomi Saito, Masanori Shigeno, Masahiko Yamaguchi. *Chem. Eur. J.* **2012**, *18*, 8994–9004. *Reproduces with permission*

#### **Supervisor's Foreword**

It is my pleasure to introduce the work of Dr. Nozomi Saito for publication in the Springer Theses series as an outstanding original work from one of the world's top universities. Dr. Saito joined my laboratory in Tohoku University in October 2005 as an undergraduate student. In April 2007, she entered the Graduate School of Pharmaceutical Sciences at Tohoku University and started her doctoral study with me and Dr. Ryo Amemiya. She was accepted as a Japan Society for the Promotion of Science (JSPS) predoctoral fellow in April 2009, and she received her doctor's degree in March 2012.

The bottom-up method for integrating synthetic small molecules and oligomeric compounds has recently attracted much interest in the field of chemistry, because novel functional materials different from materials based on biomolecules and synthetic polymers can be developed using such designed selfassembled substances. Dr. Saito was interested in the development of a bottom-up methodology for integrating dynamic double helix molecules and focused her attention on their self-assembly. Employing synthetic ethynylhelicene oligomers, she then studied various subjects including molecular level properties and nanoand micrometer-scale dynamic phenomena. The unique approach in chemistry using a broad range of substances containing small molecules, oligomeric molecules, double helices, fibers, gels, and vesicles is described in this outstanding thesis, which explicitly reveals the author's broad interests and high ability to perform molecular design, self-assembly design, and synthetic and analytical experiments, with discussions and presentations of novel concepts and future prospects. Knowing her passion, executive ability, and communication ability, I am quite convinced that Dr. Saito will become a leading chemist in our scientific society.

Sendai, March 2013

Masahiko Yamaguchi

#### Acknowledgments

I express my sincere and wholehearted appreciation to Dr. Masahiko Yamaguchi (Professor, Graduate School of Pharmaceutical Sciences, Tohoku University) for his constructive discussions, warm encouragement, and guidance in the ways of thinking as a chemist.

I am profoundly grateful for the kind support and detailed, careful guidance given to me by the late Dr. Ryo Amemiya (Graduate School of Pharmaceutical Sciences, Tohoku University).

I also would like to express my gratitude to Dr. Cho Hidetsura (Graduate School of Pharmaceutical Sciences, Tohoku University), Dr. Mieko Arisawa (Graduate School of Pharmaceutical Sciences, Tohoku University), Dr. Masanori Shigeno (Graduate School of Pharmaceutical Sciences, Tohoku University), Dr. Zengjian An (Qingdao Institute of Biochemistry and Bioprocess Technology, Chinese Academy of Sciences), Dr. Yoshizumi Yasui (Kanagawa University of Human Services), Dr. Haruo Aikawa (Tokyo Medical and Dental University), and Dr. Yoshio Nishimura (Yasuda Women's University) for valuable comments and kind encouragement.

I gratefully acknowledge Prof. Dr. Takayuki Doi (Graduate School of Pharmaceutical Sciences, Tohoku University) and Dr. Naoki Kanoh (Graduate School of Pharmaceutical Sciences, Tohoku University) for their thoughtful comments on the revision of my original manuscript.

In addition, I am grateful to Ms. Misa Sakuma, Ms. Yumiko Minakawa, Ms. Keiko Nishida, and Ms. Michiko Ohgi for their official work and to all colleagues at the Yamaguchi Laboratory, Graduate School of Pharmaceutical Sciences, Tohoku University for their cooperation, encouragement, and competitive spirit.

I thank Dr. Kazue Kurihara and Dr. Masashi Mizukami (Institute of Multidisciplinary Research for Advanced Materials, Tohoku University) for helpful discussions on AFM measurements. I also would like to thank Prof. Dr. Munetaka Akita and Dr. Daling Lu (Center for Advanced Materials Analysis, Technical Department, Tokyo Institute of Technology) for the TEM measurements. Additionally, I express my gratitude to Dr. Hiroyuki Isobe and Dr. Syunpei Hitosugi (Graduate School of Science and Faculty of Science, Tohoku University) for helpful discussions on DLS. My gratitude extends as well to Dr. Kiyoshi Kanie x Acknowledgments

and Dr. Masaki Matsubara (Institute of Multidisciplinary Research for Advanced Materials, Tohoku University) for the SAXS measurement.

The Japan Society for the Promotion of Science (JSPS) is gratefully acknowledged for financial support and for the fellowship of young Japanese scientists that I received.

Finally, I am grateful to my parents, Hidenori and Keiko Saito, and to all members of my family for their constant support and encouragement.

### **Contents**

L		ble Helix Molecules Via Self-Assembly Process	
		rences	
	Syn	thesis of Ethynylhelicene Oligomers	
	2.1	Oligomers Possessing Branched Alkyloxycarbonyl Side Chains	
	2.2	Oligomers Possessing Perfluorooctyl Side Chains	
	2.3	Oligomers Possessing Alternating	
		Decyloxycarbonyl/Perfluorooctyl Side Chains	
	Refe	rences	
	Homo-Double-Helix Formation of Ethynylhelicene		
	_	omers Possessing Various Side Chains	
	3.1	Oligomers Possessing Decyloxycarbonyl Side Chains	
	3.2	Oligomers Possessing Branched Alkyloxycarbonyl	
		Side Chains	
	3.3	Oligomers Possessing Perfluorooctyl Side Chains	
	3.4	Oligomers Possessing Decylthio Side Chains	
	3.5	Oligomers Possessing Alternating	
		Decyloxycarbonyl/Perfluorooctyl Side Chains	
	3.6	Summary of Effect of Side Chains on Stability	
		of Homo-Double Helices	
	Refe	rences	
	Hete	ero-Double-Helix Formation of Pseudoenantiomeric	
	Ethy	nylhelicene Oligomers	
	4.1	( <i>P</i> )-D-5/( <i>P</i> )-F-5 Systems	
	4.2	( <i>M</i> )-D-5/( <i>P</i> )-F-5 Systems	
	4.3	( <i>M</i> )-bD-4/( <i>P</i> )-D-5 Systems	
	4.4	(M)-D-n/ $(P)$ -DF-n Systems	
	4.5	Summary	
	Refe	rences	

xii Contents

5	Higher-Assembly Formation of Pseudoenantiomeric			
	Ethynylhelicene Oligomers	4		
	5.1 Fiber/Gel Formation in Toluene	4		
	5.2 Vesicle Formation in Diethyl Ether	5		
	5.3 Higher-Assembly Formation by Intercomplex Interactions	5		
	5.4 Summary	6		
	References	6		
6 7	Conclusions			
•	7.1 General Methods	6		
	7.2 Experimental Method for Chap. 2	6		
	7.3 Experimental Method for Chap. 4	8		
	7.4 Experimental Method for Chap. 5	8		
	References	8		
Cu	riculum Vitae	8		

### Chapter 1 Introduction: Bottom-Up Methodology for Integrating Synthetic Double Helix Molecules Via Self-Assembly Process

In nature, small molecules hierarchically form ordered assemblies with various modes and properties and are integrated into macroscopic soft substances. For example, actin proteins form secondary structures such as  $\alpha$ -helices and  $\beta$ -sheets and then fibrous higher assemblies, which further assemble to form muscles; tubulin proteins form dimers, which aggregate to form a protofilament and then a microtubule. Biological cells are vesicles that contain various vesicular organelles such as liposomes and nuclei. It is thus interesting to control the interactions between molecular complexes and to develop such hierarchical soft-assembly-forming systems using synthetic macromolecules, because such studies will lead to an understanding of natural phenomena and the development of new materials. For this purpose, I examined to develop a bottom-up methodology for integrating synthetic macromolecules via assembly formation using double-helix-forming chiral oligomers (Fig. 1.1).

A double helix is an important structural motif widely observed in nature, as shown by the structure and function of DNA. Thus, studies of synthetic double helix molecules can lead to a better understanding of biological phenomena and the development of new materials. In 2000, Lehn reported the first examples of a synthetic double helix containing no metal coordination: Aromatic oligoamides form double helices in less polar solvents by interstrand  $\pi$ - $\pi$  interactions and van der Waals interactions, and are in equilibria with single helices [1]. Since then, synthetic oligomeric compounds that form double helices have attracted interest [2–20]. However, because of difficulties in obtaining two acyclic compounds that interact by noncovalent interactions and form helical structures, the examples of these are not numerous. In addition, studies of their properties are limited. To develop the function of such double-helix-complexes, it is desirable to systematically obtain diverse double helices.

In addition to the molecular-level properties, the interactions between synthetic double helices and the formation of higher assemblies are important. This is because such interactions can integrate double helix molecules to develop new functional materials. In this work, I studied the interactions between synthetic double helix molecules and consequently their assembly formation using ethynylhelicene oligomers, which are based on molecular-level properties. The formation of soft

1

N. Saito, *Hierarchical Bottom-Up Methodology for Integrating Dynamic Ethynylhelicene Oligomers*, Springer Theses, DOI: 10.1007/978-4-431-54514-9\_1, © Springer Japan 2013

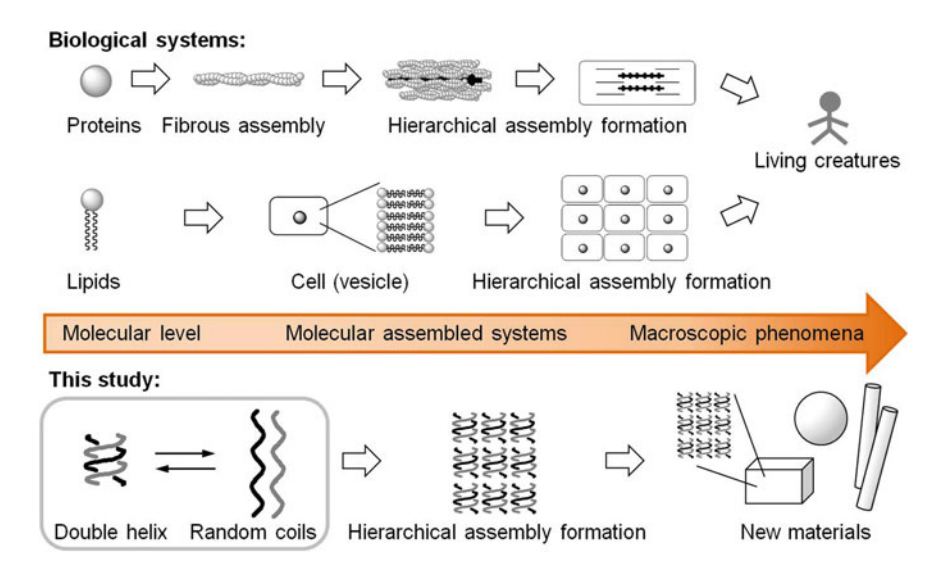


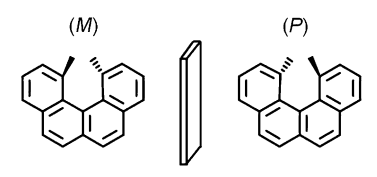
Fig. 1.1 Bottom-up methodology for integrating biological proteins and synthetic double helices

assemblies of double helices, as is observed in biological systems, had not been known when I started this work, although only a few examples of self-assembled solid films on surfaces have been reported [21, 22]. With regard to the interactions and assembly formation of single helical molecules, examples have been observed in biological and biomimetic systems. For example, peptides [23] and peptidomimetics [24–27] form bundles of several helices by the interactions between properly arranged amino acids, and four protein subunits assemble to form hemoglobin [28]. Moreover, peptides [23, 29], peptidomimetics [30–33], and synthetic oligomers [34] form single helices and their higher assemblies such as fibers or vesicles.

I employed a helical aromatic unit of 1,12-dimethylbenzo[c]phenanthrene [35], called helicene in this work, which was developed in our laboratory [36–61]. The helicene possesses four *ortho*-condensed aromatic rings and has helicity because of the steric repulsions between the methyl groups at the 1- and 12-positions (Fig. 1.2).

In 2004, the synthesis of a series of ethynylhelicene oligomers with decyloxy-carbonyl side chains, (P)-D- $\mathbf{n}$  (n = 2-9), was reported by our group, and it was found that higher analogues with large  $\mathbf{n}$  values (n = 7-9) form homo-double helices [54]. The CD spectrum obtained within 5 min after the dissolution of the

**Fig. 1.2** 1, 12-dimethylbenzo[c] phenanthrene and its helicity



heptamer (P)-D-7 in chloroform at  $5 \times 10^{-6}$  M exhibited an extremely large Cotton effects between 300 and 400 nm, which was markedly different from the spectra of oligomers from the dimer to the hexamer. Hypochromic shifts were also observed in the UV-Vis spectra. Vapor pressure osmometry (VPO) indicated the dimeric aggregate formation of (P)-D-7 when it showed the enhanced Cotton effects. The proton NMR of (P)-D-7 in chloroform at room temperature provided broad signals of aromatic protons shifted upfield, which suggested  $\pi$ -stacked structures. These results indicated the formation of a homo-double-helix by (P)-D-7. The homo-double-helix unfolded to random coils by heating. Studies of the unfolding rate using (P)-D-7 revealed that the rate constant k of unfolding was highly dependent on the type of aromatic solvent used and differed by seven orders of magnitude between iodobenzene and trifluoromethylbenzene. The log k exhibited a good correlation with the absolute hardness  $\eta$  [62]: Higher unfolding rates were observed in soft arenes and lower unfolding rates in hard-arenes. The results suggested the involvement of  $\pi$ - $\pi$ interactions in homo-double-helix formation and a notable relationship between the  $\pi$ - $\pi$  interactions and the HSAB principle: The  $\pi$ - $\pi$  interaction is a soft/soft interaction between arenes (Fig. 1.3). The structural change between homo-double helices and random coils could be reversibly conducted by changing temperature, and both the kinetic and thermodynamic stabilities of homo-double helices depended on the softness/hardness of the aromatic solvents used [54, 59].

On the basis of the above results, I planned to systematically study the molecular-level properties of homo- and hetero-double helices, and then their assembly-forming properties. Systems using ethynylhelicene oligomers have several characteristic features: (1) Because the oligomers are modularly constructed by the repetition of certain structural units, numerous derivatives can be systematically provided by changing each unit, for example, side chains, the number of helicenes, and chirality. (2) Consequently, the fine-tuning of the structures and properties of double helices and their assemblies becomes possible. By particularly employing hetero-double helices composed of two different compounds, diversity can be enhanced by changing the combination of compounds. (3) Strong intercomplex interactions occurr between hetero-double helices composed of pseudoenantiomeric oligomers, which results in higher-assembly formation. (4) Ethynylhelicene oligomers can change their structures between double helices and random coils in response to a temperature change, which can be used for the construction of stimulus-responsive dynamic materials.

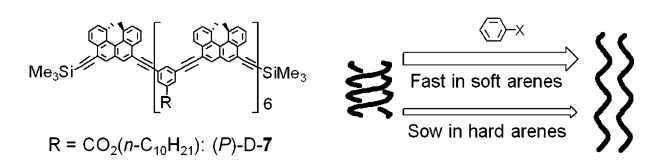


Fig. 1.3 Unfolding of (P)-D-7 and HSAB principle

Fig. 1.4 Side chain analogues of ethynylhelicene oligomers

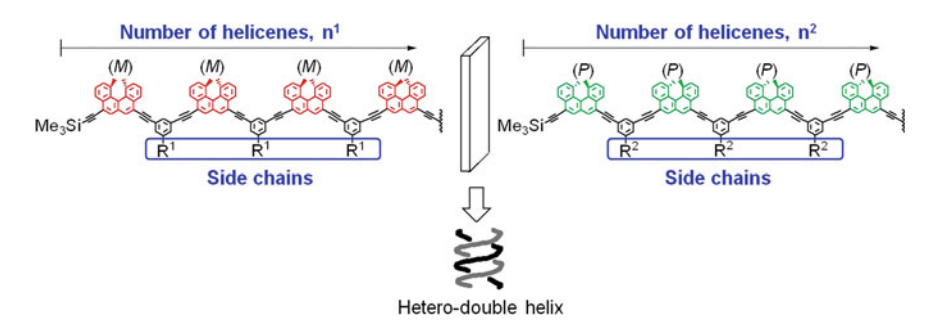


Fig. 1.5 Methodology of obtaining hetero-double helices employing pseudoenantiomeric ethynylhelicene oligomers

I first synthesized several series of side chain analogues on the basis of the results obtained with (P)-D-7. According to the absolute hardness  $\eta$  of substituted arenes [62], I considered decyloxycarbonylphenylenes in (P)-D-7 to have a relatively hard nature. Thus, I expected that the hardness of m-phenylene moieties determined by side chains would also play important roles in the properties of homo-double helices, and consequently synthesized side chain analogues (Chap. 2) (Fig. 1.4). Homo-double-helix formation was systematically studied using these compounds, and I found that side chains affect the thermodynamic stability of homo-double helices in organic media (Chap. 3).

By using these compounds and their enantiomers, hetero-double-helix formation was next examined. Pseudoenantiomers containing enantiomeric helicenes strongly aggregated and formed hetero-double helices. A methodology of forming diverse hetero-double helices and fine-tuning their properties by changing the combinations of compounds with different side chains and number of helicenes (Fig. 1.5) is shown (Chap. 4).

Hetero-double helices showed a strong tendency to form higher assemblies due to intercomplex interactions (Fig. 1.6). The assembly formation was controlled by external stimuli, and fibrous assemblies and vesicles were formed in toluene and diethyl ether, respectively. Both of them were shown to form from hetero-double helices by lateral intercomplex interactions. These results remind us of the assembly formation of biological proteins, with regard to the fact that small molecules are hierarchically bottom-upped to larger assemblies by synergism of weak interactions. Also note that slight differences in molecular structure have

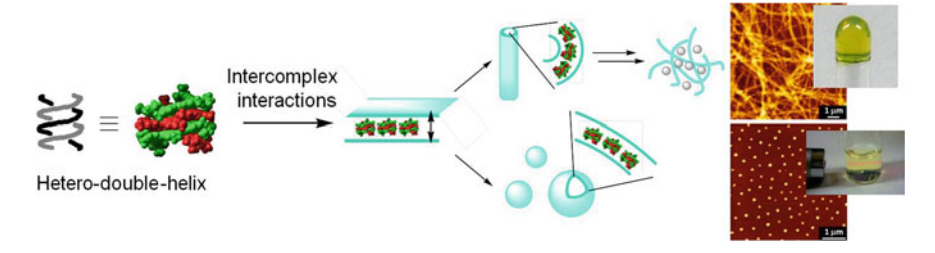


Fig. 1.6 Formation of fibers/gels and vesicles by hierarchical assembly of pseudoenantiomeric ethynylhelicene oligomers via hetero-double helices and intercomplex interaction between them

marked effects on the properties of the assemblies. The structures and properties of the assemblies were fine-tuned by changing the combination of compounds (Chap. 5).

In this thesis, I document my studies of the synthesis, homo- and hetero-double-helix formation, higher-assembly formation, and fine-tuning of their properties employing synthetic ethynylhelicene oligomers. In this work, I show a new methodology of obtaining diverse synthetic double helices and a bottom-up methodology for integrating double helix molecules into higher assemblies by intercomplex interactions.

#### References

- 1. Berl V, Huc I, Khoury RG, Krische MJ, Lehn J-M (2000) Nature 407:720
- 2. Furusho Y, Yashima E (2011) Macromol Rapid Commun 32:136
- 3. Yashima E, Maeda K, Iida H, Furusho Y, Nagai K (2009) Chem Rev 109:6102
- 4. Haldar D, Schmuck C (2009) Chem Soc Rev 38:363
- Hecht S, Huc I (eds) (2007) Foldamers: structure, properties, and applications. Wiley-VCH, Weinheim
- 6. Gan Q, Shang J, Kauffmann B, Wang Y, Bie F, Jiang H (2012) Tetrahedron 23:4479
- Makiguchi W, Kobayashi S, Furusho Y, Yashima E (2013) Angew Chem Int Ed. doi:10.1002/anie.201301005
- 8. Yamada H, Wu Z-Q, Furusho Y, Yashima E (2012) J Am Chem Soc 134:9506
- 9. Yamada H, Furusho Y, Yashima E (2012) J Am Chem Soc 134:7250
- 10. Ito H, Ikeda M, Hasegawa T, Furusho Y, Yashima E (2011) J Am Chem Soc 133:3419
- 11. Iida H, Shimoyama M, Furusho Y, Yashima E (2010) J Org Chem 75:417
- 12. Yamada H, Furusho Y, Ito H, Yashima E (2010) Chem Commun 46:3487
- 13. Wu Z-Q, Furusho Y, Yamada H, Yashima E (2010) Chem Commun 46:8962
- 14. Mudraboyina BP, Wisner JA (2012) Chem Eur J 18:14157
- 15. Wang H-B, Mudraboyina BP, Wisner JA (2012) Chem Eur J 18:1322
- 16. Wang H-B, Mudraboyina BP, Li J, Wisner JA (2010) Chem Commun 46:7343
- 17. Gan Q, Li F, Li G, Kauffmann B, Xiang J, Huc I, Jiang H (2010) Chem Commun 46:297
- Gan Q, Ferrand Y, Chandramouli N, Kauffmann B, Aube C, Dubreuil D, Huc I (2012) J Am Chem Soc 134:15656
- 19. Ferrand Y, Gan Q, Kauffmann B, Jianf H, Huc I (2011) Angew Chem Int Ed 50:7572
- 20. Baptiste B, Zhu J, Haldar D, Kauffmann B, Léger J-M, Huc I (2012) Chem Asian J 5:1364

- 21. Ikeda M, Tanaka Y, Hasegawa T, Furusho Y, Yashima E (2006) J Am Chem Soc 128:6806
- Maeda T, Furusho Y, Sakurai S-I, Kumaki J, Okoshi K, Yashima E (2008) J Am Chem Soc 130:7938
- 23. Woolfson DN (2005) Adv Protein Chem 70:79
- 24. Price JL, Horne S, Gellman SH (2010) J Am Chem Soc 132:12378
- 25. Daniels DS, Petersson J, Qiu JX, Schepartz A (2007) J Am Chem Soc 129:1532
- 26. Lee B-C, Zuckermann RN, Dill KA (2005) J Am Chem Soc 127:10999
- 27. Cheng RP, DeGrado WF (2002) J Am Chem Soc 124:11564
- 28. Petsko GA, Ringe D (2009) Protein structure and function. Oxford University Press, New York
- 29. Kojima S, Kuriki Y, Yoshida T, Yazaki K, Miura K (1997) Proc Japan Acad Ser B 73:7
- 30. Maity S, Jana P, Maity SK, Haldar D (2011) Soft Matter 7:10174
- 31. Sim S, Kim Y, Kim T, Lim S, Lee M (2012) J Am Chem Soc 134:20270
- 32. Pomerantz WC, Yuwono VM, Drake R, Hartgerink JD, Abbott NL, Gellman SH (2011) J Am Chem Soc 133:13604
- 33. Lim Y, Moon K-S, Lee M (2009) Angew Chem Int Ed 48:1601
- 34. Cuccia LA, Lehn J-M, Homo J-C, Schmutz M (2000) Angew Chem Int Ed 39:233
- 35. Yamaguchi M, Okubo H, Hirama M (1996) J Chem Soc Chem Commun 1772
- 36. Amemiya R, Yamaguchi M (2008) Org Biomol Chem 6:26
- 37. Amemiya R, Yamaguchi M (2008) Chem Rec 8:116
- 38. Kano K, Negi S, Kamo H, Kitae T, Yamaguchi M, Okubo H, Hirama M (1998) Chem Lett 27:151
- 39. Feng F, Miyashita T, Okubo H, Yamaguchi M (1998) J Am Chem Soc 120:10166
- 40. Okubo H, Yamaguchi M, Kabuto C (1998) J Org Chem 63:9500
- 41. Kano K, Kamo H, Negi S, Kitae T, Takaoka R, Yamaguchi M, Okubo H, Hirama M (1999) J Chem Soc Perkin Trans 2:15
- 42. Okubo H, Feng F, Nakano D, Hirata T, Yamaguchi M, Miyashita T (1999) Tetrahedron 55:14855
- 43. Okubo H, Yamaguchi M (2000) Heterocycles 52:863
- 44. Okubo H, Nakano D, Yamaguchi M, Kabuto C (2000) Chem Lett 29:1316
- 45. Okubo H, Nakano D, Anzai S, Yamaguchi M (2001) J Org Chem 66:557
- 46. Okubo H, Yamaguchi M (2001) J Org Chem 66:824
- 47. Nakamura K, Okubo H, Yamaguchi M (2001) Org Lett 3:1097
- 48. Honzawa S, Okubo H, Anzai S, Yamaguchi M, Tsumoto K, Kumagai I (2002) Bioorg Med Chem 10:3213
- 49. Honzawa S, Okubo H, Nakamura K, Anzai S, Yamaguchi M, Kabuto C (2002) Tetrahedron Assym 13:1043
- 50. Homzawa S, Chiba S, Okubo H, Yamaguchi M (2002) Heterocycles 57:1091
- 51. Nakano D, Yamaguchi M (2003) Tetrahedron Lett 44:4969
- 52. Saiki Y, Sugiura H, Nakamura K, Yamaguchi M, Hoshi T, Anzai J (2003) J Am Chem Soc 125:9268
- 53. Saiki Y, Nakamura K, Nigorikawa Y, Yamaguchi M (2003) Angew Chem Int Ed 42:5190
- 54. Sugiura H, Nigorikawa Y, Saiki Y, Nakamura K, Yamaguchi M (2004) J Am Chem Soc 126:14858
- 55. Sugiura H, Takahira Y, Yamaguchi M (2005) J Org Chem 70:5698
- 56. Takahira Y, Sugiura H, Yamaguchi M (2006) J Org Chem 71:763
- 57. Mizukami J, Sugiura H, Yamaguchi M, Mushiake K (2006) Bull Chem Soc Jpn 79:317
- 58. Sugiura H, Sakai D, Otani H, Teranishi K, Takahira Y, Amemiya R, Yamaguchi M (2007) Chem Lett 36:72
- 59. Sugiura H, Yamaguchi M (2007) Chem Lett 36:58
- 60. Sugiura H, Amemiya R, Yamaguchi M (2008) Chem Asian J 3:244
- 61. Sugiura H, Teranishi K, Amemiya R, Yamaguchi M (2008) Chem Lett 37:158
- 62. Pearson RG (1989) J Org Chem 54:1423

# **Chapter 2 Synthesis of Ethynylhelicene Oligomers**

Side chain analogues of ethynylhelicene oligomers were synthesized by a twodirectional method to elongate the oligomers in two directions by a repetitive Sonogashira coupling reaction with building blocks and deprotection [1, 2].

## 2.1 Oligomers Possessing Branched Alkyloxycarbonyl Side Chains

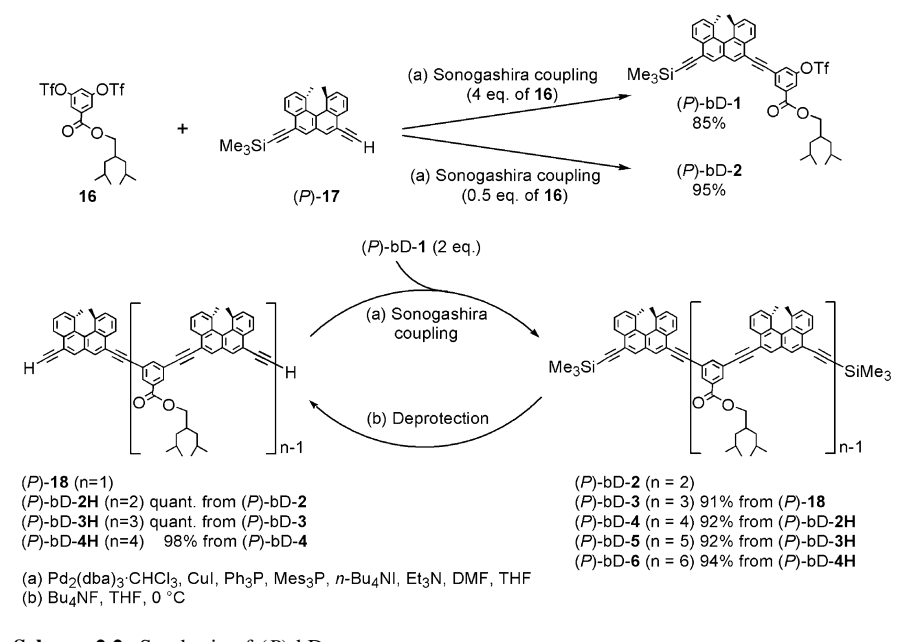
A *m*-phenylene spacer unit with a branched alkyloxycarbonyl side chain, 4-methyl-2-(2-methylpropyl)pentyl-3,5-bis(trifluoromethanesulfonyloxy) benzoate **16**, was obtained from 4-diethyl-2,2-bis(2-methylpropyl)propanedionate **12** in five steps (Scheme 2.1). The Krapcho decarboxylation of diisobutylmalonic acid diethyl ester **12** and the subsequent reduction using lithium aluminum hydride gave 4-methyl-2-(2-methylpropyl)-pentanol **14**. Benzoate **15** was prepared by the Fischer esterification of 3,5-dihydroxybenzoic acid with **14**, which was then converted to 4-methyl-2-(2-methylpropyl)pentyl-3,5-bis(trifluoromethanesulfonyloxy)benzoate **16**.

(*P*)-bD- $\mathbf{n}$  ( $\mathbf{n} = 2$ -6) were synthesized starting from  $\mathbf{16}$ . The coupling of monosilylated ethynylhelicene (*P*)- $\mathbf{17}$  and four equivalents of  $\mathbf{16}$  gave the building block (*P*)-bD- $\mathbf{1}$  (Scheme 2.2). The dimer (*P*)-bD- $\mathbf{2}$  was synthesized from  $\mathbf{16}$  and (*P*)- $\mathbf{17}$  in 95 % yield. The coupling of diethynylhelicene (*P*)- $\mathbf{18}$  and (*P*)-bD- $\mathbf{1}$  yielded the trimer (*P*)-bD- $\mathbf{3}$  in 91 % yield, and the subsequent deprotection and Sonogashira coupling converted (*P*)-bD- $\mathbf{3}$  to (*P*)-bD- $\mathbf{5}$  in 92 % yield. The tetramer (*P*)-bD- $\mathbf{4}$  ( $\mathbf{n} = \mathbf{4}$ ) and the hexamer (*P*)-bD- $\mathbf{6}$  ( $\mathbf{n} = \mathbf{6}$ ) were synthesized starting from the deprotected dimer (*P*)-bD- $\mathbf{2H}$  in 92 and 94 % yields, respectively. The enantiomers (*M*)-bD- $\mathbf{2}$ , (*M*)-bD- $\mathbf{4}$ , and (*M*)-bD- $\mathbf{6}$  were synthesized by the same method.

#### 2.2 Oligomers Possessing Perfluorooctyl Side Chains

1-Perfluorooctyl-3,5-bis(trifluoromethanesulfonyloxy)benzene **21** was synthesized in two steps (Scheme **2.3**). Trifluoromethanesulfonate **19** was obtained from

**Scheme 2.1** Synthesis of the *m*-phenylene spacer with a branched alkyloxycarbonyl side chain



Scheme 2.2 Synthesis of (P)-bD-n

**Scheme 2.3** Synthesis of the *m*-phenylene spacer with a perfluorooctyl side chain

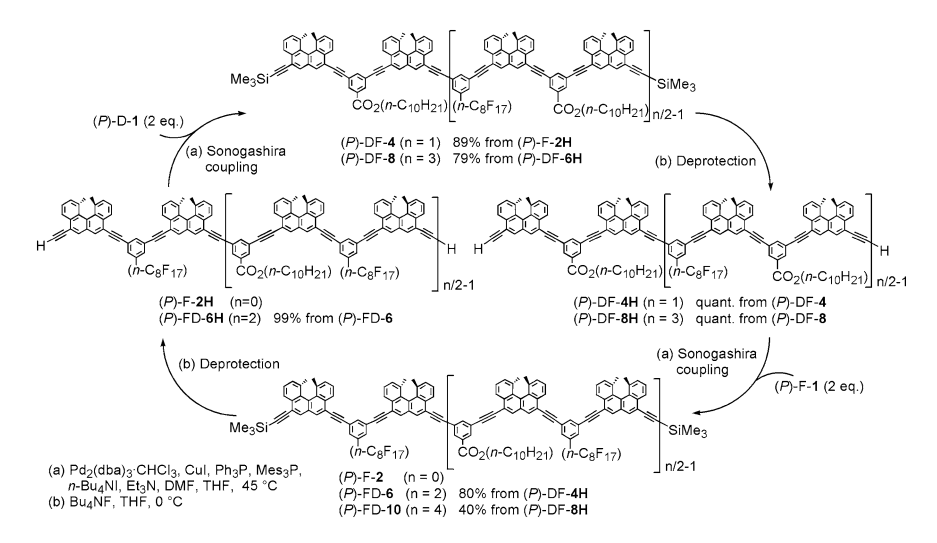
Scheme 2.4 Synthesis of (P)-F-n

3,5-dihydroxyiodobenzene **20**, which was coupled with 1-iodoperfluorooctane in the presence of copper powder and 2,2'-bipyridyl.

The building block (P)-F-1 and a series of perfluorooctylated oligomers, (P)-F-2 to (P)-F-5, were synthesized similarly to (P)-bD-n (Scheme 2.4). A repetitive coupling reaction starting from (P)-17 yielded the dimer (P)-F-2 and the tetramer (P)-F-4 in 81 and 50 % yields, respectively. The trimer (P)-F-3 and the pentamer (P)-F-5 were obtained from (P)-18 in 77 and 36 % yields, respectively. The solubility of the oligomers in organic solvents significantly decreased with an increase in the number of helicenes, and the yields of the coupling reaction decreased. Because of the solubility problem, the hexamer could not be obtained in an acceptable yield.

#### 2.3 Oligomers Possessing Alternating Decyloxycarbonyl/ Perfluorooctyl Side Chains

(*P*)-DF-**n** (**n** = 4 and 8) (*P*)-FD-**n** (**n** = 6 and 10) were synthesized by the alternative coupling of the building blocks, (*P*)-D-**1** and (*P*)-F-**1** (Scheme 2.5). The tetramer (*P*)-DF-**4** was obtained in 89 % yield by coupling (*P*)-F-**2H** and (*P*)-D-**1**. After deprotection, (*P*)-DF-**4** was converted to the hexamer (*P*)-DF-**6** in 80 % yield by coupling with (*P*)-F-**1**. Analogously, the octamer (*P*)-DF-**8** and the decamer (*P*)-FD-**10** were obtained in 79 and 40 % yields, respectively. (*P*)-FD-**6** and (*P*)-FD-**10** showed lower solubilities than (*P*)-DF-**4** and (*P*)-DF-**8**, and were not soluble at  $1.0 \times 10^{-3}$  M at room temperature in trifluoromethylbenzene.



**Scheme 2.5** Synthesis of (*P*)-DF-**n** and (*P*)-FD-**n** 

**Scheme 2.6** Synthesis of (*P*)-DF-6

Then, (P)-DF-**6** was synthesized from (P)-D-**2H** to obtain a hexamer with higher solubility than (P)-FD-**6** (Scheme 2.6). As expected, (P)-DF-**6** showed improved solubility, which was as high as that of (P)-DF-**8**.

#### References

- Nakamura K, Okubo H, Yamaguchi M (2001) Synthesis and self-aggregation of cyclic alkynes containing helicene. Org Lett 3:1097
- Sugiura H, Nigorikawa Y, Saiki Y, Nakamura K, Yamaguchi M (2004) Marked effect of aromatic solvent on unfolding rate of helical ethynylhelicene oligomer. J Am Chem Soc 126:14858

# Chapter 3 Homo-Double-Helix Formation of Ethynylhelicene Oligomers Possessing Various Side Chains

Ethynylhelicene oligomers are composed of several structural elements such as side chains, terminal groups, and chirality of helicenes. Therefore, a diversity of derivatives can be obtained by modifying these elements separately. In this study, side chain analogues were synthesized. In general, helix-forming synthetic oligomers possess an array of aromatic moieties with long alkyl side chains, which are introduced to improve their solubility in organic solvents. In some cases, however, side chains were reported to affect helix formation.

In the case of a single helix, although the m-phenylene ethynylene oligomer with triethyleneglycoxycarbonyl side chains,  $\mathbf{1}$ , forms a single helix in acetonitrile, which is a polar solvent, the oligomers with triethyleneglycoxymethyl side chains,  $\mathbf{2}$ , or triethyleneglycoxy side chains,  $\mathbf{3}$ , require more polar solvents, such as a combination of acetonitrile and water, for helix formation (Fig. 3.1) [1]. A triblock oligomer with both triethyleneglycoxycarbonyl and triethyleneglycoxymethyl side chains,  $\mathbf{4}$ , shows intermediate aggregation. It has been discussed that electron-withdrawing groups strengthen  $\pi$ -stacking [1].

The side chain effect on the homo-double-helix formation of aromatic oligoamides has also been discussed (Fig. 3.2). The dimerization constant for the homo-double-helix formation of pyridine-dicarboxamide oligomers depends on the side chains [2, 3]. A heptamer with seven decyloxy side chains,  $\bf 5$ , in CDCl<sub>3</sub> or C<sub>6</sub>D<sub>6</sub> has a dimerization constant three orders of magnitude larger than that with three decyloxy side chains,  $\bf 6$ , or that lacking a side chain,  $\bf 7$ . It was proposed that long side chains are involved in van der Waals interactions between two strands.

In CDCl<sub>3</sub>, the dimerization constants of the pyridine-dicarboxamide heptamer **5** [4] and the nonamer **10** [5] with benzyloxy side chains on pyridine rings are much higher than those with decyloxy or methoxy side chains (Fig. 3.3). This result has been ascribed to the interstrand face-to-face and edge-to-face interactions between benzyl groups. Similar dimerization constants, which were higher than those of unsubstituted oligomers, were obtained for the decyloxy and methoxy derivatives [2, 3]. The favorable dimerization of alkyloxy derivatives was explained by the reduction of unfavorable dipolar interactions.

The above examples show that side chains can affect the stability of helices formed by aromatic oligomers. However, systematic study of the side chain effect

Fig. 3.1 *m*-Phenylene ethynylene oligomers

Fig. 3.2 Pyridine-carboxamide oligomers

Fig. 3.3 Pyridine-carboxamide oligomers and effect of benzyl moiety in side chains

remains insufficient, and thus further study is needed. Then I synthesized ethynylhelicene oligomers possessing various side chains and studied the effect of the side chains on homo-double-helix formation.

As described in Chap. 1, our research group showed notable relationship between the HSAB principle and the homo-double-helix formation of ethynylhelicene oligomers possessing decyloxycarbonyl side chains: Hard aromatic solvents [6] kinetically and thermodynamically stabilize the homo-double-helix [7, 8]. Thus, to investigate the effects of the partial softness/hardness of m-phenylenes as well as of the steric and electronic nature, we synthesized a new series of ethynylhelicene oligomers with different side chains, and their homo-double-helix formation was examined (Fig. 3.4). (1) (P)-bD- $\mathbf{n}$  (n = 2-6) with 4-methyl-2-(2methylpropyl)-1-pentyloxy carbonyl side chains were synthesized, which have mphenylenes with very similar hardness and electron-withdrawing nature to (P)-D**n** but with different bulkiness. (2) (P)-F-**n** (n = 2-5) with perfluorooctyl side chains were synthesized to investigate the effect of hard and electron-withdrawing side chains on m-phenylene moieties. Although the helicene moieties can be regarded as soft aromatic moieties, the manipulation provides an alternating arrangement of soft and hard moieties to (P)-F-n. (3) A series of (P)-S- $\mathbf{n}$  (n = 2–7) with decylsulfanyl side chains containing soft and electron-donating sulfur atoms were synthesized, which possess a soft nature both at the helicene and m-phenylene moieties. (4) (P)-DF-**n** or (P)-FD-**n** (n = 4, 6, 8, 10) with alternating decyloxycarbonyl and perfluorooctyl side chains were synthesized to determine

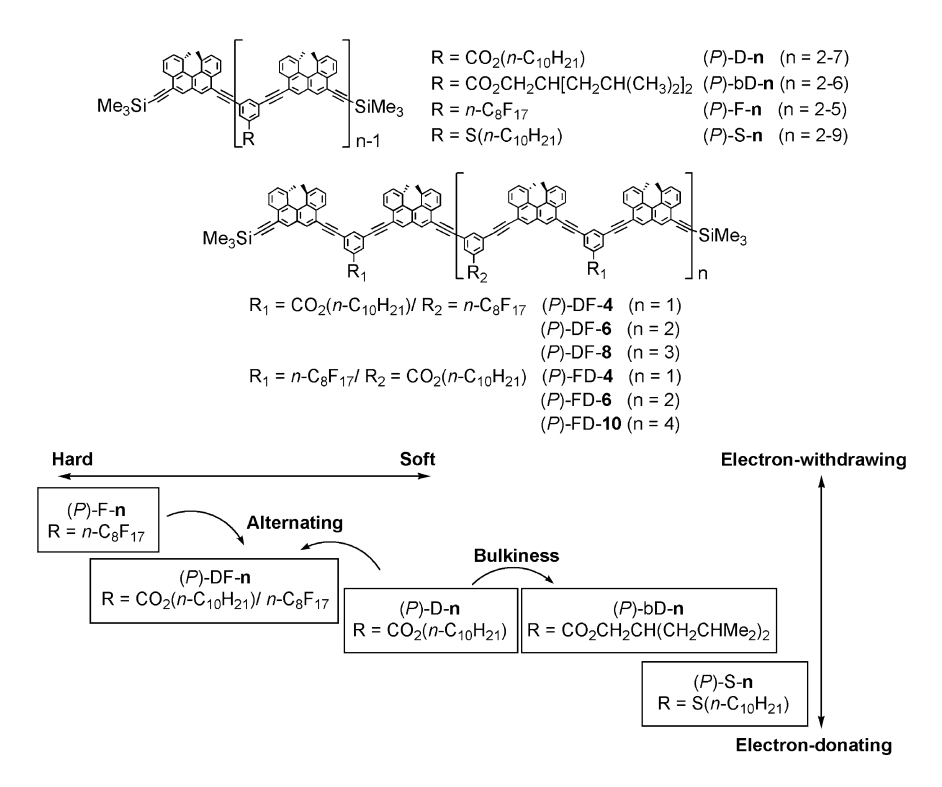


Fig. 3.4 Ethynylhelicene oligomers with various side chains and side chain effect

the effects of the arrangements of soft and hard moieties. "DF" means that an oligomer has one more decyloxycarbonyl side chain than perfluorooctyl side chains, and "FD" vice versa.

The oligomers are denoted "D", "bD", "F", "S", "DF", and "FD" derivatives, and the bold-faced number represents the number of helicenes in an oligomer. Desilylated synthetic intermediates are denoted "H", for example, (*P*)-D-**2H**.

#### 3.1 Oligomers Possessing Decyloxycarbonyl Side Chains

Before studying the newly synthesized oligomers with different side chains, the homoaggregation of (P)-D- $\mathbf{n}$  ( $\mathbf{n}=2$ –8) was re-examined in detail. CD and UV–Vis analyses were conducted in chloroform and trifluoromethylbenzene, which are relatively weak and strong helix-forming solvents, respectively [7, 8]. Although a previous spectroscopic study was conducted within 5 min after dissolution to examine unfolding rate [7], in this study, equilibrated states were examined by heating solutions of (P)-D- $\mathbf{n}$  to unfold the homo-double helices and then cooling it

to refold the helices. All the obtained spectra were confirmed to remain unchanged, which indicates the equilibrated states.

In chloroform  $(5.0 \times 10^{-6} \text{ M}, 25 ^{\circ}\text{C})$ , the CD and UV–Vis spectra of (P)-D-2, (P)-D-3, (P)-D-4, (P)-D-5, (P)-D-6, and (P)-D-7 showed monotonic increases in accordance with the number of helicenes (Fig. 3.5a). The spectra exhibited the Cotton effects of random coil states proved in a previous study [7]. (P)-D-8 showed a slightly enhanced Cotton effect at 365 nm, and the spectrum was considered to reflect partial homo-double-helix formation. This explanation was supported by the observation that (P)-D-8 showed a CD spectrum typical of a homo-double-helix at a higher concentration of  $5.0 \times 10^{-4} \text{ M}$  in chloroform at  $5 ^{\circ}$ C (Fig. 3.5b).

In trifluoromethylbenzene  $(5.0 \times 10^{-6} \text{ M}, 25 \,^{\circ}\text{C})$ , the CD spectra of (*P*)-D-**n** obtained after 15 min were confirmed to be equilibrated except those of (*P*)-D-**6** and (*P*)-D-7, which reached a steady state after 90 min and 2 h, respectively. Although the CD intensities at 335 and 385 nm showed monotonic increases in accordance with the number of helicenes for (*P*)-D-**2**, (*P*)-D-**3**, and (*P*)-D-**4**, (*P*)-D-**5** showed a slightly different shape (Fig. 3.6b), and (*P*)-D-**6**, (*P*)-D-**7**, and (*P*)-D-**8** showed quite different shapes; an enhanced Cotton effect with maxima at 323 and 365 nm was observed (Fig. 3.6a). The UV-Vis spectra of the higher oligomers, (*P*)-D-**n** (n = 6-8), showed hypochromic shifts. The results of the CD and UV-Vis studies indicated the homo-double-helix formation of (*P*)-D-**6**, (*P*)-D-**7**, and (*P*)-D-**8** in trifluoromethylbenzene.

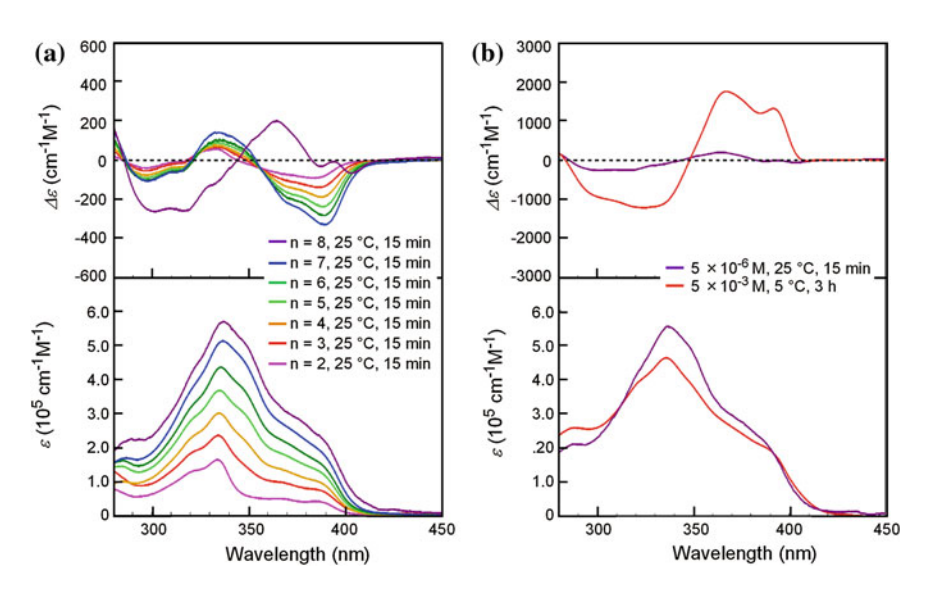


**Fig. 35** CD (*top*) and UV–Vis (*bottom*) spectra of **a** (*P*)-D-**n** (n = 2–8, chloroform,  $5.0 \times 10^{-6}$  M, 25 °C) and **b** (*P*)-D-**8** (chloroform,  $5.0 \times 10^{-4}$  M and  $5.0 \times 10^{-6}$  M). The solutions were heated at 60 °C and then cooled to 25 or 5 °C

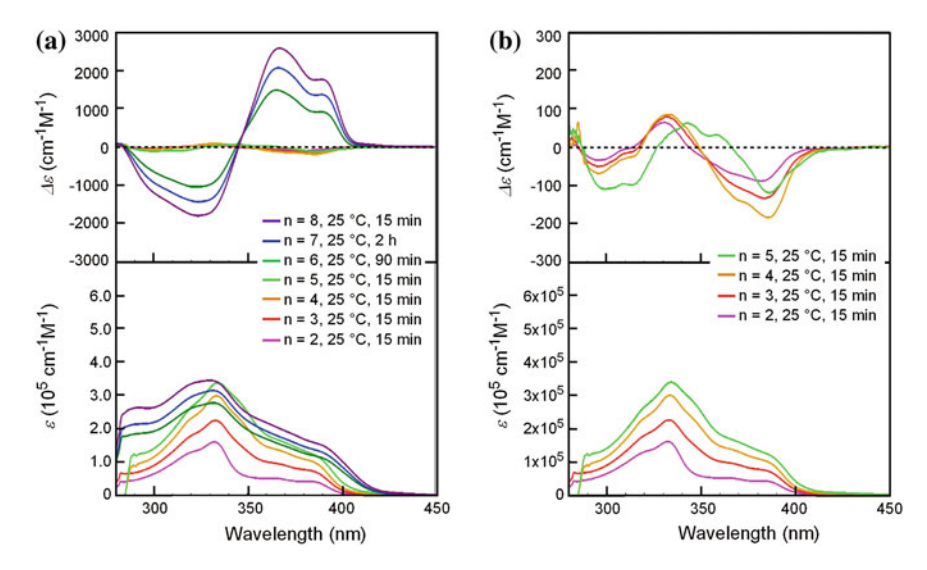


**Fig. 3.6 a** CD (*top*) and UV–Vis (*bottom*) spectra (trifluoromethylbenzene,  $5.0 \times 10^{-6}$  M, 25 °C) of (*P*)-D-**n** (n = 2–8). The solutions were heated at 80 °C and then cooled to 25 °C. **b** Magnified CD spectra (trifluoromethylbenzene,  $5.0 \times 10^{-6}$  M, 25 °C) of (*P*)-D-**n** (n = 2–5)

At a higher concentration  $(1.0 \times 10^{-3} \text{ M})$  in trifluoromethylbenzene, the equilibria of (P)-D-**n** shifted to homo-double helices, and the pentamer (P)-D-**5** exhibited the CD spectra of a homo-double-helix at 25 °C (Fig. 3.7a). At 10 °C, (P)-D-**4** also showed the enhanced Cotton effect of a homo-double-helix, whereas (P)-D-**2** and (P)-D-**3** did not (Fig. 3.7a). The dimeric aggregation of (P)-D-**4** at concentrations higher than  $1.0 \times 10^{-3}$  M was confirmed using VPO (trifluoromethylbenzene, 35 °C) (Fig. 3.7b). Taking account of this observation, we

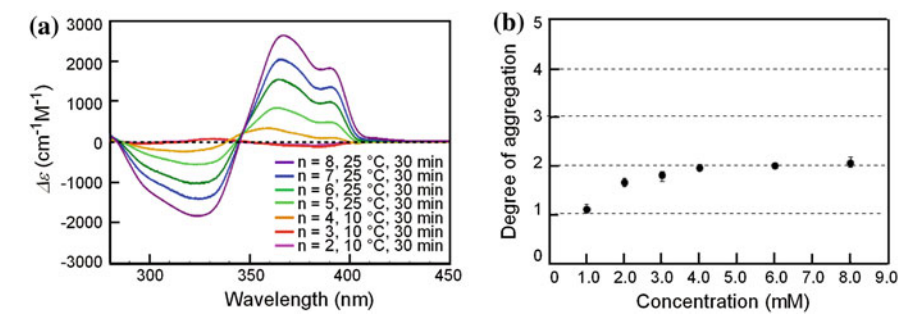


**Fig. 3.7** a CD spectra (trifluoromethylbenzene,  $1.0 \times 10^{-3}$  M) of (*P*)-D-n (n = 2–4; 10 °C and n = 5–8; 25 °C). Solutions were heated at 60 °C and then cooled to 25 or 10 °C. b Degree of aggregation determined using VPO at various concentrations of (*P*)-D-4 (trifluoromethylbenzene, 35 °C). *Circles* represent an average of more than five measurements, and *vertical lines* represent the range of obtained results

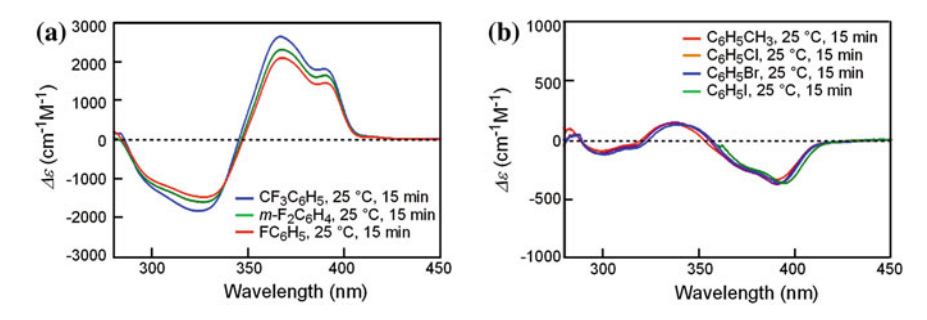


**Fig. 3.8** CD spectra  $(2.5 \times 10^{-6} \text{ M}, 25 ^{\circ}\text{C})$  of (P)-D-**8** in the following solvents: **a** trifluoromethylbenzene, m-difluorobenzene, and fluorobenzene; **b** toluene, chlorobenzene, bromobenzene, and iodobenzene. The solutions were heated at 80  $^{\circ}\text{C}$  and then cooled to 25  $^{\circ}\text{C}$ 

assumed that one turn of a homo-double-helix contained three helicenes and three *m*-phenylenes, and at least four helicenes were required to form a helical conformation, in which one terminal helicene lay on another.

In m-diffuorobenzene and fluorobenzene, which are relatively hard aromatic solvents, (P)-D-**8** showed the CD spectra of a homo-double-helix (Fig. 3.8a). In soft solvents such as toluene, chlorobenzene, bromobenzene, and iodobenzene, (P)-D-**8** provided the CD spectra of random coils (Fig. 3.8b). In the following discussions, the stability of homo-double helices formed by oligomers with different side chains is compared with that of (P)-D-**n** at equilibrium in these solvents.

## 3.2 Oligomers Possessing Branched Alkyloxycarbonyl Side Chains

$$Me_3Si$$
 $SiMe_3$ 
 $(P)-bD-n$ 

The CD and UV–Vis spectra of (*P*)-bD- $\mathbf{n}$  (n = 2–6) in chloroform (5.0 × 10<sup>-6</sup> M, 25 °C) showed a monotonic increase in accordance with the number of helicenes and were similar to those of (*P*)-D- $\mathbf{n}$  in the random coil state (Fig. 3.9a).

In trifluoromethylbenzene, the CD spectra of (*P*)-bD-6 reached equilibrium after 2 h and showed enhanced Cotton effects. Hypochromic shifts were observed in the UV–Vis spectra, which indicated homo-double-helix formation analogous to

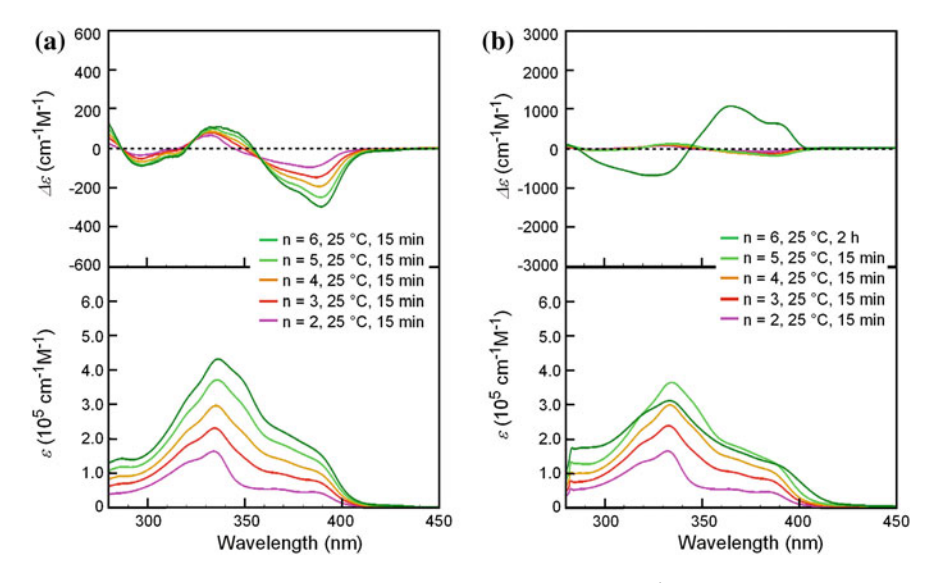


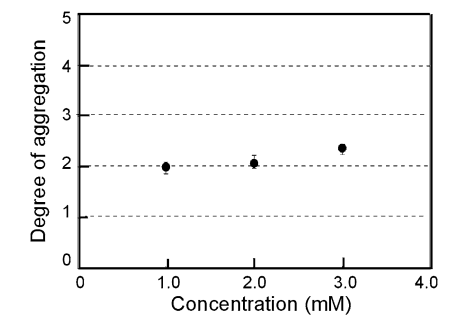
**Fig. 3.9** CD (*top*) and UV–Vis (*bottom*) spectra (25 °C,  $5.0 \times 10^{-6}$  M) of (*P*)-bD-**n** (n = 2–6) in **a** chloroform and **b** trifluoromethylbenzene. The solutions were heated at 60 °C in chloroform and at 80 °C in trifluoromethylbenzene and then cooled to 25 °C

that of (*P*)-D-**6** (Fig. 3.9b). A dimeric aggregate of (*P*)-bD-**6** was confirmed using VPO (trifluoromethylbenzene, 35 °C) (Fig. 3.10).

In *m*-difluorobenzene and fluorobenzene, (*P*)-bD-**6** showed the CD spectra of random coils (Fig. 3.11a). In soft solvents such as toluene, chlorobenzene, bromobenzene, and iodobenzene, (*P*)-bD-**6** showed the CD spectra of random coils (Fig. 3.11b). (*P*)-bD-**6** showed similar results to (*P*)-D-**6**.

The stabilities of (*P*)-D-**n** and (*P*)-bD-**n** were compared on the basis of the CD spectra in trifluoromethylbenzene. In both series, the pentamers (*P*)-D-**5** and (*P*)-bD-**5** showed the spectra of random coils at  $5.0 \times 10^{-6}$  M, and the hexamers (*P*)-D-**6** and (*P*)-bD-**6** showed the spectra of homo-double helices (Figs. 3.6a and

Fig. 3.10 Degree of aggregation of (*P*)-bD-6 determined using VPO (trifluoromethylbenzene, 35 °C) at several concentrations. *Circles* represent an average of more than five measurements, and *vertical lines* represent the range of results



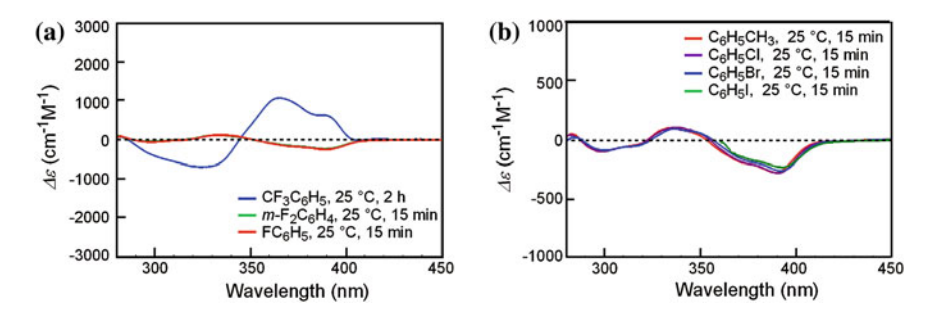


**Fig. 3.11** CD spectra  $(5.0 \times 10^{-6} \text{ M}, 25 ^{\circ}\text{C})$  of (P)-bD-6 in the following solvents: **a** trifluoromethylbenzene, *m*-difluorobenzene, and fluorobenzene; **b** toluene, chlorobenzene, bromobenzene, and iodobenzene. The solutions were heated at 80  $^{\circ}\text{C}$  and then cooled to 25  $^{\circ}\text{C}$ 

3.10b). The aggregations were compared between (P)-D-6 and (P)-bD-6 at different temperatures and concentrations. A solution of (P)-D-6 (trifluoromethylbenzene,  $5.0 \times 10^{-6}$  M) was first heated at 60 °C, and the aggregate was unfolded to random coils. Then, the solution was cooled to 25, 5, and -10 °C in this order, and allowed to stand until a steady state was reached at each temperature. The CD spectrum of (P)-D-6 showed homo-double-helix formation after 30 min at 25 °C, which did not change with cooling to 5 or -10 °C (Fig. 3.12a). The same spectra were obtained at a higher concentration of  $1.0 \times 10^{-3}$  M at 5 °C (Fig. 3.12a). Under the same conditions, (P)-bD-6 showed similar CD spectra to (P)-D-6 (Fig. 3.12b). The similar CD behaviors of (P)-D-6 and (P)-bD-6 indicated that both compounds formed homo-double helices with similar stabilities: The bulkiness at the side chains did not affect the aggregation. The  $\pi$ - $\pi$  interactions of the aromatic array of helicenes and m-phenylenes, therefore, are crucial for homo-double-helix formation, and the interaction between side chains is unimportant.

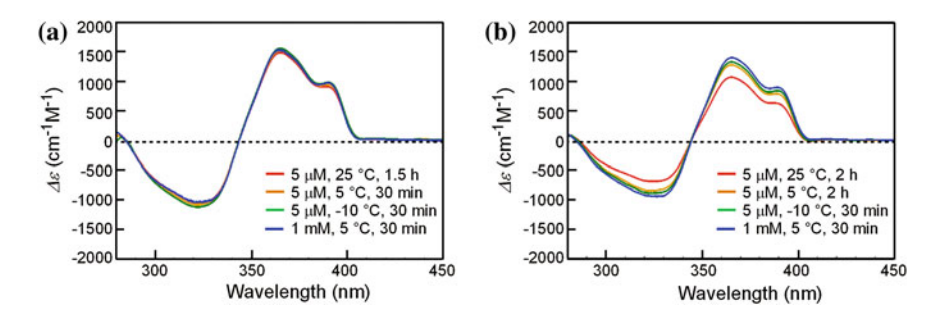


Fig. 3.12 CD spectra (trifluoromethylbenzene) of a (P)-D-6 and b (P)-bD-6 at various temperatures and concentrations. The solutions were heated at 60 °C and then cooled to 25, 5, and -10 °C

#### 3.3 Oligomers Possessing Perfluorooctyl Side Chains

$$Me_3Si$$

$$(n-C_8F_{17})$$
 $SiMe_3$ 
 $(P)-F-n$ 

(*P*)-F- $\mathbf{n}$  (n = 2–5) in chloroform (5.0 × 10<sup>-6</sup> M, 25 °C) showed the CD and UV–Vis spectra of random coils with a monotonic increase in accordance with the number of helicenes (Fig. 3.13a).

In trifluoromethylbenzene, (P)-F-5 dissolved only at concentrations below  $2.5 \times 10^{-5}$  M. A slow precipitation was observed after 30 min at 5 °C accompanied by a decrease in intensity and the poor reproducibility of the spectra. Therefore, CD and UV–Vis spectra were obtained at 5 min intervals within 30 min after cooling the solution to 5 °C. Cooling time was referred to as "within 30 min". A high reproducibility of the spectra was also confirmed. In trifluoromethylbenzene  $(5.0 \times 10^{-6} \, \text{M}, 25 \, ^{\circ}\text{C})$ , the dimer (P)-F-2 up to the tetramer (P)-F-4 showed similar CD and UV–Vis spectra to those in chloroform, whereas (P)-F-5 showed an enhanced CD with maxima at 334 and 364 nm and a hypochromic shift of the UV–Vis absorption (Fig. 3.13b).

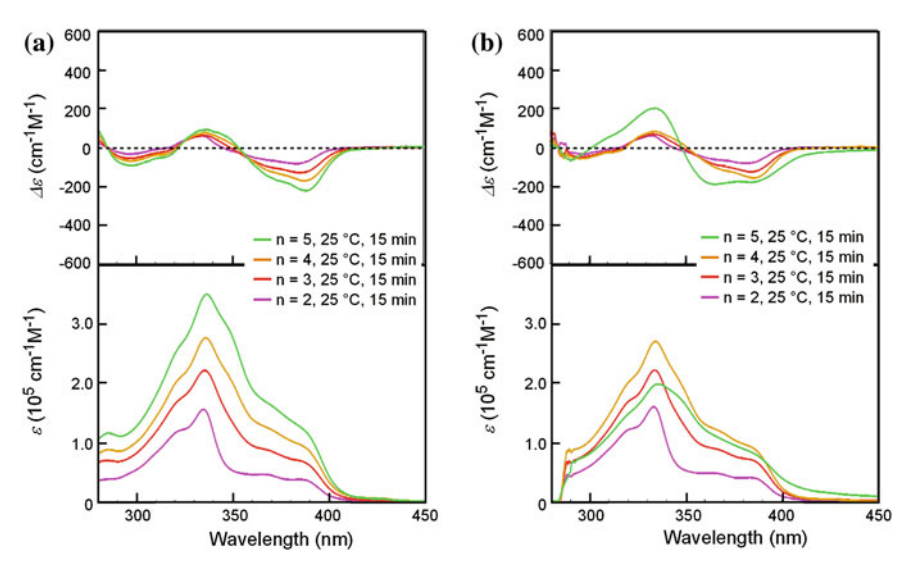


**Fig. 3.13** CD (*top*) and UV–Vis (*bottom*) spectra  $(5.0 \times 10^{-6} \text{ M}, 25 ^{\circ}\text{C})$  of (*P*)-F-n (n = 2–5) in a chloroform and b trifluoromethylbenzene. The solutions were heated at 60  $^{\circ}\text{C}$  in chloroform and 80  $^{\circ}\text{C}$  in trifluoromethylbenzene, and then cooled to 25  $^{\circ}\text{C}$ 

To determine the CD spectra of (*P*)-F-5 in the pure homo-double-helix state, the temperature, time course, and concentration dependences of the CD spectra of (*P*)-F-5 were examined. The CD spectra (trifluoromethylbenzene,  $2.0 \times 10^{-6}$  M) of (*P*)-F-5 were obtained at various temperatures between -10 and 60 °C. Precipitate was not observed at this concentration. Above 25 °C, the spectra of random coil state were obtained. Intensity increased as temperature decreased, and a steady state was reached at -10 °C with  $\Delta\varepsilon$  of approximately +800 cm<sup>-1</sup>M<sup>-1</sup> at 330 nm (Fig. 3.14a). Next,  $\Delta\varepsilon$  at 330 nm was monitored after heating the solution to 60 °C and then cooling it to -10 °C (Fig. 3.14b).  $\Delta\varepsilon$  reached a steady state after 30 min, at approximately +800 cm<sup>-1</sup>M<sup>-1</sup>.

The effect of concentration on the CD spectra was also examined. Very similar CD spectra were obtained at 5 °C at concentrations between  $5.0 \times 10^{-6}$  and  $2.5 \times 10^{-5}$  M, resulting in  $\Delta \varepsilon$  of approximately +800 cm<sup>-1</sup>M<sup>-1</sup> at 330 nm, and decreased  $\Delta \varepsilon$  at  $2.0 \times 10^{-6}$  M (Fig. 3.14c). It was concluded that the CD spectra in these steady states in trifluoromethylbenzene with  $\Delta \varepsilon$  of approximately +800 cm<sup>-1</sup>M<sup>-1</sup> at 330 nm show pure homo-double-helix states containing no random coils.

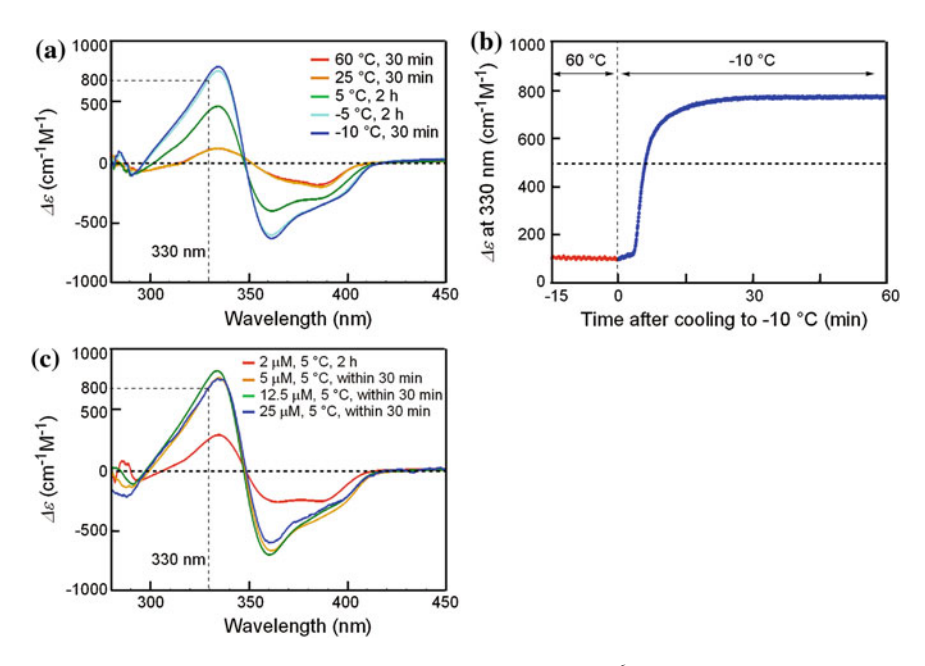
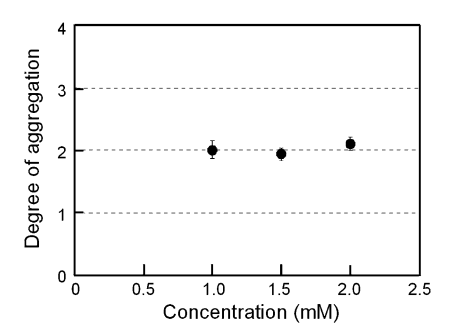


**Fig. 3.14 a** CD spectra (trifluoromethylbenzene,  $2.0 \times 10^{-6}$  M) of (*P*)-F-5 at various temperatures. **b** Profiles of  $\Delta \varepsilon$  at 330 nm (trifluoromethylbenzene,  $2.0 \times 10^{-6}$  M) of (*P*)-F-5 heated at 60 °C and then cooled to -10 °C. **c** CD spectra (trifluoromethylbenzene, 5 °C) of (*P*)-F-5 at various concentrations. The solutions were heated at 60 °C and then cooled to 5 °C

**Fig. 3.15** Degree of aggregation (*m*-difluorobenzene, 40 °C) of (*P*)-F-5 determined using VPO at various concentrations



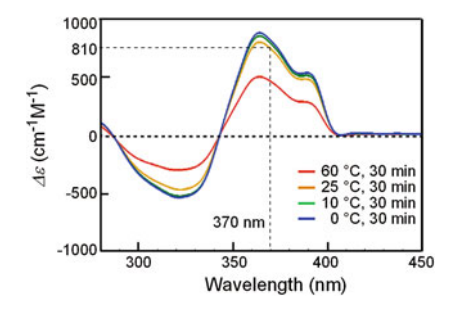
The degree of aggregation was investigated using VPO. m-Difluorobenzene was used as the solvent, since (P)-F-5 was soluble at  $1.0 \times 10^{-3}$  M at 40 °C in this solvent. At 40 °C, VPO indicated the dimeric structure at concentrations between 1.0 and  $3.0 \times 10^{-3}$  M (Fig. 3.15), which indicated homo-double-helix formation by (P)-F-5 in the solution.

On the basis of the experiments on the pentamer (P)-F-5, comparative studies were conducted with the original pentamer (P)-D-5 with decyloxycarbonyl side chains. The CDs of (P)-D-5 at  $1.0 \times 10^{-3}$  M were measured at different temperatures. Below 25 °C, typical spectra of homo-double-helix were obtained with  $\Delta\varepsilon$  of +810 cm<sup>-1</sup>M<sup>-1</sup> at 370 nm (Fig. 3.16), which was the pure homo-double-helix state, and unfolding was observed at 60 °C. Thus, both the pentamers (P)-F-5 and (P)-D-5 formed homo-double helices in trifluoromethylbenzene.

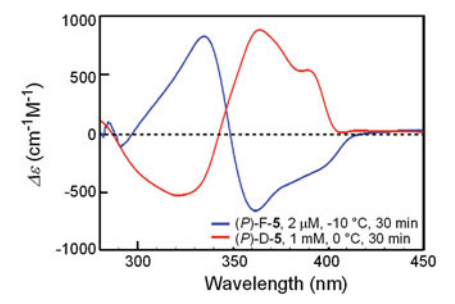
It should be noted that (P)-D-5 and (P)-F-5 in the pure homo-double-helix states showed approximately mirror-imaged CD spectra (Fig. 3.17). This means that (P)-F-5 formed similar homo-double-helix structure to (P)-D-5, but their helicities are opposite. This result was unexpected, since (P)-F-5 and (P)-D-5 had the same configuration of helicenes and differed only in the structure of the side chains. The result indicates that achiral side chains can control the helicity of homo-double helices.

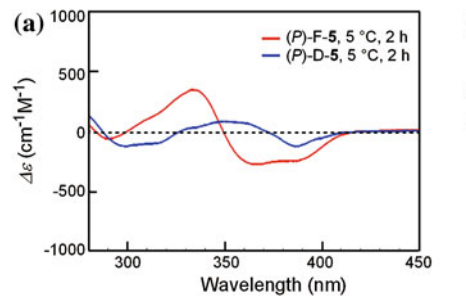
The stabilities of the homo-double-helix structure were compared between (P)-D-5 and (P)-F-5. In m-difluorobenzene  $(1.0 \times 10^{-4} \text{ M})$ , (P)-F-5 showed an intense CD compared with (P)-D-5 (Fig. 3.18a). In toluene, (P)-F-5 showed an intense CD at  $5.0 \times 10^{-5}$  M, whereas (P)-D-5 was a random coil under the same conditions, even at  $1.0 \times 10^{-4}$  M (Fig. 3.18b). (P)-F-5 formed a homo-double-helix at lower concentrations than (P)-D-5. The results indicated that the homo-double-helix of (P)-F-5 is more stable than that of (P)-D-5.

Fig. 3.16 CD spectra (trifluoromethylbenzene,  $1.0 \times 10^{-3}$  M) of (*P*)-D-5 at various temperatures



**Fig. 3.17** CD spectra (trifluoromethylbenzene) of (*P*)-D-**5**  $(1.0 \times 10^{-3} \text{ M}, 0 \text{ °C})$  and (*P*)-F-**5**  $(2.0 \times 10^{-6} \text{ M}, -10 \text{ °C})$ 





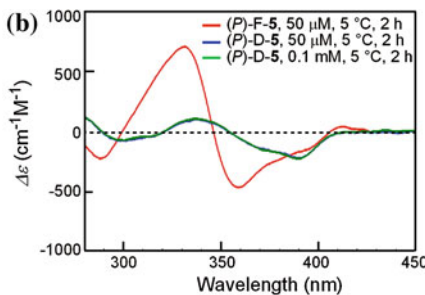


**Fig. 3.18** a CD spectra (*m*-difluorobenzene,  $1.0 \times 10^{-4}$  M, 5 °C) of (*P*)-D-**5** and (*P*)-F-**5**. b CD spectra (toluene, 5 °C) of (*P*)-D-**5** ( $5.0 \times 10^{-5}$  M and  $1.0 \times 10^{-4}$  M) and (*P*)-F-**5** ( $5.0 \times 10^{-5}$  M)

#### 3.4 Oligomers Possessing Decylthio Side Chains

In chloroform  $(5.0 \times 10^{-6} \text{ M}, 25 ^{\circ}\text{C})$ , (*P*)-S-**n** (n = 2-7) showed the CD and UV-Vis spectra of random coils that monotonically increase with the number of helicenes (Fig. 3.19a).

In trifluoromethylbenzene  $(5.0 \times 10^{-6} \text{ M}, 25 \text{ °C})$ , the CD and UV–Vis spectra of (P)-S-2, (P)-S-3, and (P)-S-4 showed a monotonic enhancement of the Cotton effect, indicating random coils. In contrast, the CD spectra of (P)-S-6 and (P)-S-7 after dissolution showed a slow change at 25 °C and reached steady states after 7 and 18 h, respectively. The spectra were different from those of random coils. Significant hypochromic shifts were observed by UV–Vis analysis (Fig. 3.19b). The results indicated aggregate formation by these longer oligomers. VPO analysis, however, could not be conducted because of their low solubility in trifluoromethylbenzene.

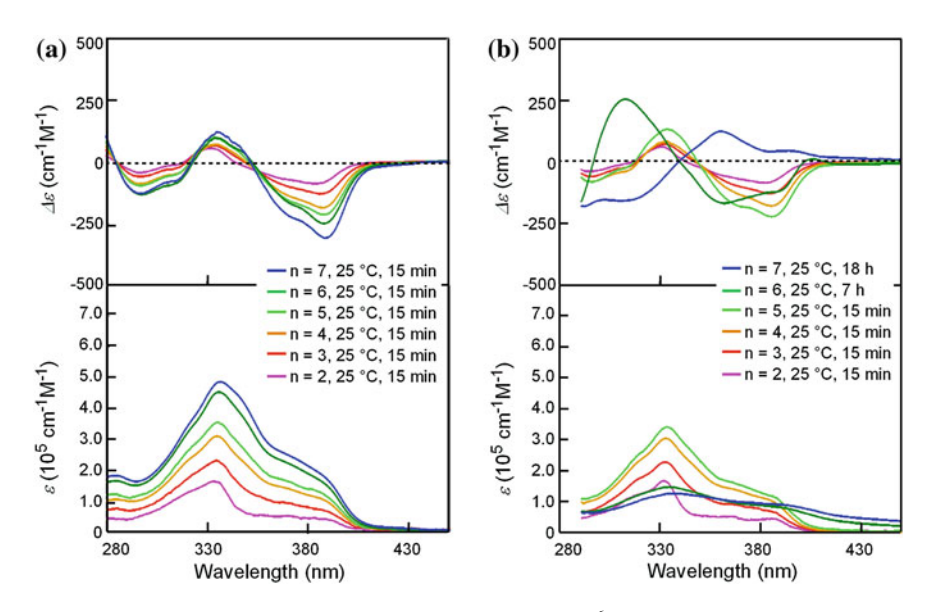


**Fig. 3.19** CD (top) and UV–Vis (bottom) spectra ( $5.0 \times 10^{-6}$  M, 25 °C) of (P)-S–n (n=2-7) in **a** chloroform and **b** trifluoromethylbenzene. The solutions were heated at 60 °C and then cooled to 25 °C

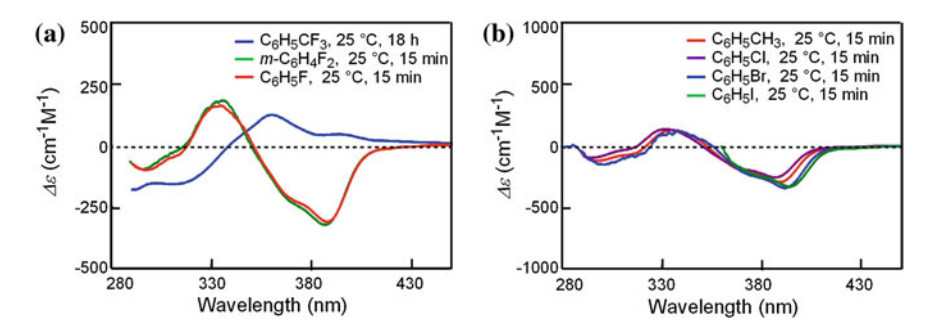


**Fig. 3.20** CD spectra  $(5.0 \times 10^{-6} \text{ M}, 25 ^{\circ}\text{C})$  of (P)-S-7 in the following solvents: **a** trifluoromethylbenzene, m-difluorobenzene, and fluorobenzene; **b** toluene, chlorobenzene, bromobenzene, and iodobenzene. The solutions were heated at 60  $^{\circ}\text{C}$  and then cooled to 25  $^{\circ}\text{C}$ 

In *m*-difluorobenzene, fluorobenzene, toluene, chlorobenzene, bromobenzene, and iodobenzene, (*P*)-S-7 gave the CD spectra ( $5.0 \times 10^{-6}$  M, 25 °C) of random coils (Fig. 3.20a, b).

The aggregations of (P)-D-7 and (P)-S-7 in toluene were compared. Solutions of (P)-D-7 and (P)-S-7 in toluene were first heated at 60 °C to unfold the heterodouble-helices to random coils, and then cooled to 25 or 5 °C. Both (P)-D-7 and (P)-S-7 at  $5.0 \times 10^{-6}$  M showed the CD spectra of random coils at 25 °C (Fig. 3.21). At  $1.0 \times 10^{-3}$  M, (P)-S-7 was a random coil at 5 °C, whereas (P)-D-7 showed the CD spectrum of a homo-double-helix (Fig. 3.21). The homo-double helix of (P)-S-7 was less stable than that of (P)-D-7.

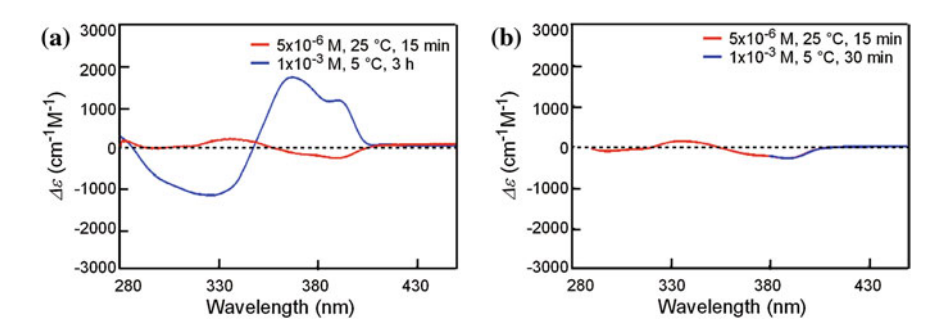


**Fig. 3.21** CD spectra (toluene) of **a** (*P*)-D-7 and **b** (*P*)-S-7 at various temperatures and concentrations. The solutions were heated at 60 °C and then cooled to 25 or 5 °C. The spectrum of (*P*)-S-7 at  $1.0 \times 10^{-3}$  M was obtained at a wavelength shorter than 380 nm because of the large UV–Vis absorption of (*P*)-S-7

#### 3.5 Oligomers Possessing Alternating Decyloxycarbonyl/ Perfluorooctyl Side Chains

$$Me_3Si$$
 $R_1$ 
 $R_2$ 
 $R_1$ 
 $SiMe_3$ 
 $n/2-1$ 

$$R_1 = CO_2(n-C_{10}H_{21})/R_2 = n-C_8F_{17}$$
 (P)-DF-**n**  
 $R_1 = n-C_8F_{17}/R_2 = CO_2(n-C_{10}H_{21})$  (P)-FD-**n**

The aggregation of (*P*)-DF-**n** (n = 4, 6, 8, 10) was examined in chloroform  $(5.0 \times 10^{-6} \text{ M}, 25 ^{\circ}\text{C})$ . The CD and UV-Vis spectra of random coils that monotonically increase with the number of helicenes were obtained (Fig. 3.22a).

In trifluoromethylbenzene  $(5.0 \times 10^{-6} \text{ M}, 5 ^{\circ}\text{C})$ , (*P*)-DF-4 showed a spectrum similar to that in chloroform (Fig. 3.22b) and was determined to be monomeric at concentrations from 1.0 to  $3.0 \times 10^{-3}$  M using VPO (45  $^{\circ}\text{C}$ ) (Fig. 3.23a). Since (*P*)-D-4 in the same solvent formed a homo-double-helix at concentrations higher than  $2.0 \times 10^{-3}$  M at 35  $^{\circ}\text{C}$  (Fig. 3.7b), (*P*)-DF-4 is consiedered to have a weaker tendency to form a homo-double-helix than (*P*)-D-4. The CD and UV–Vis spectra of (*P*)-DF-6 and (*P*)-DF-8, however, were different in trifluoromethylbenzene

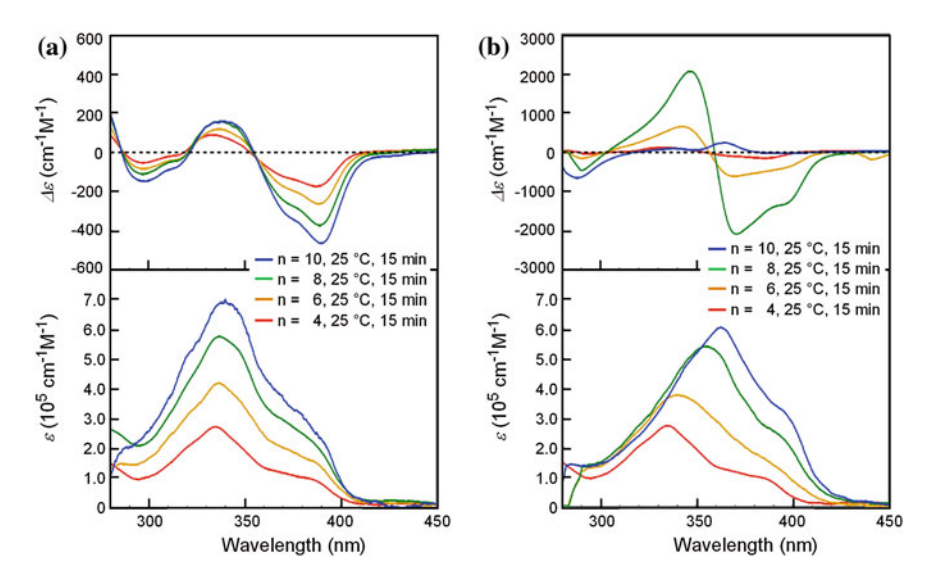


**Fig. 3.22** CD (*top*) and UV–Vis (*bottom*) spectra of (*P*)-DF-**4**, (*P*)-DF-**6**, (*P*)-DF-**8** ( $5.0 \times 10^{-6}$  M, 25 °C), and (*P*)-FD-**10** ( $2.5 \times 10^{-6}$  M) in **a** chloroform and **b** trifluoromethylbenzene. The solutions were heated at 60 °C in chloroform and at 80 °C in trifluoromethylbenzene and then cooled to 25 °C

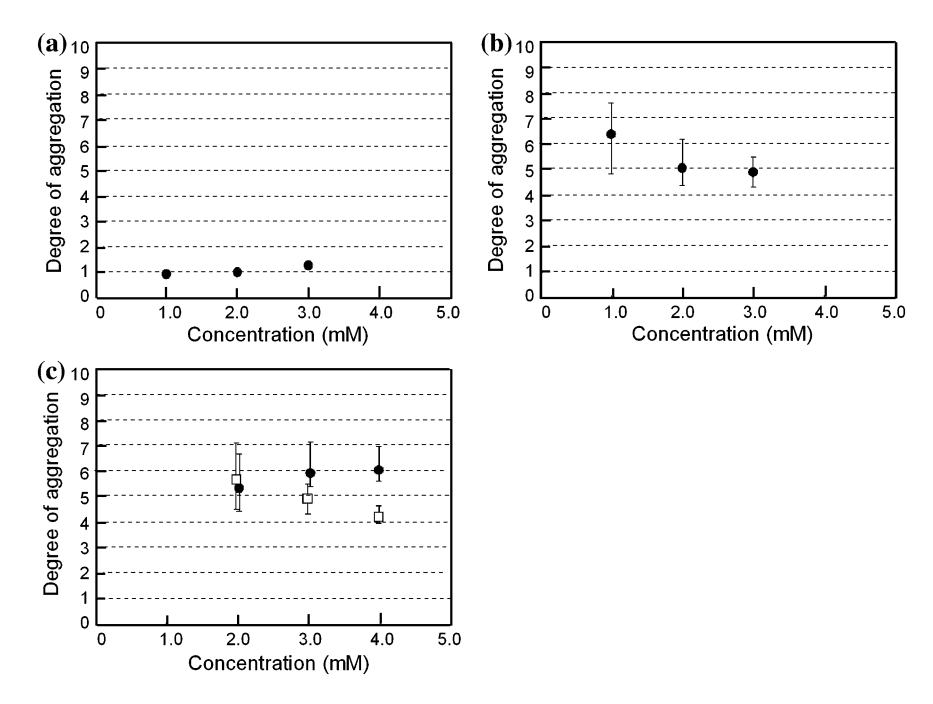


**Fig. 3.23** Degree of aggregation determined using VPO (trifluoromethylbenzene) of **a** (*P*)-DF-**4** (45 °C), **b** (*P*)-DF-**6** (60 °C), and **c** (*P*)-DF-**8** (white squares, 45 °C and black circles, 85 °C) at various concentrations. Circles represent an average of more than five measurements, and vertical lines represent the range of obtained results. The vertical lines in (**a**) are behind the circles

(Fig. 3.22b): The Cotton effects were considerably enhanced compared with those in chloroform, and the absorption maxima in UV–Vis shifted to the longer-wavelength region, from 338 to 350 nm for (P)-DF-6, and from 339 to 358 nm for (P)-DF-8. The observations were different from those for (P)-D-n, which showed a regular increase in the Cotton effect for (P)-D-4, (P)-D-5, (P)-D-6, (P)-D-7, and (P)-D-8 in trifluoromethylbenzene (Fig. 3.7a). VPO analysis indicated that (P)-DF-6 and (P)-DF-8 formed aggregates higher than dimers (Fig. 3.23b, c). The CD spectrum of (P)-FD-10 in trifluoromethylbenzene (P0-DF-8 with weak Cotton effects (Fig. 3.22b). This may not be a random coil, because a significant shift of the UV–Vis absorption maximum from 338 to 362 nm was observed, which was different from the UV–Vis spectra in chloroform. The higher oligomers of (P0-DF-n exhibited complex aggregation behaviors in trifluoromethylbenzene.

In m-difluorobenzene, fluorobenzene, toluene, chlorobenzene, bromobenzene, and iodobenzene, (P)-DF-8 showed spectra typical of random coils (Fig. 3.24). The aggregation of (P)-DF-8 was substantially less stable than that of (P)-D-8, which formed a homo-double-helix in m-difluorobenzene and fluorobenzene as well as in trifluoromethylbenzene.

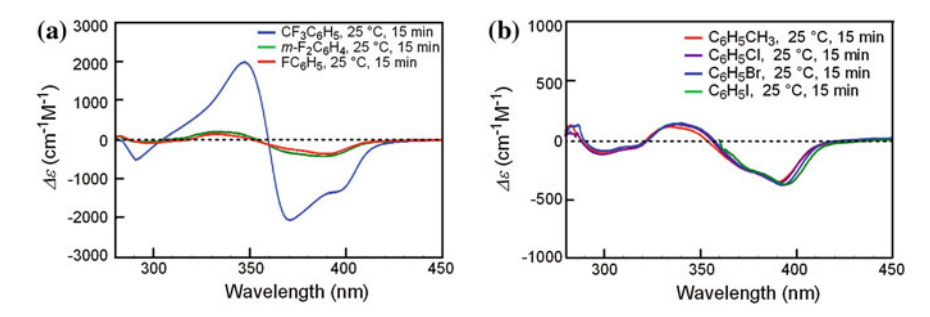


**Fig. 3.24** CD spectra  $(2.5 \times 10^{-6} \text{ M}, 25 \,^{\circ}\text{C})$  of (P)-DF-**8** in the following solvents: **a** trifluoromethylbenzene, m-difluorobenzene, and fluorobenzene; **b** toluene, chlorobenzene, bromobenzene, and iodobenzene. The solutions were heated at 80  $\,^{\circ}\text{C}$  and then cooled to 25  $\,^{\circ}\text{C}$ 

The homo-double-helix of (P)-DF-**n** was less stable than those of (P)-F-**n** and (P)-D-**n**: Although (P)-F-**n** and (P)-D-**n** formed stable homo-double helices, (P)-DF-**n** with alternating decyloxycarbonyl and perfluorooctyl side chains did not exhibit intermediate properties between them.

# 3.6 Summary of Effect of Side Chains on Stability of Homo-Double Helices

The homo-double-helix formation of ethynylhelicene oligomers with various side chains was studied. The order of stability was summarized as follows: (P)-F- $\mathbf{n} > (P)$ -D- $\mathbf{n}$  and (P)-bD- $\mathbf{n} > (P)$ -DF- $\mathbf{n}$ , (P)-FD- $\mathbf{n}$ , and (P)-S- $\mathbf{n}$ . This observation can be explained by the arrangement of soft/hard moieties. Large  $\pi$ -electron systems of helicene moieties are considered to be of soft nature, and therefore (P)-F- $\mathbf{n}$ , (P)-D- $\mathbf{n}$ , and (P)-bD- $\mathbf{n}$  have an alternating arrangement of soft helicene moieties and hard or relatively hard m-phenylene moieties, which form

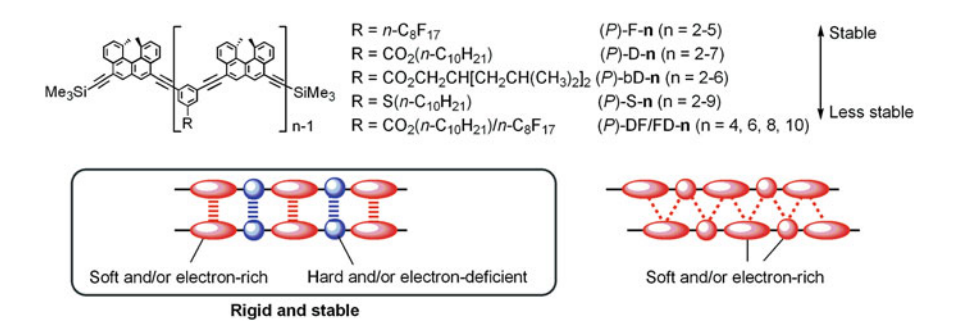


Fig. 3.25 Summary of stabilities of homo-double helices and proposed effect of side chains

stable homo-double helices. In contrast, (P)-S- $\mathbf{n}$  have soft arrays, the homo-double helices of which are less stable. The less stable nature of (P)-DF- $\mathbf{n}$  also suggests the importance of alternating arrangement: A regular alternating arrangement of soft/hard and electron-rich/deficient moieties can form a rigid aggregate (Fig. 3.25). At this stage, other possibilities that the order of stability is determined by the electronic nature of the m-phenylene moiety, and that electron-withdrawing side chains stabilize the aggregation cannot be excluded. This tendency was noted by other groups [9-12] and our group [13] in the case of arylene ethynylene macrocycles and a single helix [14].

It was shown that side chains have notable effects on the stability and structure of homo-double helices. Changing side chains can be an efficient method of obtaining a diversity of double helices.

#### References

- 1. Lahiri S, Thompson JL, Moore JS (2000) J Am Chem Soc 122:11315
- 2. Berl V, Huc I, Khoury RG, Krische MJ, Lehn J-M (2000) Nature 407:720
- 3. Berl V, Huc I, Khoury RG, Krische MJ, Lehn J-M (2001) Chem Eur J 7:2810
- 4. Haldar D, Jiang H, Légar J-M, Huc I (2007) Tetrahedron 63:6322
- 5. Haldar D, Jiang H, Légar J-M, Huc I (2006) Angew Chem Int Ed 45:5483
- 6. Pearson RG (1989) J Org Chem 54:1423
- Sugiura H, Nigorikawa Y, Saiki Y, Nakamura K, Yamaguchi M (2004) J Am Chem Soc 126:14858
- 8. Sugiura H, Yamaguchi M (2007) Chem Lett 36:58
- 9. Zhang J, Moore JS (1992) J Am Chem Soc 114:9701
- 10. Shetty AS, Zhang J, Moore JS (1996) J Am Chem Soc 118:1019
- 11. Tobe Y, Utsumi N, Kawabata K, Naemura K (1996) Tetrahedron Lett 37:9325
- 12. Tobe Y, Utsumi N, Nagano A, Naemura K (1998) Angew Chem Int Ed 37:1285
- 13. Sugiura H, Takahira Y, Yamaguchi M (2005) J Org Chem 70:5698
- 14. Goto H, Heemstra JM, Hill DJ, Moore JS (2004) Org Lett 6:889

# Chapter 4 Hetero-Double-Helix Formation of Pseudoenantiomeric Ethynylhelicene Oligomers

Hetero-double helices are an interesting group of compounds that exhibit various molecular functions in response to external stimuli. Their structural diversity is very high compared with that of homo-double helices, and various complexes can be obtained (Fig. 4.1). Whereas homo-double helices of n combinations are obtained using n compounds, hetero-double helices of  $n^2$  combinations are obtained using the same compounds. These complexes can have distinct pitch, length, and helicity. Selectivity is another notable feature of hetero-double helices. When oligomers with X and Y groups interact, the use of the homo-double-helix-method provides a mixture of XX, XY, and YY complexes. In contrast, the use of the hetero-double-helix-method provides an XY complex in a selective manner. Such diversity and selectivity can be utilized to control the properties and functions of double-helix-based materials.

For synthetic compounds to form hetero-double helices containing no metal coordination, an aromatic oligoamide and its *N*-oxide analogue [1], oligoresorcinol and oligosaccharide [2], *m*-terphenyl compounds with amidinium-carboxylate salt bridges [3–15], biphenol compound with phosphoric acid diesters [16], oligomers of heterocyclic hydrogen-bond donors and acceptors [17, 18], and fluoroquinoline and chloroquinoline oligomers [19] have recently been reported. However, when I started the present work, only a few hetero-double-helix-forming compounds were known [1–7], because of the difficulties in selectively forming complexes between two different oligomeric compounds. In the conventional examples, hydrogen bonds and salt bridges are used to make two complementary compounds aggregate. Since donor/acceptor interactions are used in such cases, it is not facile to obtain a diversity of hetero-double helices or to systematically study their properties because of structural limitation. In order to develop functional hetero-double helices and materials based on them, a methodology that can provide a diversity of hetero-double helices is needed.

In this chapter, I show a methodology of obtaining a diversity of hetero-double helices using pseudoenantiomeric ethynylhelicene oligomers, which are compounds containing enantiomeric (M) and (P) helicenes possessing different numbers of helicenes or different side chains (Fig. 4.2). In contrast to conventional methods, the present method employs  $\pi$ – $\pi$  interactions of helicenes but not donor/acceptor

	Homo-double helix	Hetero-double helix				
Combination	n Combinations by n compounds	$n^2$ Combinations by $n$ compounds				
Structure	385	Pitch Length Helicity				
Complexation	<b>&gt;-&gt;→ # # # * * * * * * * * * *</b>	<b>\}</b> + <b>\}</b> → <b>\</b> ⊗ \Y ⊗ \Y				
	Nonselective	Selective				

Fig. 4.1 Comparison between homo- and hetero-double helices

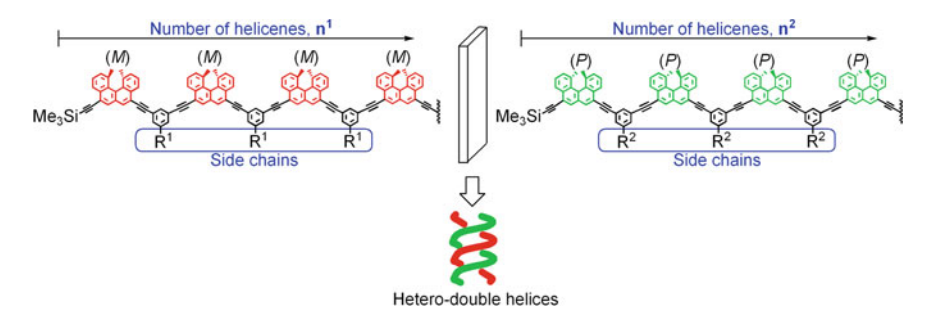


Fig. 4.2 Methodology of obtaining hetero-double helices employing pseudoenantiomeric ethynylhelicene oligomers

combination, which increased the diversity in the combination. In Chap. 2, the synthesis and homo-double-helix formation of ethynylhelicene oligomers with decyloxycarbonyl (D), branched alkyloxycarbonyl (bD), perfluorooctyl (F), and alternating decyloxycarbonyl/perfluorooctyl (DF or FD) side chains were described. It was then expected that a diversity of hetero-double helices can be obtained by taking two compounds from the list. In addition, a diversity of combination can be provided by changing the number of helicenes. I examined hetero-double-helix formation using the combinations of D/F, D/bD, and D/DF side chains.

# 4.1 (*P*)-D-5/(*P*)-F-5 Systems

Hetero-double-helix formation was examined using the pentamer (P)-D-5 or (M)-D-5 possessing decyloxycarbonyl side chains and the pentamer (P)-F-5 possessing perfluorooctyl side chains [20]. First, in order to study chiral recognition, combinations (P)-D-5/(P)-F-5 and (M)-D-5/(P)-F-5 were examined.

The aggregation of the (P)-D-5/(P)-F-5 system was examined in trifluoromethylbenzene. Solutions of (P)-D-5 and (P)-F-5 (2.5  $\times$  10<sup>-5</sup> M) were prepared and mixed in a 1:1 molar ratio at room temperature. The solution was then cooled to 5 °C, and the CD spectra were obtained within 30 min. Precipitate appeared in the solution of (P)-F-5 with cooling for longer than 30 min because of the low solubility of (P)-F-5, therefore the measurement was completed before the precipitation, which is noted as "within 30 min" in this work. When the solutions (2.5  $\times$  10<sup>-5</sup> M) were mixed, the total molar concentration of molecules in the mixed solution was 2.5  $\times$  10<sup>-5</sup> M, which is referred to here as "total 2.5  $\times$  10<sup>-5</sup> M".

The 1:1 mixture of (*P*)-D-5/(*P*)-F-5 (trifluoromethylbenzene, total  $2.5 \times 10^{-5}$  M, 5 °C) showed CD and UV-Vis spectra similar to the spectra obtained by adding the spectra of (*P*)-D-5 and (*P*)-F-5 (trifluoromethylbenzene,  $1.25 \times 10^{-5}$  M, 5 °C) called "calculated spectra" in this thesis. The results indicated no formation of hetero-complexes (Fig. 4.3a). Job plot experiments were carried out: the ratio of (*P*)-D-5 to (*P*)-F-5 was changed keeping the total concentration at  $2.5 \times 10^{-5}$  M, and the  $\Delta \varepsilon$  values at 330 and 365 nm were plotted against the mixing ratio. The plots were on approximate straight lines giving maxima of the  $\Delta \varepsilon$  values for pure (*P*)-D-5 and pure (*P*)-F-5 (Fig. 4.3b). It was therefore concluded that (*P*)-D-5 and (*P*)-F-5 did not form hetero-double helices.

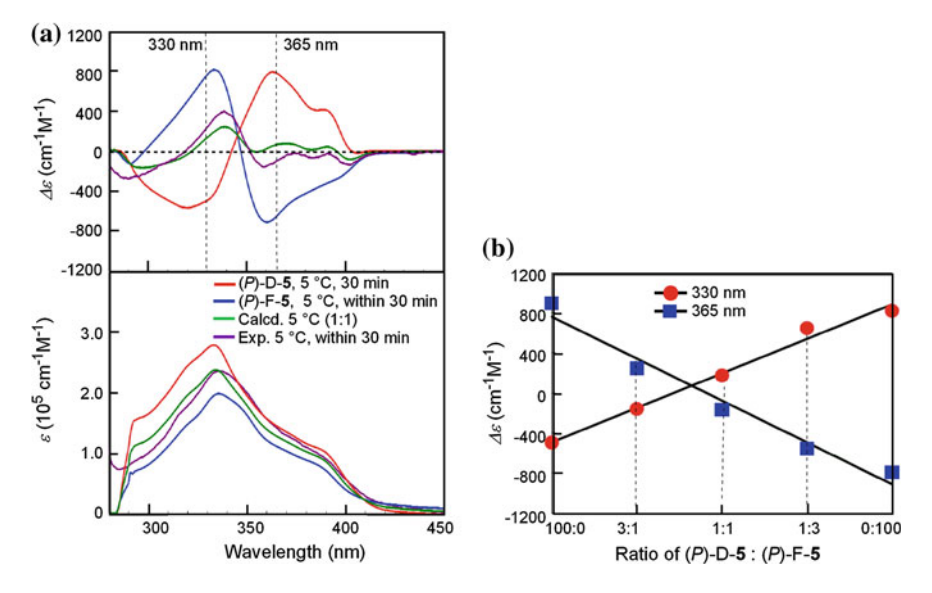
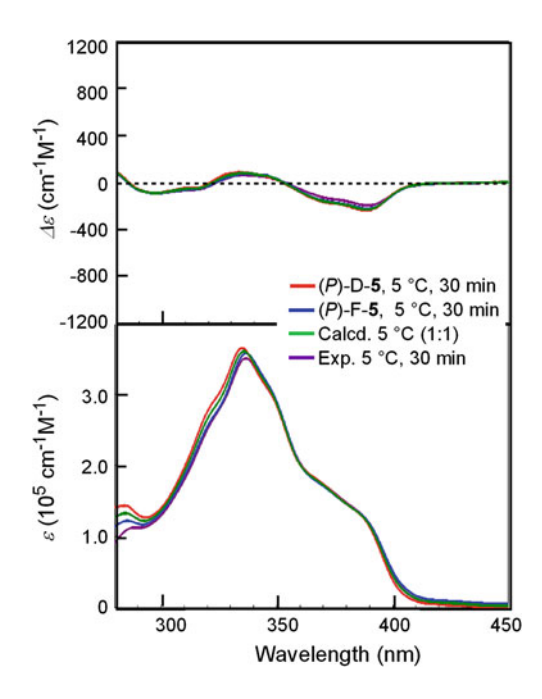


**Fig. 4.3** a CD (*top*) and UV-Vis (*bottom*) spectra of (*P*)-D-5, (*P*)-F-5 (trifluoromethylbenzene,  $1.25 \times 10^{-5}$  M, 5 °C), and 1:1 mixture of (*P*)-D-5/(*P*)-F-5 (trifluoromethylbenzene, total  $2.5 \times 10^{-5}$  M, 5 °C). The calculated spectra were obtained by adding the spectra of the components (trifluoromethylbenzene,  $1.25 \times 10^{-5}$  M, 5 °C) and dividing the total spectra by two. **b** Plots of  $\Delta\varepsilon$  at 330 nm and 365 nm (trifluoromethylbenzene, total  $2.5 \times 10^{-5}$  M, 5 °C) against ratio of (*P*)-D-5/(*P*)-F-5. Approximated *straight lines* are also shown

**Fig. 4.4** CD (*top*) and UV-Vis (*bottom*) spectra of (*P*)-D-5, (*P*)-F-5 (chloroform,  $5.0 \times 10^{-6}$  M, 5 °C), and a 1:1 mixture of (*P*)-D-5/(*P*)-F-5 (chloroform, total  $1.0 \times 10^{-5}$  M, 5 °C). The calculated spectra were obtained by adding the spectra of the components (chloroform,  $5.0 \times 10^{-6}$  M, 5 °C) and dividing the total spectra by two



Similar experiments were conducted in chloroform, which is a relatively weak helix-forming solvent for ethynylhelicene oligomers [21, 22] (See Chap. 3). CD and UV-Vis spectra (chloroform,  $5.0 \times 10^{-6}$  M, 5 °C) showed that both (*P*)-D-5 and (*P*)-F-5 were random coils (Fig. 4.4). When the 1:1 mixture of (*P*)-D-5/(*P*)-F-5 (chloroform, total  $1.0 \times 10^{-5}$  M, 5 °C) was cooled to 5 °C, it showed spectra similar to the calculated spectra (Fig. 4.4). It was concluded that (*P*)-D-5 and (*P*)-F-5 formed no hetero-double-helix regardless of the solvent.

# 4.2 (M)-D-5/(P)-F-5 Systems

Next, the combination of (M)-D-5 and (P)-F-5 was examined in trifluoromethylbenzene. (M)-D-5 is an enantiomer of (P)-D-5, and (M)-D-5 and (P)-F-5 contain enantiomeric helicenes. It is a notable feature of ethynylhelicene oligomers that chirality can change their interaction to form hetero-complexes. In the following discussion, ethynylhelicene oligomers containing enantiomeric (M) and (P) helicenes with different numbers are referred to as "pseudoenantiomers".

Both (M)-D-5 and (P)-F-5 showed the CD and UV-Vis spectra of random coils in chloroform  $(2.5 \times 10^{-6} \text{ M}, 25 ^{\circ}\text{C})$  (Fig. 4.5a). Solutions of (M)-D-5 and (P)-F-5 (chloroform,  $5.0 \times 10^{-6} \text{ M})$  were prepared and mixed in a 1:1 ratio, which was then allowed to stand at 25 °C. The mixture after 30 min of mixing showed intense CD with a positive maximum at 326 nm and a negative maximum at 370 nm

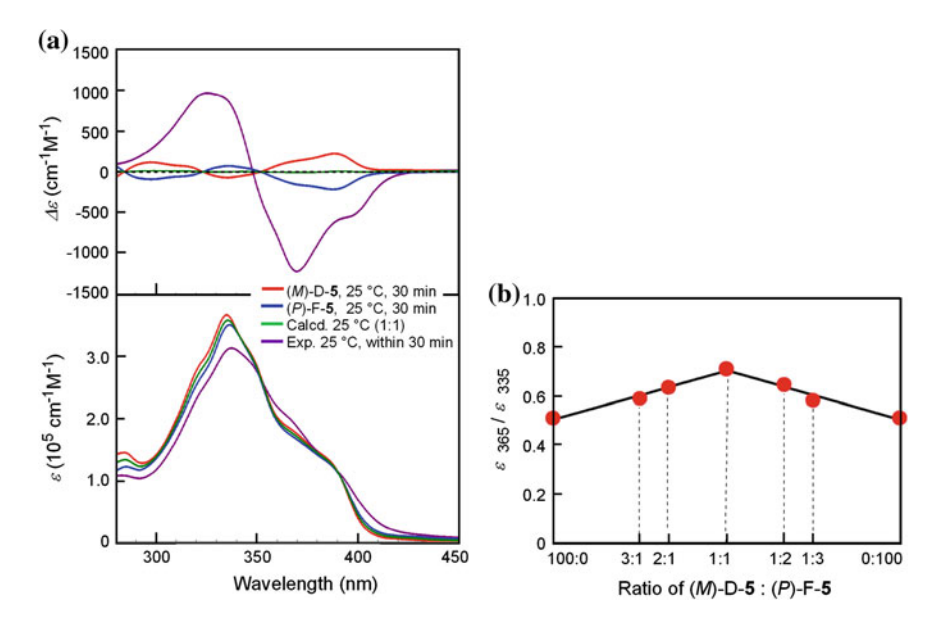


**Fig. 4.5 a** CD (*top*) and UV-Vis (*bottom*) spectra of (*M*)-D-5, (*P*)-F-5 (chloroform,  $2.5 \times 10^{-6}$  M, 25 °C), and 1:1 mixture of (*M*)-D-5/(*P*)-F-5 (chloroform, total  $5.0 \times 10^{-6}$  M, 25 °C). The calculated spectra were obtained by adding the spectra of the components (chloroform,  $2.5 \times 10^{-6}$  M, 25 °C). **b** Plot of  $\varepsilon_{365}/\varepsilon_{335}$  (chloroform, total  $5.0 \times 10^{-6}$  M, 25 °C, 30 min) against ratio of (*M*)-D-5/(*P*)-F-5. Approximated *straight lines* are also shown

(Fig. 4.5a, top). Since both (M)-D-5 and (P)-F-5 are random coils under these conditions (chloroform,  $5.0 \times 10^{-6}$  M, 25 °C), the calculated spectra show very small Cotton effects because of the enantiomeric nature of (M)-D-5 and (P)-F-5 (Fig. 4.5a). However, a 1:1 mixture of (M)-D-5 and (P)-F-5 provided a CD spectrum quite different from the calculated spectrum. The UV-Vis spectrum of the mixture was also different from the calculated one (Fig. 4.5a, bottom), and showed a decrease in  $\varepsilon$  at 335 nm and an increase in  $\varepsilon$  at 365 nm. The  $\varepsilon_{365}/\varepsilon_{335}$  value was 0.71, which was larger than the value of 0.51 of random coils. As will be noted later, the  $\varepsilon_{365}/\varepsilon_{335}$  values are approximately 0.5 in random coil states, and increase close to 1 when hetero-double helices are formed. The results indicated that a hetero-complex was formed in the (M)-D-5/(P)-F-5 system.

Job plot experiments (chloroform, total  $5.0 \times 10^{-6}$  M, 25 °C) gave a maximum of  $\varepsilon_{365}/\varepsilon_{335}$  value at a 1:1 ratio, which indicates the 1:1 stoichiometry of (*M*)-D-5 and (*P*)-F-5 (Fig. 4.5b). (*M*)-D-5/(*P*)-F-5 formed a chiral 1:1 complex, which was considered to be a hetero-double-helix.

The 1:1 mixture of (M)-D-5/(P)-F-5 (chloroform, total  $5.0 \times 10^{-6}$  M, 25 °C) gave a precipitate after 2 h, which was accompanied by decreases in the CD and UV-Vis intensities [20]. The precipitate isolated by centrifugation showed Cotton effects similar to that in chloroform solution [20]. The precipitate is suggested to be an assembly of the hetero-double helices.

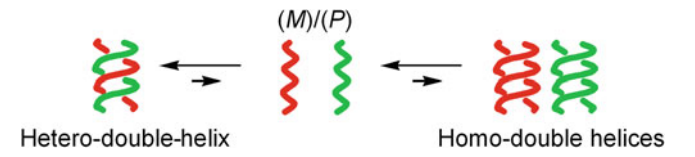


Fig. 4.6 Hetero-double-helix formation by pseudoenantiomeric (M)-D-5 and (P)-F-5

Pseudoenantiomeric (*M*)-D-5 and (*P*)-F-5 formed a hetero-double-helix, despite the fact that each (*P*)-D-5 and (*P*)-F-5 were random coils under these conditions. Therefore, hetero-double-helix formation is much stronger than homo-double-helix formation (Fig. 4.6). It was also observed that the hetero-double-helix tends to further assemble to form precipitates. Such properties of the hetero-double-helix are studied in the next section.

### 4.3 (M)-bD-4/(P)-D-5 Systems

An issue that had to be considered in the study of the (M)-D- $\mathbf{n}/(P)$ -D- $\mathbf{n}$  system was its tendency to form gels. Previously, our group reported that pseudoenantiomers form gels in toluene via higher aggregation [23, 24]. I considered that the gels are formed from hetero-double helices, and thus it is critical to examine a system that does not form a gel in order to analyze hetero-double-helix formation. It was expected that bulky bD side chains would reduce the interactions between hetero-double-helix complexes and the gel formation (Fig. 4.7). Among the combinations of the (M)-bD- $\mathbf{n}/(P)$ -bD- $\mathbf{n}$ , (M)-bD- $\mathbf{n}/(P)$ -D- $\mathbf{n}$  was found to be suitable for this purpose (See Chap. 5). Since it was also previously observed that combinations of different n values, particularly those smaller than 6, showed less tendency to form gels than combinations of the same  $\mathbf{n}$ , (M)-bD- $\mathbf{4}/(P)$ -D- $\mathbf{5}$  was used.

Solutions of (*M*)-bD-4 and (*P*)-D-5 (*m*-difluorobenzene,  $5.0 \times 10^{-4}$  M) were prepared and mixed in a 1:1 ratio at room temperature. The mixture remained transparent and homogeneous for at least 12 h. The CD spectra of a 1:1 mixture of

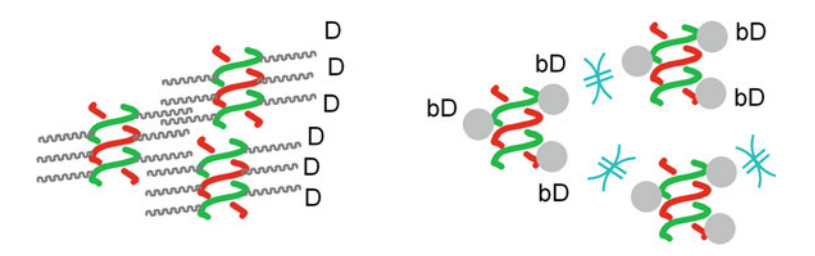


Fig. 4.7 Side chain effect on interaction between hetero-double-helix complexes

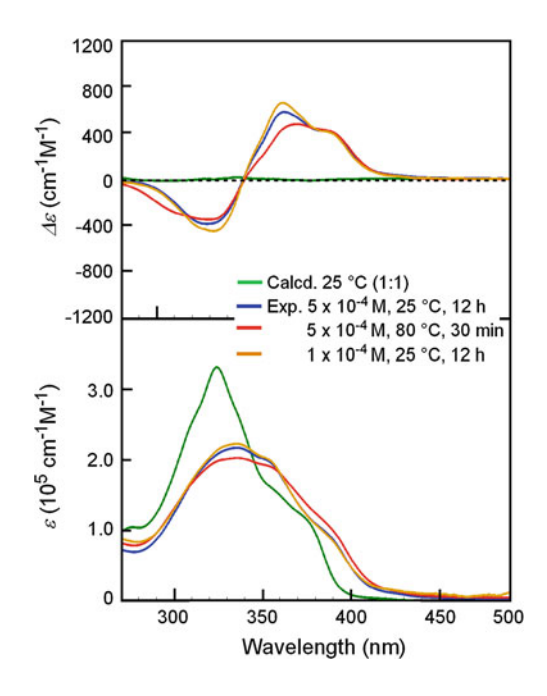
(*M*)-bD-4/(*P*)-D-5 (*m*-difluorobenzene, total  $5.0 \times 10^{-4}$  M, 25 °C) immediately showed enhanced Cotton effects, while the calculated spectrum showed very small Cotton effects. The intensity slightly decreased, reaching a steady state after 12 h with a negative maximum at 329 nm and a positive maximum at 371 nm (Fig. 4.8, top). The UV-Vis spectra (*m*-difluorobenzene, total  $5.0 \times 10^{-4}$  M, 25 °C) in the steady state showed an  $\varepsilon_{365}/\varepsilon_{335}$  value of 0.97 (Fig. 4.8, bottom), which was similar to that observed in the hetero-complex formation by the (*M*)-D-5/(*P*)-F-5 system. The CD and UV-Vis spectra (*m*-difluorobenzene, total  $5.0 \times 10^{-4}$  M) showed only a slight change with heating at 80 °C (Fig. 4.8). The results showed a strong heteroaggregate formation by (*M*)-bD-4/(*P*)-D-5 in *m*-difluorobenzene.

At a lower concentration of  $1.0 \times 10^{-4}$  M, the CD and UV-Vis spectra were similar to those at  $5.0 \times 10^{-4}$  M (Fig. 4.8). The small differences between the spectra at  $5.0 \times 10^{-4}$  and  $1.0 \times 10^{-4}$  M indicated that the equilibrium was shifted to the hetero-double-helix state at higher concentrations than  $1.0 \times 10^{-4}$  M.

Job plots (*m*-difluorobenzene, total  $5.0 \times 10^{-4}$  M, 35 °C) were obtained using  $\varepsilon_{365}/\varepsilon_{335}$  values, which indicated the 1:1 complex formation of (*M*)-bD-4 and (*P*)-D-5 (Fig. 4.9a).

The apparent molecular weight of the heteroaggregate was determined by VPO (m-difluorobenzene, 40 °C), taking advantage of the high solubility of (M)-bD-4/(P)-D-5 in this solvent:  $4.9 \times 10^3$  at  $5.0 \times 10^{-4}$  M and  $4.6 \times 10^3$  at  $1.0 \times 10^{-3}$  M (Fig. 4.9b). These values coincided with the calculated molecular weight of the heterodimer of (M)-bD-4/(P)-D-5, 4836.7: Bimolecular heteroaggregate formation was confirmed.

Fig. 4.8 CD (top) and UV-Vis (bottom) spectra of 1:1 mixture of (M)-bD-4/(P)-D-5 (m-difluorobenzene) at total concentration of  $5.0 \times 10^{-4}$  and  $1.0 \times 10^{-4}$  M. The calculated spectra were obtained by adding the spectra of the components (m-difluorobenzene,  $5.0 \times 10^{-4}$  M, 25 °C) and dividing the total spectra by two



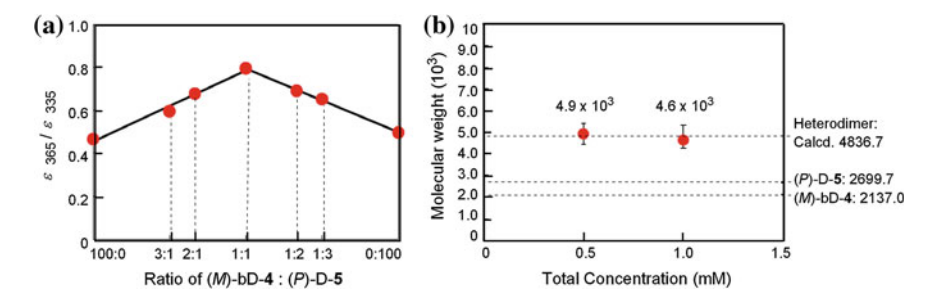


**Fig. 4.9** a Plot of  $\varepsilon_{365}/\varepsilon_{335}$  (*m*-diffuorobenzene, total 5.0  $\times$  10<sup>-4</sup> M, 35 °C) against ratio of (*M*)-bD-4/(*P*)-D-5. The plot were based on the UV-Vis data obtained after 30 min of mixing. Approximated *straight lines* are also shown. **b** Apparent molecular weight of heteroaggregate in 1:1 mixture of (*M*)-bD-4/(*P*)-D-5 (*m*-diffuorobenzene, 40 °C). The measurements were conducted between 30 min and 1 h after mixing. *Circles* represent the average of more than five measurements, and *vertical lines* represent the range of the obtained results. The *dashed lines* show the calculated molecular weights of (*M*)-bD-4, (*P*)-D-5, and their 1:1 complex

On the basis of the intense CD, change of UV-Vis absorption, 1:1 stoichiometry, and bimolecular aggregation determined by VPO, it was concluded that (M)-bD-4/(P)-D-5 formed a hetero-double-helix in m-difluorobenzene. The hetero-double-helix of the (M)-bD-4/(P)-D-5 system exhibited an  $\varepsilon_{365}/\varepsilon_{335}$  value close to 1, and  $\varepsilon_{365}/\varepsilon_{335}$  values are used to elucidate hetero-double-helix formation in the following discussions.

Note that (M)/(P) combinations form hetero-double helices that are much more stable than homo-double helices of (M)/(M) or (P)/(P) combinations. The substantial chiral recognition between pseudoenantiomers was consistent with the formation of three-dimensional chiral structures of hetero-double helices.

Also note that the (M)-D-5/(P)-F-5 system showed similar CD spectra to the (M)-bD-4/(P)-D-5 system, except for the inverted Cotton effects. The presence of two types of mirror-image CD spectrum can also be explained by the formation of a hetero-double-helix and its enantiomer. Among the synthetic hetero-double helices containing no metal coordination [1–19], this is a rare example employing neither hydrogen bonds [1, 16–19], salt bridges [3–15] as the driving force of aggregation.

The molecular structure of the (*M*)-tetramer/(*P*)-pentamer complex with side chains simplified to methoxycarbonyl groups was obtained by calculations using MacroModel 8.6 [25] in the MMFFs force field [26–30]. A double-helix structure was obtained as the energy-minimum structure (See Chap. 7), in which main chains were intertwined in cylindrical shape, and side chains protrude outside (Fig. 4.10). One turn of a double helix contained approximately three helicenes and three *m*-phenylenes, in accordance with the speculation obtained from the spectroscopic studies (Chap. 3, Fig. 3.7a). The aromatic rings stack in an offset manner. The diameter and length of that were 2.4 and 1.9 nm, respectively. In order to compare the structures of the hetero- and homo-double helices, calculations of the (*P*)-tetramer/

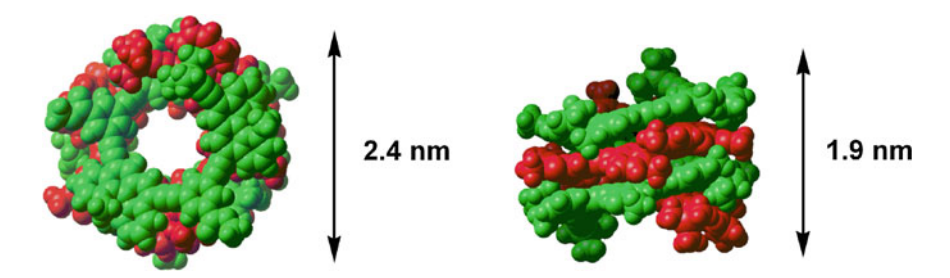


Fig. 4.10 Top view (left) and side view (right) of hetero-double-helix structure formed by (M)-tetramer/(P)-pentamer calculated using MacroModel 8.6 in MMFFs force field starting from loosely twisted right-handed structure. Side chains were simplified to CO<sub>2</sub>Me. The molecule is presented using a CPK model with red for the (M)-tetramer and green for the (P)-pentamer

(P)-pentamer complex with the same absolute configuration of helicenes was conducted. A double-helix structure was obtained (Fig. 4.11, right), which was similar to the (M)-tetramer/(P)-pentamer complex except for slight differences in the stacking mode of helicenes and in symmetry. The hetero-double-helix structure of the (M)-tetramer/(P)-pentamer is more symmetrical, and the stacking area is larger than that of the (P)-tetramer/(P)-pentamer, which might be related to the difference in stability: (M)/(P) hetero-double helices are more stable than (M)/(M) or (P)/(P) homodouble helices.

Also note that there was an obvious difference between (M)/(P) and (P)/(P) combinations with regard to higher aggregate formation, as indicated by the ready precipitation and gel formation of (M)/(P) combinations. This will be discussed in Chap. 5.

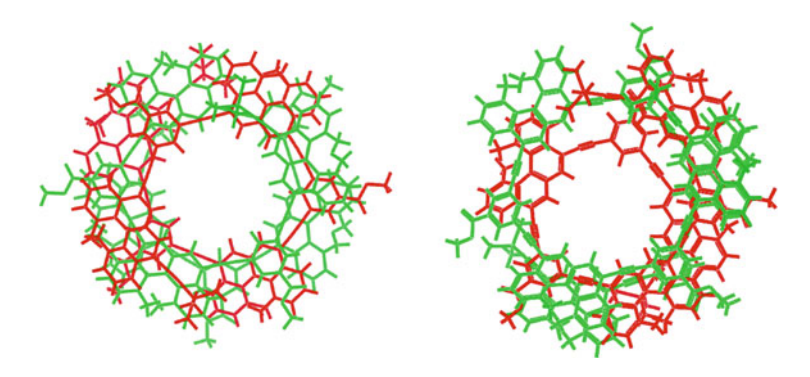


Fig. 4.11 Top view of double helices formed by (M)-tetramer/(P)-pentamer (left) and (P)-tetramer/(P)-pentamer (right) obtained using MacroModel 8.6 in MMFFs force field starting from loosely twisted left-handed structure. Side chains were simplified to  $CO_2Me$ . The molecule is presented using a wire model with red for the (M)- or (P)- tetramer, and green for the (P)-pentamer

## 4.4 (M)-D-n/(P)-DF-n Systems

The reversible structural change between hetero-double helices and random coils is an important property of double-helix-forming compounds, because it can be used to induce stimulus-responding switching. For example, length and flexibility change between cylindrical rigid hetero-double helices and long flexible random coils, and such molecules can be used to switch the properties of bulk materials. It should also be noted that such functions can be fine-tuned using combinations of compounds to form hetero-double helices.

Among known synthetic hetero-double helices, no reversible change has been observed with only one exception. Yashima showed that a hetero-double-helix polymer associating by amidinium-carboxylate salt bridges and its shorter analogue cause the structural change by repetitive additions of excess amounts of acid and base [8]. In contrast, the present system using pseudoenantiomeric oligomers changes the structure by thermal stimuli, and broad applications can be expected.

For this purpose, reversible structural changes of the following (M)-D- $\mathbf{n}$  ( $\mathbf{n}=4$ , 6, 8)/(P)-DF- $\mathbf{n}$  ( $\mathbf{n}=4$ , 6, 8) systems induced by heat were examined by changing the number of helicenes: (M)-D- $\mathbf{4}/(P)$ -DF- $\mathbf{4}$ , (M)-D- $\mathbf{4}/(P)$ -DF- $\mathbf{6}$ , (M)-D- $\mathbf{6}/(P)$ -DF- $\mathbf{6}$  systems (chlorobenzene, total  $5.0 \times 10^{-6}$  M). It is a notable feature of the hetero-double-helix formation of ethynylhelicene oligomers that the properties can be fine-tuned using a combination of compounds. Chlorobenzene was used as a solvent, which is a weak homo-double-helix-forming solvent for ethynylhelicene oligomers [21, 22] (See Chap. 3). It should also be noted that gels were not formed in this solvent at a concentration of  $5.0 \times 10^{-6}$  M.

Hetero-double-helix formation was examined using various (M)-D- $\mathbf{n}/(P)$ -DF- $\mathbf{n}$  combinations by mixing solutions of oligomers (chlorobenzene,  $5.0 \times 10^{-6}$  M) in a 1:1 ratio. Then, the mixtures were heated at 100 °C and cooled to 5 °C for 30 min for CD and UV-Vis analysis. The combinations of the (M)-D- $\mathbf{4}/(P)$ -DF- $\mathbf{4}$ , (M)-D- $\mathbf{4}/(P)$ -DF- $\mathbf{6}$ , (M)-D- $\mathbf{4}/(P)$ -DF- $\mathbf{8}$ , (M)-D- $\mathbf{6}/(P)$ -DF- $\mathbf{4}$ , and (M)-D- $\mathbf{8}/(P)$ -DF- $\mathbf{4}$  systems containing the tetramers did not form hetero-double helices and showed CD spectra with very weak Cotton effects at 5 °C (Fig. 4.12a). The aggregation of the combinations containing tetramers was too weak to form hetero-double helices under the conditions examined.

The combinations containing longer oligomers were then examined: (M)-D-8/(P)-DF-8, (M)-D-8/(P)-DF-6, (M)-D-6/(P)-DF-8, and (M)-D-6/(P)-DF-6 systems (chlorobenzene, total 5.0  $\times$  10<sup>-6</sup> M). Each of these oligomers were random coils under the conditions examined (chlorobenzene, 5.0  $\times$  10<sup>-6</sup> M).

A 1:1 mixture of (M)-D-8/(P)-DF-8 (chlorobenzene, total  $5.0 \times 10^{-6}$  M) was prepared and cooled to 5 °C for 30 min, which showed an enhanced Cotton effects in the CD spectra and an increase in the  $\varepsilon_{365}/\varepsilon_{335}$  value in the UV-Vis spectra to 1.3 (Fig. 4.13a). The CD and UV-Vis spectra only slightly changed with heating at 100 °C for 30 min, and an  $\varepsilon_{365}/\varepsilon_{335}$  value of 1.2 was obtained at 100 °C

**Fig. 4.12** CD spectra of 1:1 mixture of (M)-D-4/(P)-DF-4, (M)-D-4/(P)-DF-6, (M)-D-4/(P)-DF-8, (M)-D-6/(P)-DF-4, and (M)-D-8/(P)-DF-4 (chlorobenzene, total  $5.0 \times 10^{-6}$  M, 5 °C, 30 min)

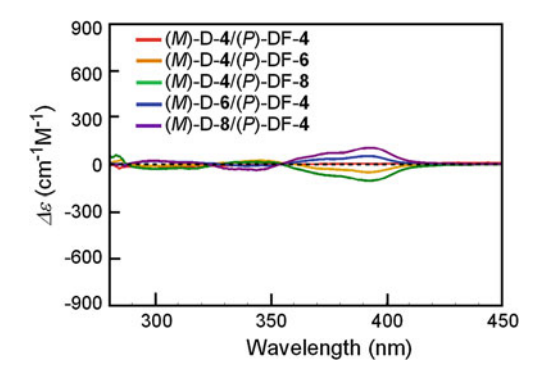


(Fig. 4.13a). Once the hetero-double-helix was formed at 5 °C, it did not unfold to random coils.

The (M)-D-8/(P)-DF-6, (M)-D-6/(P)-DF-8, and (M)-D-6/(P)-DF-6 systems showed similar results with  $\varepsilon_{365}/\varepsilon_{335}$  values of 1.0 at 5 °C. Their responses to heating, however, were different. At 100 °C, these systems showed decreases in  $\varepsilon_{365}/\varepsilon_{335}$  value to 0.61, 0.59, and 0.56, respectively (Fig. 4.13b–d, bottom). The decrease in the  $\varepsilon_{365}/\varepsilon_{335}$  value from ca. 1 to ca. 0.5 indicated unfolding to random coils.

Job plot experiments (chlorobenzene, total  $5.0 \times 10^{-6}$  M) using the  $\varepsilon_{365}/\varepsilon_{335}$  values obtained in the (M)-D-6/(P)-DF-6 system gave a maximum of  $\varepsilon_{365}/\varepsilon_{335}$  value at a 1:1 ratio at 5 °C, while the plot was linear and constant at 100 °C (Fig. 4.14). The results are consistent with the hetero-double-helix formation at 5 °C and unfolding to random coils at 100 °C. Similar results were obtained using the (M)-D-8/(P)-DF-6 and (M)-D-6/(P)-DF-8 systems (chlorobenzene, total  $5.0 \times 10^{-6}$  M, 5 °C), and hetero-double helices were also formed in these systems.

Using the above systems, reversible switching between hetero-double helices and random coils was attained. The (M)-D-6/(P)-DF-8 and (M)-D-6/(P)-DF-6 systems showed highly reproducible and reversible structural changes induced by heating at 100 °C and cooling at 5 °C for 30 min, as shown by the change in  $\Delta \varepsilon$  at 370 nm, which changed between -24/-2600 and +0.7/-2700, respectively (Fig. 4.15a). (M)-DF-8/(P)-D-6 also showed a reversible change in the repeating cycles of heating/cooling every 30 min, but the change was less reversible because of the slowness of the structural change (Fig. 4.15b).

The side chain and number of helicenes have significant effects on the stability of hetero-double helices (Fig. 4.16): The hetero-double helices of the combinations containing tetramers were unstable under the conditions examined. The combinations containing hexamers and octamers formed stable hetero-double helices, but the thermal stability and the rate of the structural change differed depending on the combination. A reversible and reproducible structural change

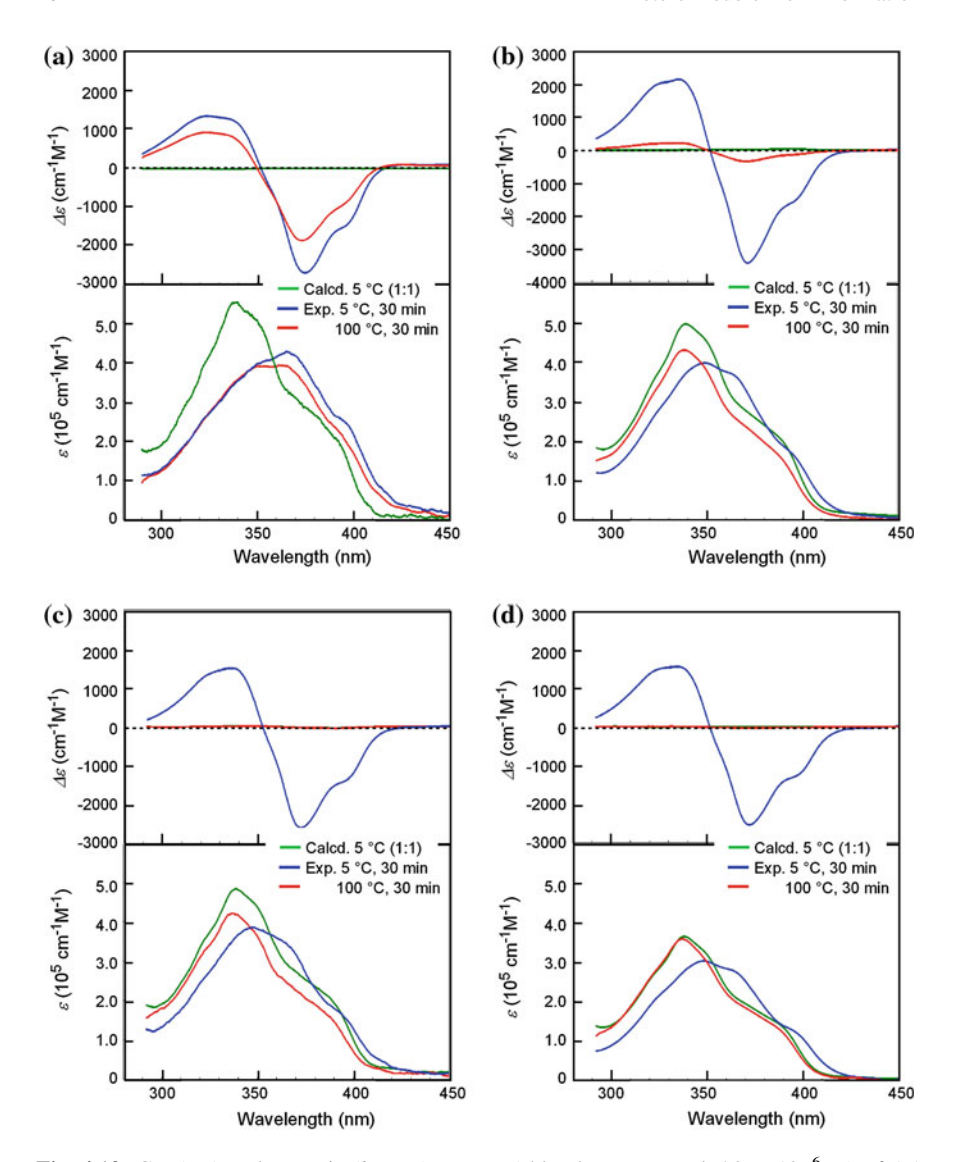


**Fig. 4.13** CD (*top*) and UV-Vis (*bottom*) spectra (chlorobenzene, total  $5.0\times10^{-6}$  M) of 1:1 mixtures of **a** (*M*)-D-**8**/(*P*)-DF-**8**, **b** (*M*)-D-**8**/(*P*)-DF-**6**, **c** (*M*)-D-**6**/(*P*)-DF-**8**, and **d** (*M*)-D-**6**/(*P*)-DF-**6** systems

between hetero-double helices and random coils by thermal stimuli was attained using the (M)-D-6/(P)-DF-8 and (M)-D-6/(P)-DF-6 systems. The methodology can be used to fine-tune the dynamic properties of hetero-double helices.

4.5 Summary 41

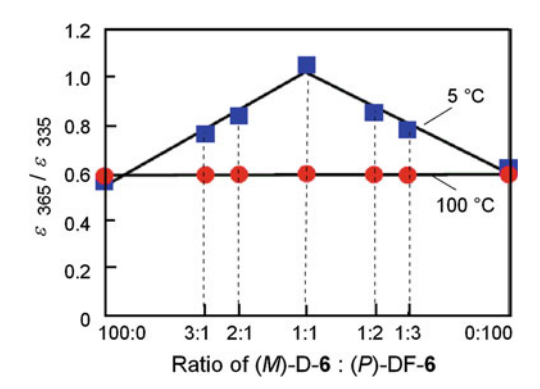


**Fig. 4.14** Plots of  $\varepsilon_{365}/\varepsilon_{335}$  (chlorobenzene, total  $5.0 \times 10^{-6}$  M) against ratio of (*M*)-D-6/(*P*)-DF-6. The plots were based on the UV-Vis data obtained after 30 min of mixing. Approximated *straight lines* are also shown

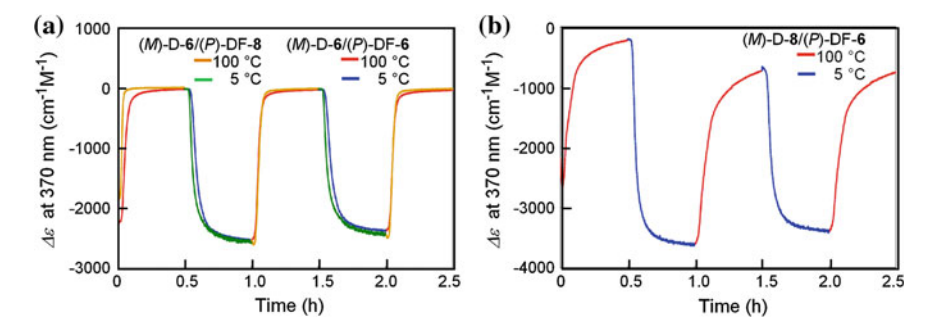


**Fig. 4.15**  $\Delta \varepsilon$  at 370 nm/time profiles (chlorobenzene, total  $5.0 \times 10^{-6}$  M) of 1:1 mixtures of **a** (*M*)-D-**6**/(*P*)-DF-**8**, (*M*)-D-**6**/(*P*)-DF-**6**, and **b** (*M*)-D-**8**/(*P*)-DF-**6** systems for repeating cycles of 100 /5 °C every 30 min

# 4.5 Summary

Pseudoenantiomeric (M)/(P) combinations of ethynylhelicene oligomers formed hetero-double helices, which are more stable than homo-double helices of (M)/(M) or (P)/(P) combinations. Side chains and number of helicenes had significant effects on the properties of hetero-double helices. Bimolecular hetero-double-helix formation was confirmed using the (M)-bD-4/(P)-D-5 system without forming higher assemblies. A reversible structural change between hetero-double helices and random coils was attained using the (M)-D-6/(P)-DF-8 and (M)-D-6/(P)-DF-6 systems. The methodology of fine-tuning the properties of hetero-double helices by combinations of compounds provided a diversity of hetero-double helices (Fig. 4.17).

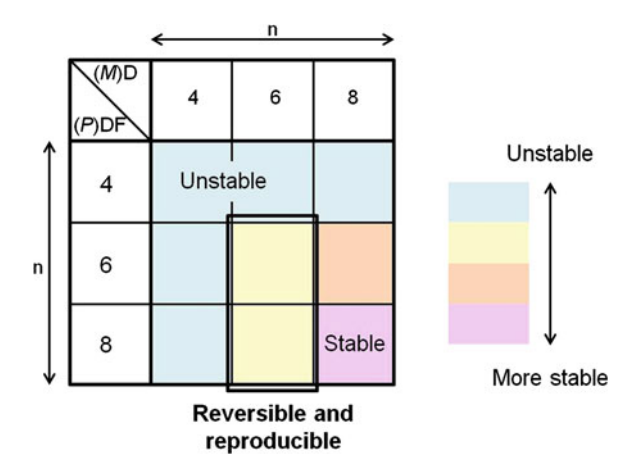


Fig. 4.16 Summary of stability of hetero-double helices formed by (M)-D- $\mathbf{n}/(P)$ -DF- $\mathbf{n}$  systems

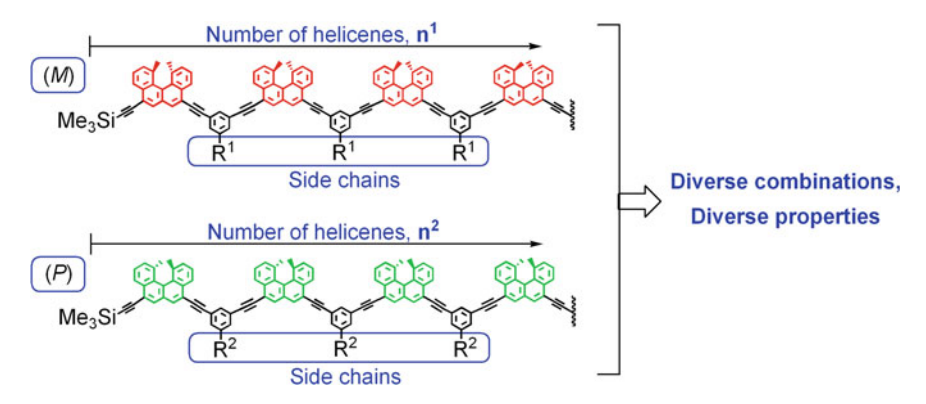


Fig. 4.17 Methodology of obtaining a diversity of hetero-double helices by changing combination of compounds

#### References

- 1. Zhan C, Léger JM, Huc I (2006) Angew Chem Int Ed 45:4625
- 2. Goto H, Furusho Y, Yashima E (2007) J Am Chem Soc 129:9168
- 3. Tanaka Y, Katagiri H, Furusho Y, Yashima E (2005) Angew Chem Int Ed 44:3867
- 4. Ikeda M, Tanaka Y, Hasegawa T, Furusho Y, Yashima E (2006) J Am Chem Soc 128:6806
- 5. Furusho Y, Tanaka Y, Yashima E (2006) Org Lett 8:2583
- 6. Hasegawa T, Furusho Y, Katagiri H, Yashma E (2007) Angew Chem Int Ed 46:5885
- 7. Furusho Y, Tanaka Y, Maeda T, Ikeda M, Yashima E (2007) Chem Commun 43:3174
- 8. Maeda T, Furusho Y, Sakurai SI, Kumaki J, Okoshi K, Yashima E (2008) J Am Chem Soc 130:7938
- 9. Ito H, Furusho Y, Hasegawa T, Yashima E (2008) J Am Chem Soc 130:14008
- 10. Yamada H, Furusho Y, Ito H, Yashima E (2010) Chem Commun 46:3487

References 43

- 11. Wu Z-Q, Furusho Y, Yamada Y, Yashima E (2010) Chem Commun 46:8962
- 12. Iida H, Shimoyama M, Furusho Y, Yashima E (2010) J Org Chem 75:417
- 13. Ito H, Ikeda M, Hasegawa T, Furusho Y, Yashima E (2011) J Am Chem Soc 133:3419
- 14. Yamada H, Furusho Y, Yashima E (2012) J Am Chem Soc 134:7250
- 15. Yamada H, Wu Z-Q, Furusho Y, Yashima E (2012) J Am Chem Soc 134:9506
- 16. Yamada H, Maeda K, Yashima E (2009) Chem Eur J 15:6794
- 17. Wang H-B, Mudrabovine BP, Li J, Wisner JA (2010) Chem Commun 46:7343
- 18. Wang HB, Mudraboyina PB, Wisner JA (2012) Chem Eur J 18:1322
- 19. Gan O, Li F, Li G, Kauffmann B, Xiang J, Huc I, Jiang H (2010) Chem Commun 46:297
- 20. Amemiya R, Saito N, Yamaguchi M (2008) J Org Chem 73:7137
- Sugiura H, Nigorikawa Y, Saiki Y, Nakamura K, Yamaguchi M (2004) J Am Chem Soc 126:14858
- 22. Sugiura H, Yamaguchi M (2007) Chem Lett 36:58
- 23. Amemiya R, Mizutani M, Yamaguchi M (2010) Angew Chem Int Ed 49:1995
- 24. Saito N, Shigeno M, Yamaguchi M (2012) Chem Eur J 18:8994
- Mahamadi F, Richards NGJ, Guida WC, Liskamp R, Lipton CC, Chang G, Hendrickson T, Still WC (1990) J Compt Chem 11:440
- 26. Halgren TA (1996) J Compt Chem 17:490
- 27. Halgren TA (1996) J Compt Chem 17:520
- 28. Halgren TA (1996) J Compt Chem 17:553
- 29. Halgren TA, Nachbar RB (1996) J Compt Chem 17:587
- 30. Halgren TA (1996) J Compt Chem 17:616

# Chapter 5 Higher-Assembly Formation of Pseudoenantiomeric Ethynylhelicene Oligomers

In biological systems, molecules form nanoscale assemblies, organelles, and cells in a step-by-step manner, in which fibers and vesicles are fundamental three-dimensional molecular assemblies. For example, actin proteins form filaments, which further assemble to form muscles; tubulin proteins form dimers, which aggregate to form a protofilament and then a microtubule. Biological cells are vesicles that contain various vesicular organelles such as liposomes and nuclei. Then, the development of such elaborate assembled systems of fibers and vesicles using synthetic molecules is an interesting subject for understanding biological functions and creating novel functional materials [1–3].

An issue that needs to be considered in assembly formation of synthetic compounds is the driving force for association and the diversity of substances. Synthetic amphiphilic compounds [4–19] and amide compounds including peptides [20-34] are known to assemble into both fibers and vesicles. Hydrophobic interactions, electrostatic interactions, and hydrogen bonds are the predominant driving forces of forming these assemblies. These systems, however, are generally sensitive, and subtle changes in the component structure and external stimuli such as solvent, temperature, and concentration can often cause the loss of assemblyforming abilities. Therefore, it is not facile to systematically obtain a diversity of closely related assemblies. To obtain an assembled system with the desired structures and properties, the development of a methodology that can fine-tune the structures and properties of assemblies is needed. In this regard, assembly formation using non-amphiphilic/non-amide compounds was considered attractive, since the assemblies were expected to exhibit properties and the diversity not observed in the conventional systems. However, very little is known on the ability of such systems to form fibers and vesicles [35, 36].

In this chapter, I describe a methodology of forming two-component assemblies of fibers and vesicles employing pseudoenantiomeric ethynylhelicene oligomers, which are non-amphiphilic/non-amide compounds [37]. As described in Chap. 4, hetero-double helices formed by pseudoenantiomeric ethynylhelicene oligomers showed a strong tendency to form higher assemblies. I then considered it interesting to construct a higher assembly of hetero-double helices in a systematic manner and to construct a structure that responds to external stimuli (Fig. 5.1).

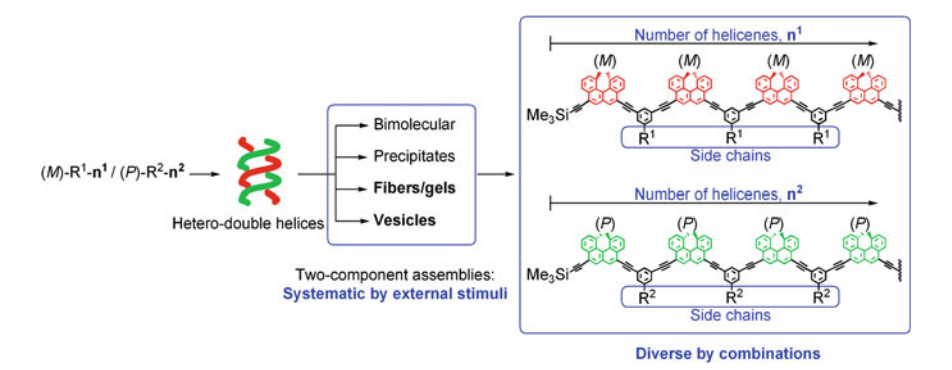


Fig. 5.1 Methodology of constructing a diversity of two-component assemblies by controlling the higher-assembly formation of hetero-double helices by external stimuli and combination of compounds

The driving forces in assembly formation, most likely  $\pi$ – $\pi$  interactions and van der Waals interactions, were different from those in conventional systems, and notable responses to external stimuli were observed. Also note that oligomers are modularly constructed by the repetition of structural units, and therefore have an intrinsic diversity. Thus, numerous derivatives can be systematically obtained by changing each unit such as the number of helicenes and the structure of side chains. In addition, a two-component method employing hetero-double helices further increases diversity (Fig. 5.1). Such systematic molecular assemblies have not been identified in conventional fiber- and vesicle-forming systems.

In Chap. 2, the synthesis of several series of optically active ethynylhelicene oligomers with decyloxycarbonyl (D) [38, 39], perfluorooctyl (F) [40], 4-methyl-2-(2-methylpropyl)-1-pentyloxycarbony (bD), decylsulfanyl (S), and alternating D and F (DF and FD) [41] side chains (Fig. 5.2) was described (See Chap. 2). In this chapter, several tetramer/pentamer systems were taken and studied: Assembly

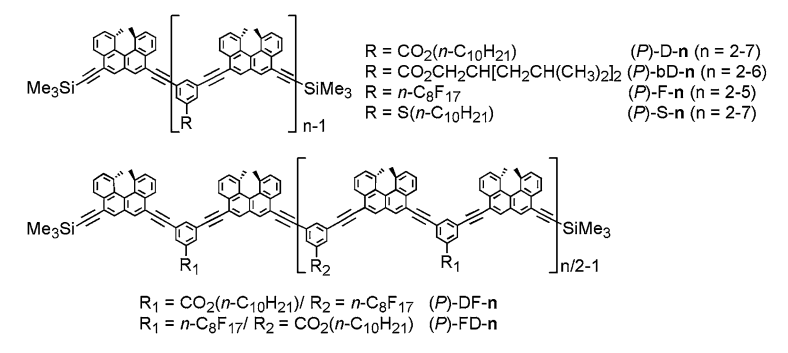


Fig. 5.2 Side chain analogues of ethynylhelicene oligomers

formation was examined using combinations of (M)-bD-4/(P)-bD-5, (M)-bD-4/(P)-D-5, (M)-D-5/(P)-DF-4.

#### 5.1 Fiber/Gel Formation in Toluene

When solutions (toluene,  $5.0 \times 10^{-4}$  M, 25 °C) of (M)-bD-4 and (P)-bD-5 were mixed in a 1:1 ratio, the vellow color of the mixture immediately turned deeper, and the solution became turbid within 10 min. Turbid partial gels were formed after 24 h. CD and UV-Vis studies were carried out using this system. Each solution of (M)-bD-4 and (P)-bD-5 showed the CD spectra of random coils, and the calculated spectra (See Chap. 7) obtained by adding these spectra and then dividing the total spectra by two showed a very small Cotton effect due to the pseudoenantiomeric nature of (M)-bD-4 and (P)-bD-5 (Fig. 5.3a). In contrast, the experimental CD spectra of the 1:1 mixture (toluene, total  $5.0 \times 10^{-4}$  M, 25 °C) immediately showed enhanced Cotton effects. Then the intensity slightly decreased, reaching a steady state after 3 h with a positive maximum at 320 nm and a negative maximum at 371 nm (Fig. 5.3a, top). The UV-Vis spectra (toluene, total  $5.0 \times 10^{-4}$  M, 25 °C) in the steady state showed an  $\varepsilon_{365}/\varepsilon_{335}$  value of 0.90 (Fig. 5.3a, bottom), which was typical of hetero-double-helix formation (See Chap. 4). These spectral features indicate that the gels are formed from hetero-double-helices. When the (M)-bD-4/ (P)-D-5 gel formed after 24 h was heated to 80 °C, the soft turbid gel turned to a less turbid and less viscous suspension, but was not fully transparent. The CD and UV-Vis spectra at 80 °C showed stronger Cotton effects and stronger absorption than those at 25 °C probably because of the increased transparency (Fig. 5.3a). The hetero-double-helix and higher assembly did not substantially dissociate at 80 °C.

The combination of (M)-bD-4/(P)-D-5 (toluene, total  $5.0 \times 10^{-4}$  M, 25 °C) was then examined. A deep-yellow color appeared immediately after mixing, and the solution became turbid. A turbid gel was formed after 24 h, which showed a CD with a negative maximum at 302 nm and a positive maximum at 402 nm (Fig. 5.3b, top). The UV-Vis spectra showed an  $\varepsilon_{365}/\varepsilon_{335}$  value of 0.82 (Fig. 5.3b, bottom). A hetero-double-helix formation was suggested, but the opaque nature of the mixture resulted in a weaker CD and lower UV–Vis intensities of the mixture than of (M)-bD-4/(P)-bD-5. When the (M)-bD-4/(P)-D-5 gel formed after 24 h was heated into 80 °C, the turbid soft gel turned to a less turbid suspension, and the spectra showed only a small change (Fig. 5.3b).

When the solutions (toluene,  $5.0 \times 10^{-4}$  M, 25 °C) of (*M*)-D-4 and (*P*)-D-5 were mixed in a 1:1 ratio, the resulting mixture immediately became deep yellow, forming a transparent gel after 6 h. The CD spectra gradually increased in intensity and reached a steady state after 18 h with a negative maximum at 337 nm and a positive maximum at 370 nm (Fig. 5.3c, top), and the UV-Vis spectra provided an  $\varepsilon_{365}/\varepsilon_{335}$  value of 0.95 (Fig. 5.3c, bottom). The gel changed into a transparent solution with heating to 80 °C, and the intensity of Cotton effect and the  $\varepsilon_{365}/\varepsilon_{335}$  value substantially decreased (Fig. 5.3c). The higher aggregates and hetero-double-helix of (*M*)-

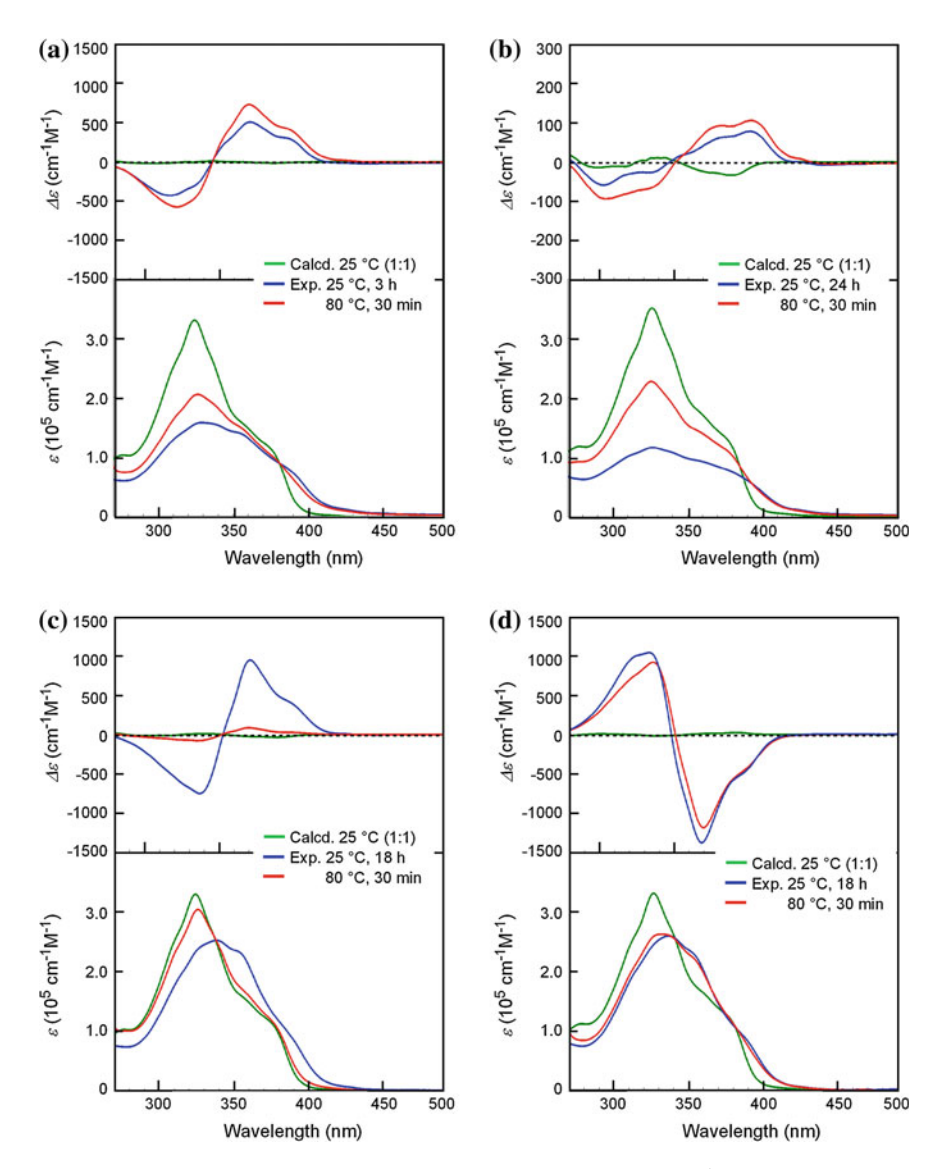


**Fig. 5.3** CD (*top*) and UV-Vis (*bottom*) spectra (toluene, total  $5.0 \times 10^{-4}$  M) of 1:1 mixtures of a (*M*)-bD-4/(*P*)-bD-5, b (*M*)-bD-4/(*P*)-D-5, c (*M*)-D-4/(*P*)-D-5, and d (*M*)-D-5/(*P*)-DF-4. The calculated spectra obtained by adding the spectra of the components (toluene,  $5.0 \times 10^{-4}$  M, 25 °C) and dividing the total spectra by two are also shown

D-4/(P)-D-5 considerably disaggregated to random coils with heating, and exhibited a lower thermal stability than those of the (M)-bD-4/(P)-bD-5 and (M)-bD-4/(P)-D-5 systems.

A 1:1 mixture (toluene,  $5.0 \times 10^{-4}$  M, 25 °C) of (*M*)-D-5 and (*P*)-DF-4 also formed a deep-yellow transparent gel after 24 h. The CD spectra reached a steady state after 18 h with a positive maximum at 333 nm and a negative maximum at 368 nm (Fig. 5.3d, top), and the UV-Vis spectra provided an  $\varepsilon_{365}/\varepsilon_{335}$  value of 0.93 (Fig. 5.3d, bottom). Cotton effects opposite to those of the above three combinations were obtained, which originated from the combination containing the pentamer with the (*M*) configuration. The gel changed into a slightly less viscous gel with heating to 80 °C, but the spectra showed only a small change (Fig. 5.3d). It is shown that the change in the combination of oligomers with different side chains can be used to fine-tune the thermal stability of gels.

Also note that the CD and UV-Vis spectra of all these combinations were similar to those of the hetero-double-helix formed by the (M)-bD-4/(P)-D-5 system (m-difluorobenzene,  $5.0 \times 10^{-4}$  M) (See Chap. 4). It was therefore concluded that these fibers/gels are formed from hetero-double helices.

Atomic force microscopy (AFM) images of four xerogels were obtained. The mixtures in a 1:1 ratio (toluene,  $1.0 \times 10^{-4}$  M) were heated at 110 °C for 3 min and allowed to stand at room temperature for 24 h, a portion of which was dropped on mica surfaces for AFM. Entangled fibrous networks of thin fibers partially forming thick bundles were observed (Fig. 5.4). The heights and widths of the thin fibers were about 5–80 nm, respectively, for all four gels. The results indicated a similar fiber formation of the four combinations. The images of the turbid gelforming (*M*)-bD-4/(*P*)-bD-5 and (*M*)-bD-4/(*P*)-D-5 systems showed more bundles than those of the transparent gel-forming (*M*)-D-4/(*P*)-D-5 and (*M*)-D-5/(*P*)-DF-4 systems.

Minimum gel-forming concentrations (MGCs) in toluene were compared using the (*M*)-bD- $\bf n$  (n = 2, 4, 6)/(*P*)-bD- $\bf n$  (n = 2-6), (*M*)-bD- $\bf n$  (n = 2, 4, 6)/(*P*)-D- $\bf n$  (n = 2-6), and (*M*)-D- $\bf n$  (n = 2, 4, 6)/(*P*)-D- $\bf n$  (n = 2-6) systems (Table 5.1). Two-component gels were formed with the oligomers possessing three or more helicenes. The result indicated a broad scope of the gel formation method using the pseudoenantiomeric oligomers. The MGCs of the combinations of (*M*)-bD- $\bf n$ /(*P*)-bD- $\bf n$  and (*M*)-bD- $\bf n$ /(*P*)-D- $\bf n$  were generally lower than that of (*P*)-D- $\bf n$ /(*M*)-D- $\bf n$ . For example, (*M*)-bD- $\bf n$ /(*P*)-bD- $\bf n$ , (*M*)-bD- $\bf n$ /(*P*)-bD- $\bf n$ , and 1.0 × 10<sup>-3</sup>, 5.0 × 10<sup>-4</sup>, and 1.0 × 10<sup>-4</sup> M, respectively. The branched side chains of (*P*)-bD- $\bf n$  tended to provide turbid gels and suppress the gel formation to some extent. The MGC of the (*M*)-D-5/(*P*)-DF-4 system was 1.0 × 10<sup>-4</sup> M.

All the combinations of (*M*)-bD-4/(*P*)-bD-5, (*M*)-bD-4/(*P*)-D-5, (*M*)-D-4/(*P*)-D-5, and (*M*)-D-5/(*P*)-DF-4 formed fibers/gels in toluene. CD and UV-Vis studies indicated that the fibers are considered to be formed from hetero-double helices. The macroscopic properties of the gels such as bundle formation, thermal stability, transparency, and MGC, differed depending on the combination of the compounds (Table 5.2). The properties of two-component gels can be fine-tuned by changing the side chain structure without losing gel-forming ability.

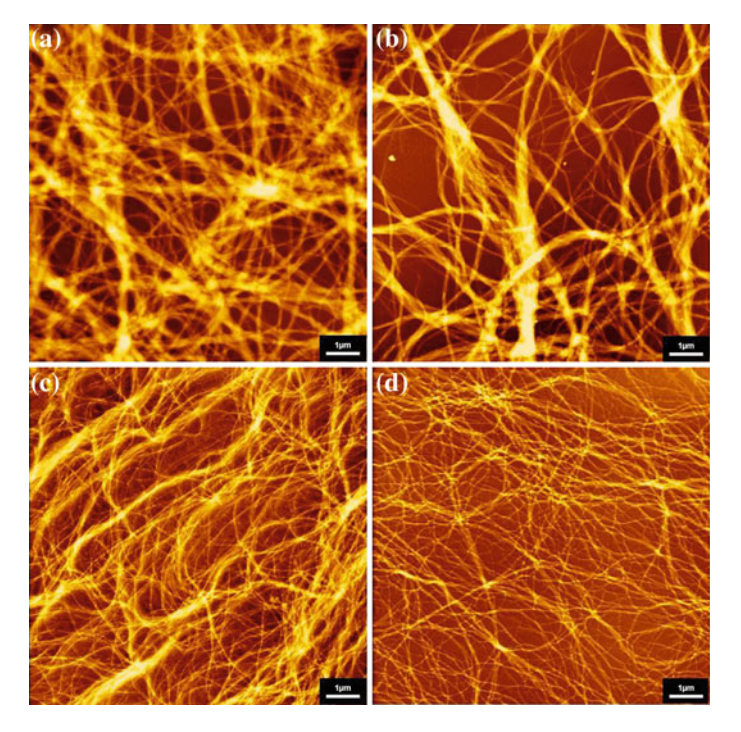


**Fig. 5.4** AFM height images of dried samples prepared from 1:1 mixtures (toluene, total  $1.0 \times 10^{-4}$  M) of **a** (*M*)-bD-4/(*P*)-bD-5, **b** (*M*)-D-4/(*P*)-bD-5, **c** (*M*)-D-4/(*P*)-D-5, and **d** (*M*)-D-5/(*P*)-DF-4 on mica surfaces. The samples were prepared after allowing the mixed solutions to stand at room temperature for 24 h. Scale bars:  $1.0 \times 10^{-6}$  m

**Table 5.1** MGCs ( $10^{-3}$  M) of (M)-bD- $\mathbf{n}'(P)$ -bD- $\mathbf{n}'$  (top), (M)-bD- $\mathbf{n}'(P)$ -D- $\mathbf{n}'$  (middle), and (M)-D- $\mathbf{n}'(P)$ -D- $\mathbf{n}'$  (bottom) examined in the range between total 0.1 mM and 10 mM at room temperature

(P)	n = 2		n = 3			n = 4		n = 5			n = 6				
	bD	D	D	bD	D	D	bD	D	D	bD	D	D	bD	D	D
(M)	bD	bD	D	bD	bD	D	bD	bD	D	bD	bD	D	bD	bD	D
n=2	С	С	С	S	S	S	S	S*	S*	S	S	S*	S	S*	S*
n = 4	S	S	S	2	2	5*	P	10	2	1	0.5	0.1*	1	0.5*	0.1*
n = 6															

C crystalline, S soluble at total 10 mM, Asterisks examined using the enantiomeric combination, Underbars a turbid gel was formed

# **5.2** Vesicle Formation in Diethyl Ether

Vesicular assembly was observed in diethyl ether, which was different from the fibers/gels in toluene. When solutions (diethyl ether,  $1.0 \times 10^{-4}$  M) were mixed in a 1:1 ratio, the mixtures of all the (*M*)-bD-4/(*P*)-bD-5, (*M*)-bD-4/(*P*)-D-5,

	(M)-bD- <b>4</b> / $(P)$ -bD- <b>5</b>	( <i>M</i> )-bD- <b>4</b> /( <i>P</i> )-D- <b>5</b>	(M)-D- $4/(P)$ -D- $5$	( <i>M</i> )-D-5/( <i>P</i> )-DF-4
$\varepsilon_{365}/\varepsilon_{335}$	0.9	0.82	0.95	0.93
Morphology	Fiber/gel	Fiber/gel	Fiber/gel	Fiber/gel
Bundles	Large amount	Large amount	Small amount	Small amount
Thermal stability	Stable	Stable	Less stable	Stable
Transparency	Turbid	Turbid	Clear	Clear
MGC	1 mM	0.5 mM	0.1 mM	0.1 mM
-				

Table 5.2 Comparison of properties of fibers/gels in four combinations

(*M*)-D-4/(*P*)-D-5, and (*M*)-D-5/(*P*)-DF-4 systems immediately turned deep yellow and semitransparent. Tyndall scattering was observed by passing laser light (532 nm) through the solutions, which indicated the formation of small particles. Soft precipitates, and not gel, appeared and gradually increased in amount.

The CD and UV-Vis spectra of (M)-bD-4 and (P)-bD-5 (diethyl ether,  $2.5 \times 10^{-5}$ M, 25 °C) were typical of a double helix and a random coil, respectively, and the calculated spectra showed relatively intense Cotton effects (Fig. 5.5a, top). The CD spectra of a 1:1 mixture of (M)-bD-4/(P)-bD-5 (diethyl ether, total  $2.5 \times 10^{-5}$  M, 25 °C) immediately showed an enhanced Cotton effects, which was different from the calculated spectrum. A steady state was reached after 3 h with a negative maximum at 315 nm and a positive maximum at 370 nm (Fig. 5.5a, top). The UV-Vis spectra also reached a steady state after 3 h, giving an  $\varepsilon$   $_{365}/\varepsilon$   $_{335}$  of 0.78 (Fig. 5.5a, bottom).

The (M)-bD-4/(P)-D-5 and (M)-D-4/(P)-D-5 systems (diethyl ether, total  $2.5 \times 10^{-5}$  M, 25 °C) also showed CD with Cotton effects with a negative maximum of approximately 330 and a positive maximum of approximately 370 nm in the steady state after 18 h and 3 h, respectively (Fig. 5.5b and c, top). The UV-Vis spectra showed increased  $\varepsilon_{365}/\varepsilon_{335}$  of 1.0 and 0.85, respectively (Fig. 5.5b and c, bottom). The low intensities of CD and UV-Vis are considered to be due to partial precipitation.

The (M)-D-5/(P)-DF-4 system (diethyl ether, total  $2.5 \times 10^{-5}$  M, 25 °C) showed similar UV-Vis spectra with an  $\varepsilon_{365}/\varepsilon_{335}$  value of 0.92, except for the Cotton effects with positive broad maxima ranging from 310 to 320 nm and a negative maximum at 370 nm, which is opposite to those of other systems (Fig. 5.5d).

CD and UV-Vis studies provided observations similar to the hetero-double helix formation of (M)-bD-4/(P)-D-5 (m-difluorobenzene,  $5.0 \times 10^{-4}$  M) (See Chap. 4), and therefore these vesicles are concluded to be formed from hetero-double helices.

Dynamic light scattering (DLS) studies of the 1:1 mixture using the (M)-bD-4/(P)-bD-5 system (diethyl ether, total 1.0  $\times$  10<sup>-4</sup> M, 25 °C) showed the presence of aggregates with a diameter of ca. 175 nm after 1 min of mixing, together with small particles of 0.7 nm diameter, probably random coils of (M)-bD-4 and (P)-bD-5. The small particles disappeared after 30 min, and the size of the large particles increased to reach a steady state with a diameter ca. 400 nm after 1 h (Fig. 5.6).

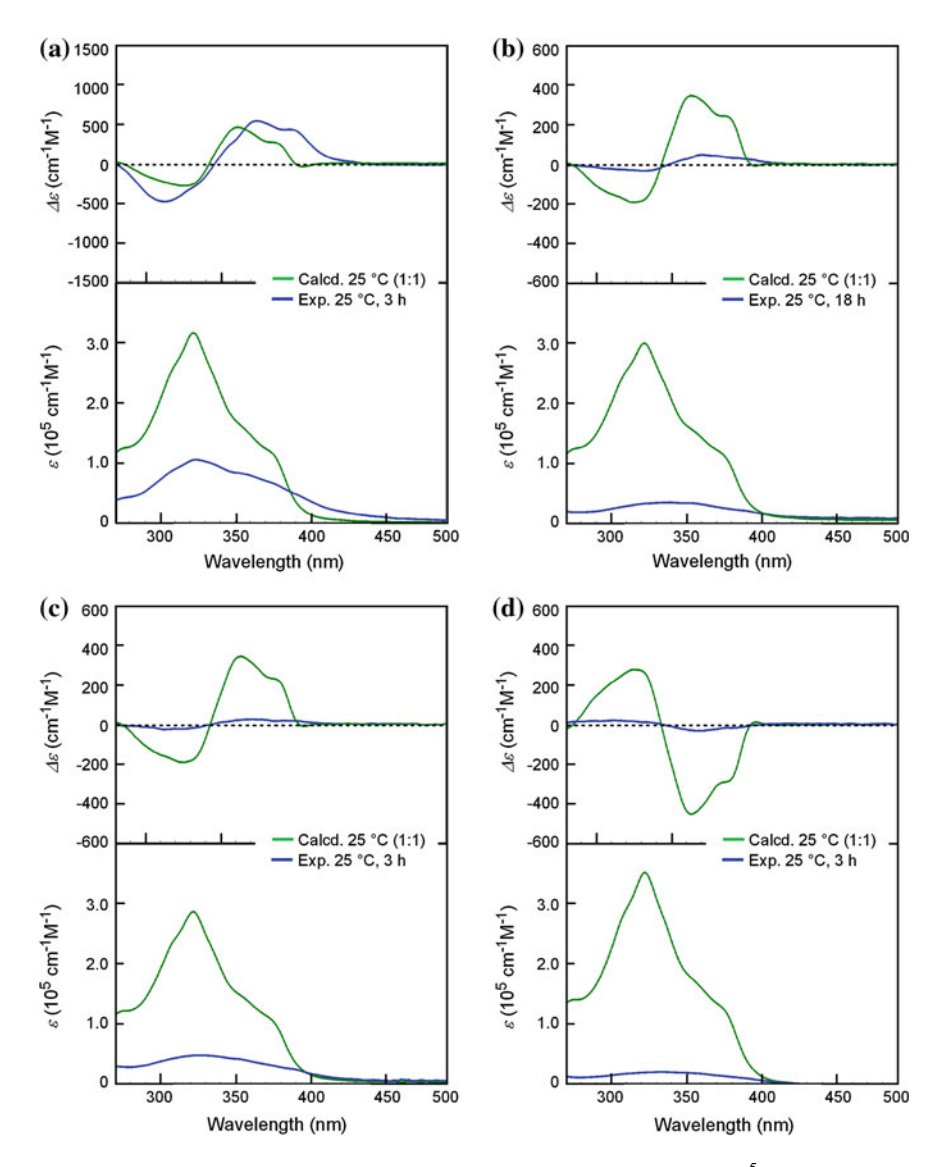
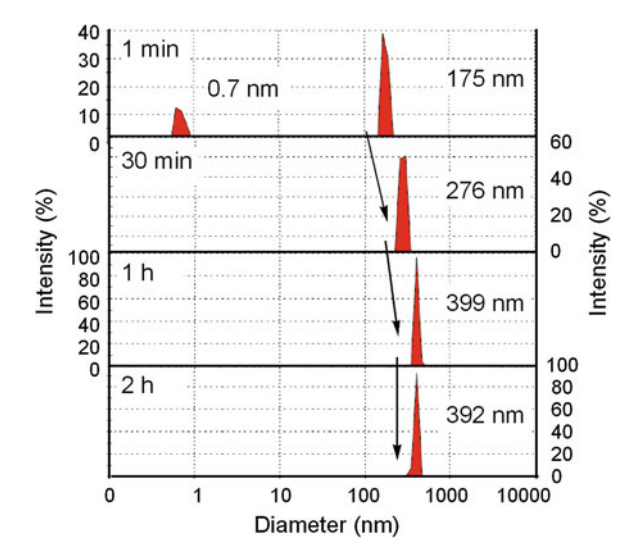


**Fig. 5.5** CD (*top*) and UV-Vis (*bottom*) spectra (diethyl ether, total  $2.5 \times 10^{-5}$  M, 25 °C) of 1:1 mixtures of **a** (*M*)-bD-4/(*P*)-bD-5, **b** (*M*)-bD-4/(*P*)-D-5, **c** (*M*)-D-4/(*P*)-D-5, and **d** (*M*)-D-5/(*P*)-DF-4. Calculated spectra obtained by adding the spectra of the components (diethyl ether,  $2.5 \times 10^{-5}$  M, 25 °C) and dividing the total spectra by two are also shown

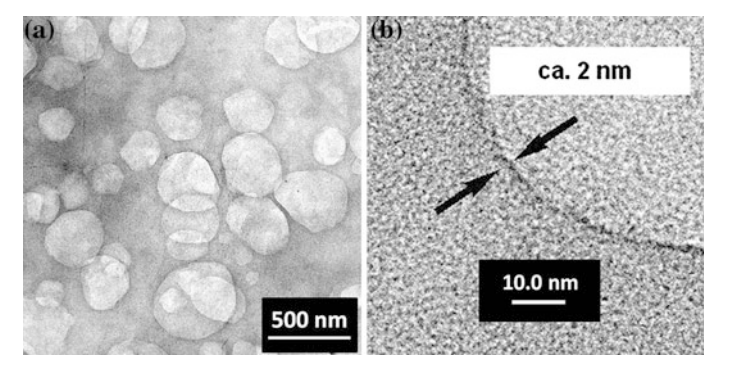
The morphologies of the aggregates in diethyl ether were determined by transmission electron microscopy (TEM). TEM image of a 1:1 mixture of (M)-bD-4/(P)-bD-5 (diethyl ether, total 1.0 × 10<sup>-4</sup> M, r.t., 1 h) showed spherical objects (Fig. 5.7a), and the contrast between the light internal region and the dark outer

Fig. 5.6 Diameter-intensity distribution of assemblies in 1:1 mixture of (M)-bD-4/(P)-bD-5 (diethyl ether, total  $1.0 \times 10^{-4}$  M, 25 °C) measured using DLS



edges indicated a hollow structure (Fig. 5.7a). The assemblies formed in diethyl ether were shown to be vesicles. The thickness of the exterior wall was estimated to be ca. 2 nm (Fig. 5.7b). Although two-component vesicles composed of amphiphilic compounds [5, 7, 42–48] and one-component vesicles composed of non-amphiphilic compounds [22, 27, 35, 36, 49–51] have been found, it should be noted that two-component vesicle formation by non-amphiphilic compounds is unprecedented.

The morphologies and sizes of the assemblies were determined by AFM and compared among the four combinations of (M)-bD-4/(P)-bD-5, (M)-bD-4/(P)-D-5, and (M)-D-5/(P)-DF-4. 1:1 mixtures (diethyl ether, total  $1.0 \times 10^{-4}$  M) were allowed to stand at room temperature for 1 h then gently



**Fig. 5.7 a** TEM images of dried sample prepared from 1:1 mixture of (M)-bD-4/(P)-bD-5 (diethyl ether, total  $1.0 \times 10^{-4}$  M). Scale bar: 500 nm. **b** Magnified TEM image of exterior part of the vesicle. Scale bar: 10.0 nm

stirred. A portion of each mixture was dropped on a freshly cleaved mica surface, and the solvent was removed under ambient pressure and then in vacuo. AFM images of all four systems showed spherical assemblies (Fig. 5.8a, c, and d). In the (M)-bD-4/(P)-bD-5 system, the average diameter and height of 126 particles were 108 and 15 nm, respectively. The diameter was considerably larger than the height of the particles (Fig. 5.8b). Such results were observed for vesicles, which indicated that vesicles were flattened on the surface owing to their hollow and soft nature [52-54]. The different average diameters obtained by AFM and DLS may be due to the difference between swollen and dried vesicles [44, 55, 56], (M)-bD-4/ (P)-D-5 and (M)-D- $\frac{4}{P}$ -D-5 systems showed similar images with diameters of 59 and 20 nm, and heights of 9.9 and 2.9 nm, respectively. These systems provided smaller particles with relatively broader distributions of vesicle sizes than the (M)bD-4/(P)-bD-5 system. The average sizes of vesicles were in the order of (M)-bD-4/(P)-bD-5 > (M)-bD-4/(P)-D-5 > (M)-D-4/(P)-D-5. Note that the AFM image of the (M)-D-5/(P)-DF-4 system (diethyl ether, total  $1.0 \times 10^{-4}$  M) showed large vesicles with an average diameter of 243 nm and a height of 14 nm, which had holes at the edge (Fig. 5.8e). Considering that the TEM image of a vesicle obtained in the (M)-D-5/(P)-DF-4 system (diethyl ether, total  $1.0 \times 10^{-4}$  M, r.t., 1 h) showed smooth vesicles without holes (Fig. 5.8f), the holes are likely to emerge when the relatively large and hydrophobic vesicles possessing perfluorooctyl moiety contact with the hydrophilic mica surface. This deformation property can be utilized for functions such as drug delivery and release.

Solvents had a notable effect on assembly formation, and all the combinations of (M)-bD-4/(P)-bD-5, (M)-bD-4/(P)-D-5, (M)-D-5, (M)-D-5, (M)-D-5, and (M)-D-5/(P)-DF-4 formed vesicles in diethyl ether, as shown by AFM and TEM studies. CD and UV–Vis studies indicated that the vesicles in diethyl ether as well as the fibers/gels in toluene are formed from hetero-double helices. In contrast, the macroscopic properties of the vesicles such as size and fragility differed depending on the combination (Table 5.3). The properties of two-component vesicles can be fine-tuned by changing the combination of oligomers.

Transformation from vesicles into fibers occurred with a solvent change, which was consistent with the higher-assembly formation from hetero-double helices. A soft precipitate of vesicles formed by (M)-bD-4/(P)-bD-5 in diethyl ether  $(1.0 \times 10^{-4} \text{ M}, \text{ r.t.}, 1 \text{ h})$  was isolated by centrifugation (6400 rpm, 10 min), and then toluene was added to the precipitate after washing it with the solvents (See Chap. 7). The residual soft substance was heated at 80 °C for 1 h and left to stand at r.t. for 3 h. The AFM images of a dried sample prepared in a similar manner showed fibrous aggregates (Fig. 5.9a), which were similar to the fibers formed by (M)-bD-4/(P)-bD-5 (Fig. 5.4a). This transformation was also analyzed using CD and UV-Vis spectra. When the precipitate was heated at 80 °C for 1 h, the CD spectrum of the mixture showed relatively weak Cotton effects with a negative maximum at 318 nm and a positive maximum at 368 nm (Fig. 5.9b, top), and the UV-Vis spectrum showed an  $\varepsilon_{365}/\varepsilon_{335}$  value of 0.62 (Fig. 5.9b, bottom). Both CD

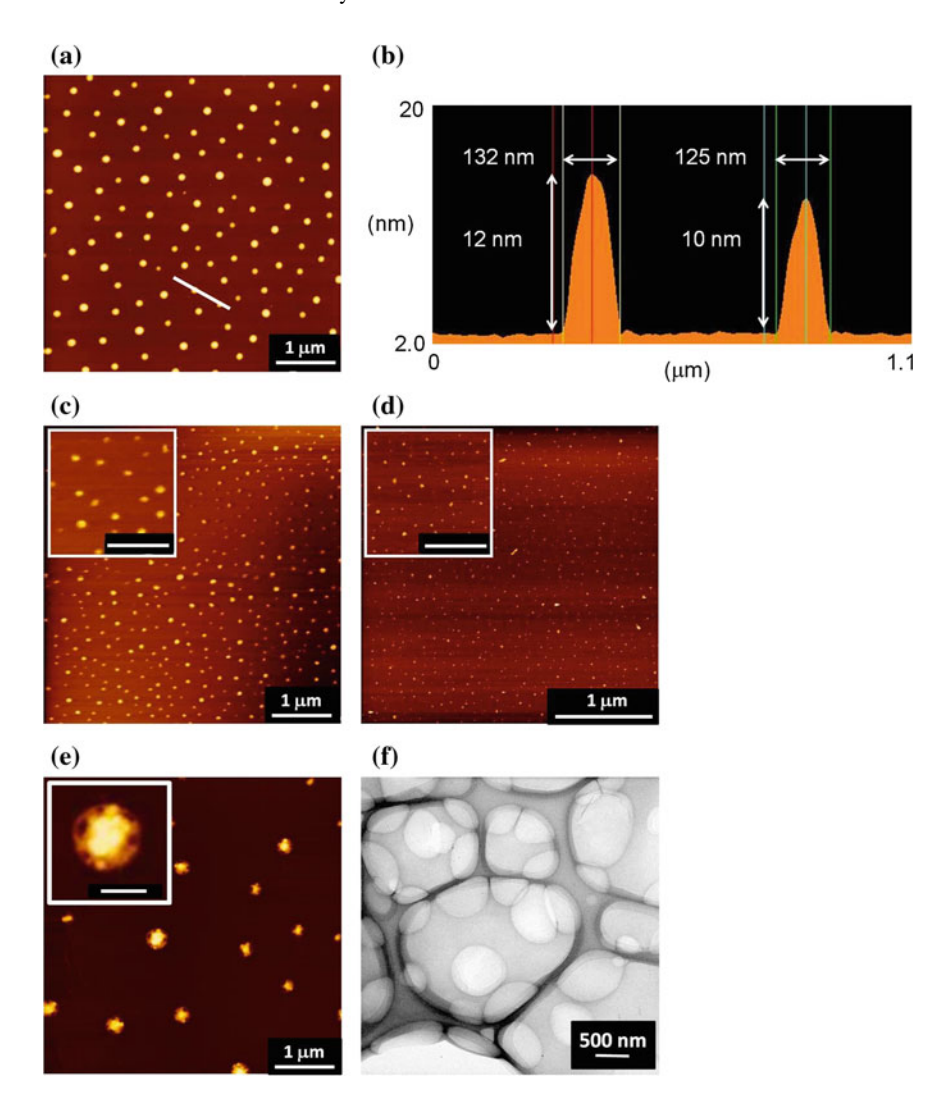


**Fig. 5.8** a AFM height image and **b** cross-sectional analysis at white line in (**a**) of dried sample prepared from 1:1 mixture of (M)-bD-4/(P)-bD-5 (diethyl ether, total  $1.0 \times 10^{-4}$  M). AFM height images of dried samples prepared from 1:1 mixtures of **c** (M)-bD-4/(P)-D-5, and **e** (M)-D-5/(P)-DF-4 (diethyl ether, total  $1.0 \times 10^{-4}$  M). Scale bars:  $1.0 \times 10^{-6}$  m (5.0  $\times 10^{-7}$  m in insets). **f** TEM image of dried sample prepared from 1:1 mixture of (M)-D-5/(P)-DF-4 (diethyl ether, total  $1.0 \times 10^{-4}$  M). Scale bars: 500 nm

and UV-Vis spectra were different from the calculated spectrum obtained by adding the spectra of (M)-bD-4 and (P)-bD-5 in random coil state (toluene, total  $1.0 \times 10^{-4}$  M, 80 °C, 30 min) (Fig. 5.9b). Vesicles are considered to dissociate

	( <i>M</i> )-bD- <b>4</b> /		( <i>M</i> )-bD- <b>4</b> /		(M)-D- <b>4</b> /	(M)-D- <b>5</b> /
	( <i>P</i> )-bD- <b>5</b>		( <i>P</i> )-D- <b>5</b>		(P)-D- <b>5</b>	(P)-DF- <b>4</b>
$\varepsilon_{365}/\varepsilon_{335}$	0.78		1		0.85	0.92
Morphology	Vesicle		Vesicle		Vesicle	Vesicle
Average diameter (nm)	108	>	59	>	20	243 (with holes)
Average diameter (nm)	15		9.9		2.9	14 (with holes)

**Table 5.3** Comparison of properties of vesicles in four combinations

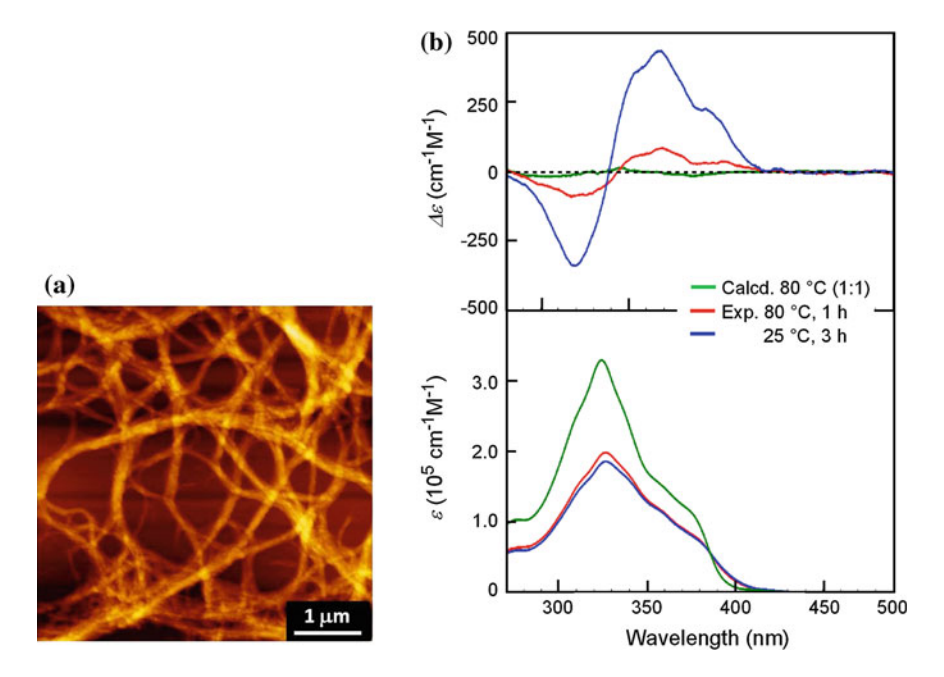


**Fig. 5.9 a** AFM height image of precipitate of (M)-bD-4/(P)-bD-5 (diethyl ether, total  $1.0 \times 10^{-4}$  M, r.t., 1 h) isolated by centrifugation, dissolved in toluene (total ca.  $1.0 \times 10^{-4}$  M, 80 °C, 1 h), and allowed to stand at r.t. for 3 h. Scale bar:  $1.0 \times 10^{-6}$  m. **b** CD (*top*) and UV-Vis (*bottom*) spectra of precipitate obtained in 1:1 mixture of (M)-bD-4/(P)-bD-5 (diethyl ether, total  $1.0 \times 10^{-4}$  M, r.t., 1 h) and then dissolved in toluene (total ca.  $1.0 \times 10^{-4}$  M, 80 °C, 1 h). The calculated spectrum of (M)-bD-4/(P)-bD-5 (toluene,  $1.0 \times 10^{-4}$  M, 80 °C, 30 min) is also shown

to hetero-double helices and random coils at 80 °C. After allowing the mixture to stand at 25 °C for 3 h, the CD showed the enhanced Cotton effects, and the  $\varepsilon_{365}/\varepsilon_{335}$  value increased to 0.65. The results indicated that the solvent exchange induced the morphological transition from vesicles to fibers via hetero-double helices and random coils.

# 5.3 Higher-Assembly Formation by Intercomplex Interactions

As discussed above, all the (M)-bD-4/(P)-bD-5, (M)-bD-4/(P)-D-5, (M)-D-4/(P)-D-5, and (M)-D-5/(P)-DF-4 systems formed fibers/gels in toluene and vesicles in diethyl ether. All four systems showed CD and UV-Vis spectra similar to those of the hetero-double-helix of (M)-bD-4/(P)-D-5 (m-difluorobenzene, total  $1.0 \times 10^{-4}$  M, 25 °C, 12 h) in both toluene (total  $1.0 \times 10^{-4}$  M, 25 °C) and diethyl ether (total  $2.5 \times 10^{-5}$  M, 25 °C), except for the inverted Cotton effects of the CD spectra of the (M)-D-5/(P)-DF-4 system originating from the combination containing the pentamer with the (M) configuration (Fig. 5.10). The results indicated that fibers/gels and vesicles were formed from hetero-double helices.

It should be noted that the TEM image of a vesicle obtained in the (M)-bD-4/(P)-bD-5 system (diethyl ether, total  $1.0 \times 10^{-4}$  M, r.t., 1 h) showed a wall thickness of ca. 2 nm (Fig. 5.7b). Then, the structure of vesicles could be related to the heterodouble-helix structure of (M)-bD-4/(P)-bD-5. Information on the length and height of the (M)-tetramer/(P)-pentamer complex with methoxycarbonyl side chains was obtained using MacroModel 8.6 [57] in the MMFFs force field [58–62] (Chap. 4,

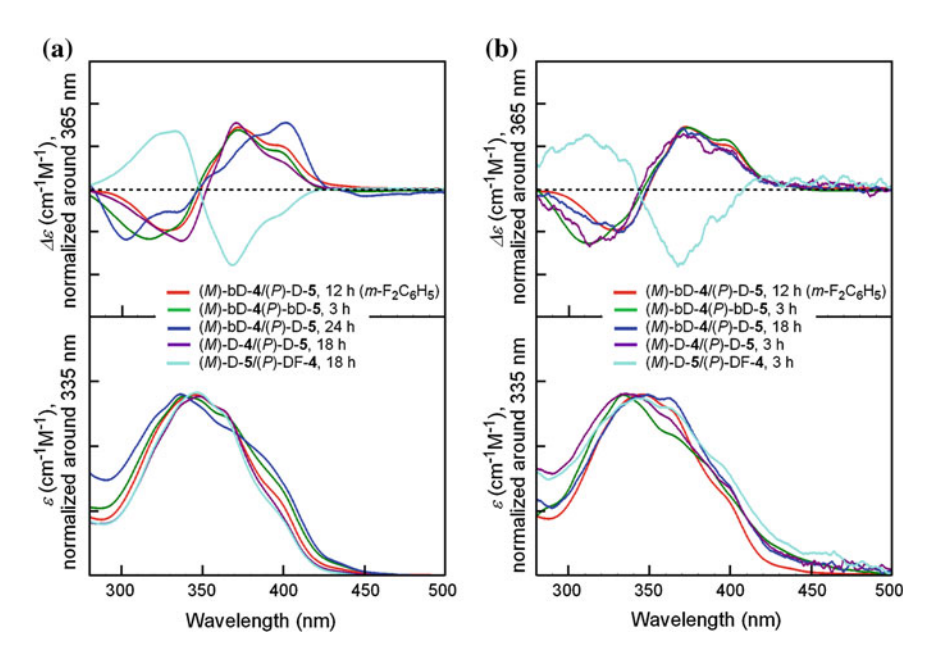


**Fig. 5.10** CD (*top*) and UV-Vis (*bottom*) spectra of 1:1 mixtures of (*M*)-bD-4/(*P*)-bD-5, (*M*)-bD-4/(*P*)-D-5, (*M*)-D-5, (*M*)-D-5/(*P*)-DF-4 in a toluene (total  $1.0 \times 10^{-4}$  M. 25 °C) and b diethyl ether (total  $2.5 \times 10^{-5}$  M, 25 °C). Spectra of a 1:1 mixture of (*M*)-bD-4/(*P*)-D-5 (*m*-difluorobenzene, total 0.5 mM, 25 °C, 12 h) are also shown. The spectra are shown on a normalized scale at absorption maxima at approximately 365 nm for CD and 335 nm for UV-Vis

Fig. 4.10). 4-Methyl-2-(2-methylpropyl)pentyl (bD) side chains were attached to the calculated hetero-double-helix structure of the (*M*)-tetramer/(*P*)-pentamer complex, and energy minimization was carried out without the conformational search (See Chap. 7). A hetero-double-helix structure of (*M*)-bD-4/(*P*)-bD-5 with a diameter and a width of 3.2 and 1.9 nm, respectively, was obtained, in which seven side chains were arranged at mutual angles of approximately 60° (Fig. 5.11). The height of 1.9 nm coincided well with the thickness of the vesicle, and it was therefore considered that hetero-double helices formed a monolayer structure by lateral interaction, which then forms vesicles. The lateral interactions between hetero-double helices were named "intercomplex interactions" in this study. It may reasonably be assumed that the fibers formed in toluene also possess membrane like structures, which resulted in the formation of hollow cylindrical fibers in toluene (Fig. 5.14). Differences between the growing rates of the membranes in toluene and diethyl ether might result in differences in anisotropy and morphology between the fibers/gels and vesicles.

At this stage, it is worthwhile discussing the observations that hetero-double helices composed of (M)/(P) combinations of ethynylhelicene oligomers formed fiber/gels and vesicles in solution, but (P)/(P) combinations did not form such higher assemblies. The chemical structures are the same for both combinations, and only the chirality of the helicenes differs. The strong intercomplex interactions between hetero-double helices composed of pseudoenantiomeric (M)/(P) ethynylhelicene oligomers may originate from the molecular shape of the hetero-double helices. For comparison, a computational calculation of (P)-bD-4/(P)-bD-5 with the same absolute configuration of helicenes was conducted using MacroModel 8.6 in the similar manner to that of (M)-bD-4/(P)-bD-5. 4-Methyl-2-(2-methylpropyl)pentyl (bD) side chains were attached to the calculated hetero-double-helix structure of the (P)-tetramer/(P)-pentamer with methoxycarbonyl side chains, and energy minimization was carried out without the conformational search (See Chap. 7) (Fig. 5.12).

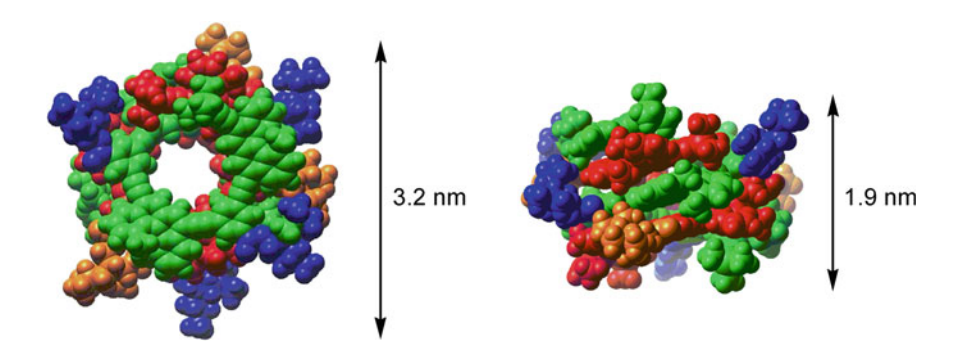
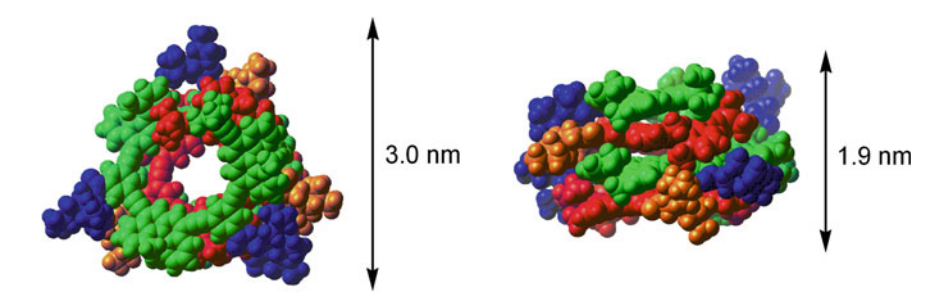


Fig. 5.11 Top view (left) and side view (right) of hetero-double-helix structure formed from (M)-bD-4/(P)-bD-5 calculated using MacroModel 8.6 in MMFFs force field. The molecule is presented using a CPK model with red (main chain) and orange (side chains) for (M)-bD-4, and green (main chain) and blue (side chains) for (P)-bD-5



**Fig. 5.12** Top view (*left*) and side view (*right*) of double-helix structure formed from (*P*)-bD-4/ (*P*)-bD-5 calculated using MacroModel 8.6 in MMFFs force field. The molecule is presented using a CPK model with *red* (main chain) and *orange* (side chains) for (*P*)-bD-4, and *green* (main chain) and *blue* (side chains) for (*P*)-bD-5

Despite the similar cylindrical double-helix structures of (M)-bD-4/(P)-bD-5 and (P)-bD-4/(P)-bD-5, substantial differences were observed in the arrangement of side chains. It is noted that (M)-bD-4/(P)-bD-5 has side chains arranged at mutual angles of approximately 60°, while (P)-bD-4/(P)-bD-5 has side chains arranged at mutual angles of approximately 120°. The molecular shape of heterodouble helices formed by (M)/(P) systems of a higher symmetry may have a larger surface area, which induces better packing by van der Waals interactions. Then, stronger intercomplex interactions occur in (M)/(P) systems than in (M)/(M) or (P)/(P) systems (Fig. 5.13).

The results shown here is an interesting example of hierarchical buildup from molecules of nanometer level to substances of micrometer or centimeter level. Pseudoenantiomeric ethynylhelicene oligomers form hetero-double helices, which then form membranes by intercomplex interactions. The membranes form higher assemblies of cylindrical fibers or vesicles (Fig. 5.14). The phenomena that weak interactions sinergistically and hierarchically form assemblies and that slight differences in molecular structure have marked effects on assembly formation remind us of the assembly of proteins in biological systems.

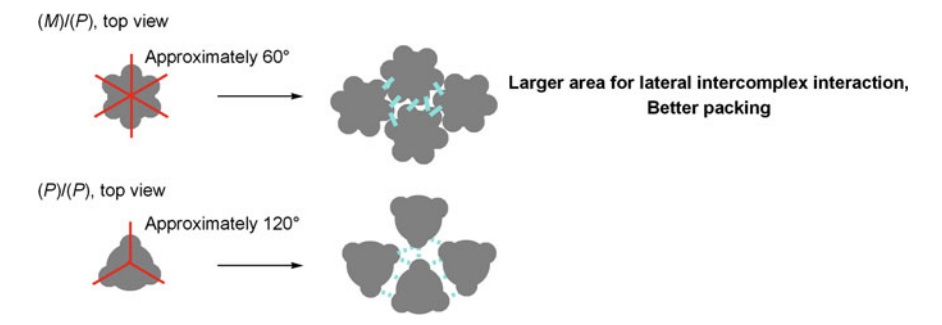


Fig. 5.13 Difference in lateral intercomplex interaction between (M)/(P) and (P)/(P) combinations

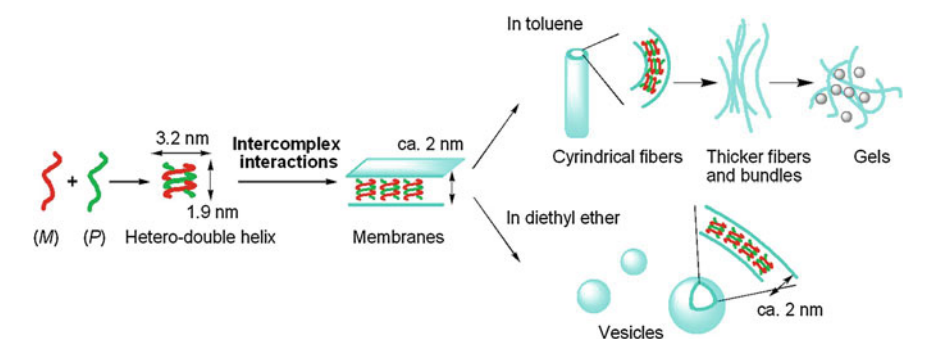


Fig. 5.14 Plausible pathways of forming fibers/gels and vesicles by hierarchical assembly of pseudoenantiomeric ethynylhelicene oligomers

### **5.4 Summary**

Pseudoenantiomeric (M)/(P) ethynylhelicene oligomers form hetero-double helices. Their shape of higher symmetry and larger surface area than homo-double helices is considered to induce strong lateral intercomplex interactions. Hetero-double helices initially form membranes by the intercomplex interactions and ultimately fibers or vesicles, the morphology of which is determined by the solvent used. The structures and properties of the assemblies were fine-tuned by changing the combination of compounds with different side chains, without losing assembly-forming ability. A methodology of systematically obtaining a diversity of assemblies by taking advantage of the two-component system was shown. This methodology reminds us of the assembly formation of biological proteins, with regard to the fact that small molecules are hierarchically bottom-upped to larger assemblies by synergistic weak interactions, and that slight differences in molecular structure have marked effects on the properties of the assemblies.

#### References

- 1. Wang BY, Xu H, Zhang X (2009) Adv Mater 21:2849
- 2. Pramod P, Thomas KG, George MV (2009) Chem Asian J 4:806
- Kim H-J, Kim T, Lee M (2011) Responsive nanostructures from aqueous assembly of rigidflexible block molecules. Acc Res Chem 44:72
- 4. Park C, Lee IH, Lee S, Rhue YM, Kim C (2006) Proc Natl Acad Sci 103:1199
- 5. Ryu J-H, Kim H-J, Huang Z, Lee E, Lee M (2006) Angew Chem Int Ed 45:5304
- 6. Ajayaghosh A, Chithra P, Varghese R (2007) Angew Chem Int Ed 46:230
- 7. Wang C, Yin S, Chen S, Xu H, Wang Z, Zhang X (2008) Angew Chem Int Ed 47:9049
- 8. Wang C, Guo Y, Wang Y, Xu H, Wang R, Zhang X (2009) Supramolecular amphiphiles based on a water-soluble charge-transfer complex: fabrication of ultralong nanofibres with tunable straightness. Angew Chem Int Ed 48:8962

References 61

 Versluis F, Tomatsu I, Kehr S, Fregonese C, Tepper AWJW, Stuart MCA, Ravoo BJ, Koning RI, Kros A (2009) J Am Chem Soc 131:13186

- 10. Wang BC, Chen Q, Xu H, Wang Z, Zhang X (2010) Adv Mater 22:2553
- 11. Kim T-H, Han Y-S, Seong B-S, Hong K-P (2011) Soft Matter 7:10070
- 12. Köth A, Appenhans D, Robertson D, Tiersch B, Koetz J (2011) Use of weakly cationic dentritic glycopolymer for morphological transformation of phospholipid vesicles into tube-like networks. Soft Matter 7:10581
- Moghaddam MJ, Campo L, Waddington LJ, Weerawardena A, Kirby N, Drummond CJ (2011) Soft Matter 7:10994
- 14. Rana U, Chakrabarti K, Malik S (2011) J Mater Chem 21:11098
- 15. Fernández G, García F, Sánchez L (2008) Chem Commun 44:6567
- 16. Wang T, Jiang J, Liu Y, Li Z, Liu M (2010) Langmuir 26:18694
- 17. Po C, Tam AY-Y, Wong KM-C, Yam VW-W (2011) J Am Chem Soc 133:12136
- 18. Liang Q, Chen G, Guan B, Jiang M (2011) J Mater Chem 21:13262
- Muños A, Illecas BM, Sánchez-Navarro M, Rojo J, Martín N (2011) J Am Chem Soc 133:16758
- 20. Ghosh S, Verma S (2008) Tetrahedron 64:6202
- Yan X, Cui Y, He Q, Wang K, Li J, Mu W, Wang B, Ou-yang Z-C (2008) Chem Eur J 14:5974
- 22. Cai W, Wang G-T, Xu Y-X, Jiang X-K, Li Z-T (2008) J Am Chem Soc 130:6936
- 23. Naskar J, Banerjee A (2009) Chem Asian J 4:1817
- 24. You L-Y, Wang G-T, Jiang X-K, Li Z-T (2009) Tetrahedron 65:9494
- 25. Du P, Wang G-T, Zhao T, Li GY, Jiang K-X, Li Z-T (2009) Tetrahedron Lett 51:188
- 26. Alfonso I, Bru M, Burguete I, García-Verdugo E, Luis SV (2010) Chem Eur J 16:1246
- 27. Xu Y-X, Wang GT, Zhao X, Jiang X-K, Li ZT (2010) Soft Matter 6:1246
- 28. Ke D, Zhan C, Li ADQ, Yao J (2011) Angew Chem Int Ed 50:3715
- 29. Maity S, Jana P, Maity SK, Haldar D (2011) Langmuir 27:3835
- 30. Ran X, Wang H, Zhang P, Binglian B, Zhao C, Yu Z, Li M (2011) Soft Matter 7:8561
- 31. Lee J, Kim JM, Yun M, Park C, Park J, Lee KH, Kim C (2011) Soft Matter 7:9021
- 32. Rubio J, Alfonso I, Burguete MI, Luis SV (2011) Soft Matter 7:10737
- 33. Ajayaghosh A, Chithra P, Varghese R (2007) Angew Chem Int Ed 46:230
- Yagai S, Nakano Y, Seki S, Asano A, Okubo T, Isoshima T, Karatsu T, Kitamura A, Kikkawa Y (2010) Angew Chem Int Ed 49:9990
- 35. Ajayaghosh A, Varghese R, Praveen VK, Mahesh S (2006) Angew Chem Int Ed 45:3261
- 36. Ajayaghosh A, Varghese R, Mahesh S, Praveen VK (2006) Angew Chem Int Ed 45:7729
- 37. Saito N, Shigeno M, Yamaguchi M (2012) Chem Eur J 18:8994
- 38. Sugiura H, Nigorikawa Y, Saiki Y, Nakamura K, Yamaguchi M (2004) J Am Chem Soc 126:14858
- 39. Sugiura H, Yamaguchi M (2007) Chem Lett 36:58
- 40. Amemiya R, Saito N, Yamaguchi M (2008) J Org Chem 73:7137
- 41. Saito N, Terakawa R, Shigeno M, Amemiya R, Yamaguchi M (2011) J Org Chem 76:4841
- 42. Wang C, Guo C, Wang Y, Xu H, Zhang X (2009) Chem Commun 45:5380
- 43. Greenfield MA, Palmer LC, Vernizzi G, Cruz MO, Stupp SI (2009) J Am Chem Soc 131:12030
- 44. Zhang H, Shen J, Liu Z, Hao A (2010) Supramol Chem 22:297
- 45. Krishna S, Nalluri M, Ravoo BJ (2010) Angew Chem Int Ed 49:5371
- 46. Wang K, Guo D-S, Liu Y (2010) Chem Eur J 16:8006
- Voskuhl J, Fenske T, Stuart MCA, Wibbeling B, Schmuck C, Ravoo BJ (2010) Chem Eur J 16:8300
- 48. Wang K, Guo D-S, Wang X, Liu Y (2011) ACS Nano 5:2880
- 49. Wang Q, Wu J, Gong Z, Zou Y, Yi T, Huang C (2010) Soft Matter 6:2679
- 50. Zhang K-D, Wang G-T, Zhao X, Li Z-T (2010) Langmuir 26:6878
- 51. Easwaramoorthi S, Kim P, Lim JM, Song S, Suh H, Sessler JL, Kim D (2010) J Mater Chem 20:9684

- 52. Yang M, Wang W, Yuan F, Zhang X, Li J, Liang F, He B, Minch B, Wegner G (2005) J Am Chem Soc 127:15107
- 53. Seo SH, Chang JY, Tew GC (2006) Angew Chem Int Ed 45:7526
- 54. Rehm T, Stepanenko V, Zhang X, Würthner F, Gröhn F, Klein K, Schmuck C (2008) Org Lett 10:1469
- 55. Zou J, Tao F, Jiang M (2007) Langmuir 23:12791
- 56. Sun T, Li Y, Zhang H, Li J, Xin F, Kong L, Hao A (2011) Collid Surf A 375:87
- 57. Mahamadi F, Richards NGJ, Guida WC, Liskamp R, Lipton CC, Chang G, Hendrickson T, n Still WC. (1990) J Compt Chem 11:440
- 58. Halgren TA (1996) J Compt Chem 17:490
- 59. Halgren TA (1996) J Compt Chem 17:520
- 60. Halgren TA (1996) J Compt Chem 17:553
- 61. Halgren TA, Nachbar RB (1996) J Compt Chem 17:587
- 62. Halgren TA (1996) J Compt Chem 17:616

## Chapter 6 Conclusions

- 1. Ethynylhelicene oligomers possessing different side chains were synthesized: (*P*)-bD-**n** (**n** = 2–6) with 4-methyl-2-(2-methylpropyl)pentyl side chains, (*P*)-F-**n** (**n** = 2–5) with perfluorooctyl side chains, (*P*)-DF-**n** (**n** = 4, 6, 8) with alternating decyloxycarbonyl/perfluorooctyl side chains, and (*P*)-FD-**n** (**n** = 4, 6, 10) with alternating perfluorooctyl/decyloxycarbonyl side chains. A two-directional method was employed to elongate the oligomers by a repetitive Sonogashira coupling reaction with building blocks and deprotection.
- 2. The homo-double-helix formation of ethynylhelicene oligomers with various side chains was studied. The order of stability was (*P*)-F-**n** > (*P*)-D-**n** and (*P*)-bD-**n** > (*P*)-DF-**n**, (*P*)-FD-**n**, and (*P*)-S-**n**. It is considered that a regular alternating arrangement of soft/hard and electron-rich/deficient moieties is important for stable homo-double-helix. (*P*)-D-**5** and (*P*)-F-**5** in pure homo-double-helix states showed approximately mirror-image CD spectra, which indicated that their helicities are opposite. Side chains have notable effects on the stability and structure of homo-double helices.
- 3. Mixtures of pseudoenantiomeric (*M*)/(*P*)-ethynylhelicene oligomers formed hetero-double helices, which are thermodynamically more stable than homodouble helices of (*M*)/(*M*) or (*P*)/(*P*) combinations. Bimolecular hetero-doublehelix formation was confirmed using the (*M*)-bD-4/(*P*)-D-5 system, which did not form higher assemblies. The side chains and the number of helicenes had significant effects on the properties of hetero-double helices, and a reversible structural change between hetero-double helices and random coils was attained under appropriate conditions using the (*M*)-D-6/(*P*)-DF-8 and (*M*)-D-6/(*P*)-DF-6 systems. A methodology of fine-tuning the properties of hetero-double helices by a combination of compounds is presented.
- 4. The hetero-double-helix complex aggregated to form higher assemblies, and fibers were formed in toluene and vesicles in diethyl ether. It is considered that the high symmetry and large surface area in hetero-double-helix complexes induce strong lateral intercomplex interactions, which result in the hierarchical formation of membranes and ultimately of fibers and vesicles. The structures and properties of the assemblies were fine-tuned by changing the combination

64 6 Conclusions

of compounds with different side chains without losing the assembly-forming ability. A methodology of systematically obtaining diverse higher assemblies using two-component systems is shown.

# **Chapter 7 Experimental Section**

#### 7.1 General Methods

Melting points were determined with a Yanaco micro melting point apparatus without correction. Elemental analyses were conducted with a Yanaco CHN CORDER MT-6 and a Yanaco HNS-15/HSU-20. Optical rotations were measured on a JASCO DIP-340 digital polarimeter. IR spectra were measured on a JASCO FT/IR-400 spectrophotometer. UV-Vis spectra were measured on a BECKMAN DU 640 or a JASCO J-720 spectropolarimeter. <sup>1</sup>H NMR and <sup>13</sup>C NMR spectra were recorded on a Varian Mercury (400 MHz), a Varian Vnmr J2.2C (400 MHz), or a JEOL JNM-ECA 600 (600 MHz) with tetramethylsilane as an internal standard. Chemical shifts are expressed in parts per million (ppm,  $\delta$ ). The abbreviations of signal patterns are as follows: s, singlet; d, doublet; t, triplet; q, quartet; quin, quintet; sep, septet; m, multiplet. <sup>13</sup>C NMR spectra taken in CDCl<sub>3</sub> ( $\delta$  77.0) was referenced to the residual solvents. <sup>19</sup>F NMR spectra were also recorded on a Varian Vnmr J2.2C (400 MHz) or a JEOL JNM-ECA 600 (565 MHz) with trifluoroacetic acid as an internal standard ( $\delta$  -79.0). Low- and High- resolution mass spectra were recorded on a JEOL JMS-DX-303, a JMS-AX-500, or a JEOL JMS-700. FAB mass spectra were recorded on a JEOL JMS-700 spectrometer by using m-nitrobenzyl alchohol matrix. MALDI-TOF MS spectra were recorded on a Perseptive Biosystems Voyager<sup>TM</sup> DE or a Shimadzu Axima using α-cyano-4hydroxycinnamic acid as the matrix. CD spectra were measured on a JASCO J-720 spectropolarimeter. Vapor pressure osmometry (VPO) was conducted with KNAUER K-7000 molecular weight apparatus using benzyl as a standard. Atomic force microscopic (AFM) images were obtained on a Veeco Digital Instrument Multimode Nanoscope IIIa or a SEIKO SPA400 operating in the tapping mode regime under ambient temperature and pressure. Micro-fabricated silicon cantilever tips (Olympus OMCL-AC160TS-C2 or Veeco MPP-11100-10) were used. Transmission Electron Microscopy (TEM) images were obtained on a JEOL JEM-2010F operating with an accerelating voltage of 200 kV. Samples were prepared by drop casting a solution on a 400 mesh carbon-coated copper grids. DLS measurements were conducted with Malvern Zetasizer Nano N. Polarizing optical microscopic observations were carried out using an Olympus BX53 polarizing optical microscope equipped to a CCD camera. Gel permeation chromatography (GPC) was conducted with Recycling Preparative HPLC LC-908 or LC-918 (Japan Analytical Industry, Co. Ltd.). CD and UV–Vis spectra were recorded using distilled or spectrophotomeric grade commercial solvents. Solvents used for AFM, TEM, and DLS experiments were used after filtration through 0.2  $\mu$ m pore membrane filters. The ratio of solvent mixture was shown by volume/volume.

## 7.2 Experimental Method for Chap. 2

4-Methyl-2-(2-methylpropyl)-pentanoic acid ethyl ester, 13. Under an argon atmosphere, a mixture of diisobutylmalonic acid diethyl ester 12 (6.38 g. 23.4 mmol), lithium chloride (5.96 g, 0.141 mol), and water (2.50 mL, 0.140 mmol) in dimethyl sulfoxide (68 mL) was heated under reflux for 24 h. Then the mixture was cooled to room temperature, and saturated aqueous ammonium chloride was added. After being stirred for 1 h, the organic materials were extracted with ethyl acetate three times. The organic layer was washed with water, brine, and dried over magnesium sulfate. The solvent was evaporated under reduced pressure, and separation by silica gel chromatography gave 13 as colorless oil (3.88 g, 19.4 mmol, 83 %). LRMS (EI, 70 eV) m/z: 201 ([M + H]<sup>+</sup>, 1.1 %), 144 ( $[M-C_4H_8]$ , 81 %), 101 ( $[M-C_7H_{15}]^+$ , 100 %). HRMS m/z Calcd for  $C_{12}H_{25}O_2^+$ : 201.1834. Found: 201.1855. IR (KBr) 2957, 2871, 1736, 1178 cm<sup>-1</sup>. <sup>1</sup>H NMR (400 MHz, CDCl<sub>3</sub>)  $\delta$  0.87 (6H, d, J = 6.4 Hz), 0.90 (6H, d, J = 6.4 Hz), 1.16–1.22 (2H, m), 1.25 (3H, t, J = 7.2 Hz), 1.49–1.51 (4H, m), 2.50 (1H, sep, J = 4.8 Hz), 4.13 (2H, q, J = 7.2 Hz). <sup>13</sup>C NMR (100 MHz, CDCl<sub>3</sub>).  $\delta$  14.3, 22.0, 23.0, 26.1, 41.7, 42.2, 59.9, 176.9.

4-Methyl-2-(2-methylpropyl)-pentanol, 14. Under an argon atmosphere, to a suspension of lithium alminium hydride (878 mg, 23.1 mmol) in THF (67 mL), 13 (3.86 g, 19.3 mmol) in THF (10 mL) was slowly added at  $-100 \,^{\circ}\text{C}$ . Then the mixture was warmed to 0 °C, and stirred for 2 h. At the temperature, sodium sulfate decahydrate was added slowly until formation of hydrogen stopped. Then, water (2-3 mL) was added, which was followed by excess sodium sulfate. After being stirred at room temperature overnight, insoluble materials were filtrated through Celite, and washed with THF three times. The solvent was evaporated under reduced pressure, and separation by silica gel chromatography gave 14 as colorless oil (2.95 g, 19.3 mmol, 97 %). LRMS (EI, 70 eV) m/z: 140.15 ([M- $H_2O$ ], 9.9 %), 83 ( $[C_5H_7O]^+$ , 65 %), 71 ( $[C_4H_7O]^+$ , 95 %), 57 ( $[C_4H_9]^+$ , 100 %), 43 ( $[C_3H_7]^+$ , 72 %). HRMS (FAB) m/z Calcd for  $C_{20}H_{45}O_2^+$  ( $[2 M-H]^+$ ): 317.3414. Found: 317.3432. IR (KBr) 3325 (br), 2954, 2917, 2871, 1468, 1048 cm<sup>-1</sup>. <sup>1</sup>H NMR (400 MHz, CDCl<sub>3</sub>)  $\delta$  0.88 (6H, d, J = 6.4 Hz), 0.89 (6H, d, J = 6.4 Hz), 1.07 (2H, quin, J = 6.4 Hz), 1.22 (2H, quin, J = 6.4 Hz), 1.55–1.71 (3H, m), 1.71–1.83 (1H, m, br), 3.51 (2H, d, J = 4.8 Hz). <sup>13</sup>C NMR (100 MHz, CDCl<sub>3</sub>)  $\delta$  22.8, 23.0, 25.2, 35.6, 41.1, 66.0.

4-Methyl-2-(2-methylpropyl)-pentyl 3,5-dihydroxy benzoate, 15. Under an argon atmosphere, a mixture of 14 (1.02 g, 6.43 mmol), 3,5-dihydroxybenzoic acid (1.04 g, 6.75 mmol), and conc. sulufonic acid (0.010 mL) in dry 1,4-dioxane (13 mL) was heated under reflux for 22 h. After the mixture was cooled to room temperature, saturated aqueous ammonium chloride was added. The organic materials were extracted with ethyl acetate. The organic layer was washed with water, brine, and dried over magnesium sulfate. The solvent was evaporated under reduced pressure, and separation by silica gel chromatography gave 15 as white solid (1.38 g, 4.68 mmol, 73 %), Mp 98–100 °C (ethyl acetate-hexane), LRMS  $(EI, 70 \text{ eV}) \text{ } m/z: 294 ([M]^+, 24 \%), 154 ([M-C_{10}H_{20}], 100 \%), 138 ([M-C_{10}H_{20}O], 100 \%)$ 85 %). HRMS m/z Calcd for C<sub>17</sub>H<sub>26</sub>O<sub>4</sub>: 294.1831. Found: 294.1840. IR (KBr) 3648 (br), 3304 (br), 2956, 1688, 1607, 1453, 1242, 1150 cm<sup>-1</sup>. <sup>1</sup>H NMR (400 MHz, CDCl<sub>3</sub>)  $\delta$  0.90 (6H, d, J = 6.4 Hz), 0.91 (6H, d, J = 6.4 Hz), 1.17 (2H, quin, J = 6.4 Hz), 1.28 (2H, quin, J = 6.4 Hz), 1.70 (2H, sep, J = 6.4 Hz), 1.85–1.94 (1H, m), 4.18 (2H, d, J = 5.2 Hz), 5.22 (2H, s), 6.58 (1H, t, J = 2.4 Hz), 7.11 (2H, d, J = 2.4 Hz). <sup>13</sup>C NMR (100 MHz, CDCl<sub>3</sub>)  $\delta$  22.7, 23.0, 25.2, 32.9, 41.6, 68.7, 107.5, 109.1, 132.5, 156.9, 166.8.

4-Methyl-2-(2-methylpropyl)pentyl 3,5-bis(trifluoromethanesulfoxy)benzoate, 16. To a solution of 15 (1.15 g, 3.91 mmol) in pyridine (15 mL), trifluoromethanesulfonic acid anhydride (1.6 mL, 9.7 mmol) was slowly added at -30 °C. The mixture was gradually warmed to room temperature, and stirred for 3 h. The reaction mixture was diluted with ethyl acetate, and saturated aqueous ammonium chloride was added. The organic materials were extracted with ethyl acetate. The organic layer was washed with saturated aqueous sodium hydrogencarbonate, water, brine, and dried over magnesium sulfate. The solvent was evaporated under reduced pressure, and separation by silica gel chromatography gave 17 as white solid (2.15 g, 3.84 mmol, 98 %). Mp 76-77 °C (hexane-methanol). LRMS (EI, 70 eV) m/z: 401 ([M–C<sub>10</sub>H<sub>21</sub>O]<sup>+</sup>, 54 %), 83 ([C<sub>6</sub>H<sub>11</sub>]<sup>+</sup>, 100 %). HRMS (FAB) m/zCalcd for  $C_{19}H_{23}F_6O_8S_2$  ([M–H]<sup>+</sup>): 557.0733. Found: 557.0735. IR (KBr) 2960, 1719, 1434, 1250, 1224, 1138 cm<sup>-1</sup>. <sup>1</sup>H NMR (400 MHz, CDCl<sub>3</sub>)  $\delta$  0.91 (6H, d, J = 6.8 Hz, 0.93 (6H, d, J = 6.8 Hz), 1.16–1.30 (4H, m), 1.67–1.74 (2H, m), 1.89-1.99 (1H, m), 4.26 (2H, d, J = 5.6 Hz), 7.44 (1H, t, J = 2.4 Hz), 7.98 (2H, d, J = 2.4 Hz). <sup>13</sup>C NMR (100 MHz, CDCl<sub>3</sub>)  $\delta$  22.6, 23.0, 25.3, 32.9, 41.8, 70.0, 118.6 (q,  $J_{\text{C-F}} = 319 \text{ Hz}$ ), 119.6, 122.4, 134.7, 149.4, 162.9. <sup>19</sup>F NMR (376 MHz, CDCl<sub>3</sub>, trifluoroacetic acid ( $\delta$  –79.0) as an external standard)  $\delta$  –75.3 (6F, s).

(*P*)-Building block with 4-methyl-2-(2-methylpropyl)-pentanoxycarbonyl side chains, (*P*)-bD-1. Under an argon atmosphere, a mixture of 16 (1.23 g, 2.20 mmol), tris(dibenzylideneacetone)dipalladium(0) chloroform adduct 45.6 mg, 0.0440 mmol), cuprous iodide (101 mg, 0.0528 mmol), tris(2,4,6-trimethylphenyl)phosphine (103 mg, 0.264 mmol), triphenylphosphine (69.3 mg, 0.264 mmol), tetrabutylammonium iodide (1.30 g, 2.20 mmol), triethylamine (0.70 mL), *N*,*N*-dimethylformamide (6.6 mL), and THF (2.6 mL) was freeze-evacuated three times in flask A. In flask B, a solution of monosilylated ethynylhelicene (*P*)-17 (332 mg, 0.881 mmol) in THF (4.0 mL) was freeze-evacuated three times, and the mixture was slowly added to flask A. The mixture was stirred

at room temperature for 1 h. The reaction was quenched by adding saturated aqueous ammonium chloride, and the organic materials were extracted with toluene. The organic layer was washed with water, brine, and dried over magnesium sulfate. The solvents were evaporated under reduced pressure, and separation by silica gel chromatography and recycling GPC gave (P)-bD-1 as yellow solid (588 mg, 0.749 mmol, 85 %). Mp 64–66 °C (toluene-methanol).  $[\alpha]_D^{27}$  –348 (c 0.50, CHCl<sub>3</sub>). MALDI-TOF MS *m/z* Calcd for C<sub>45</sub>H<sub>47</sub>F<sub>3</sub>O<sub>5</sub>SSi: 784.2866. Found: 784.4. UV–Vis (CHCl<sub>3</sub>, 5.0 ×  $10^{-6}$  M)  $\lambda_{\text{max}}$  ( $\epsilon$ ) 334 nm (7.3 ×  $10^{4}$ ). CD (CHCl<sub>3</sub>,  $5.0 \times 10^{-6}$  M)  $\lambda(\Delta \varepsilon)$  261 nm (57), 295 nm (-19), 331 nm (27), 383 nm (-44). IR (KBr) 2956, 2148, 1729, 1429, 1248 cm<sup>-1</sup>. Anal. (C<sub>45</sub>H<sub>47</sub>F<sub>3</sub>O<sub>5</sub>SSi) Calcd: C, 68.85; H, 6.03. Found: C, 68.82; H, 6.00.  $^{1}$ H NMR (400 MHz, CDCl<sub>3</sub>)  $\delta$  0.39 (9H, s), 0.94 (6H, d, J = 6.4 Hz), 0.96 (6H, d, J = 6.4 Hz), 1.24 (2H, quin, J = 6.4 Hz), 1.32 (2H, quin, J = 6.4 Hz), 1.75 (2H, sep, J = 6.4 Hz), 1.92 (6H, s), 1.93 (6H, s), 1.93–2.01 (1H, m), 4.28 (2H, d, J = 5.6 Hz), 7.45 (1H, d, J = 8.4 Hz), 7.47 (1H, d, J = 8.4 Hz), 7.67 (1H,t, J = 8.4 Hz), 7.69 (1H, t, J = 8.4 Hz), 7.76 (1H, t, J = 1.6 Hz), 7.92 (1H, dd, J = 1.6, 1.2 Hz), 8.01 (1H,s), 8.06 (1H, s), 8.35 (1H, dd, J = 1.6, 1.2 Hz), 8.43 (2H, d, J = 8.4 Hz). <sup>13</sup>C NMR  $(100 \text{ MHz}, \text{CDCl}_3) \delta 0.097, 22.7, 23.06, 23.14, 23.2, 25.3, 33.0, 41.8, 69.5, 91.1,$ 91.4, 100.3, 102.9, 118.7 (q,  $J_{C-F} = 319$  Hz), 118.9, 120.4, 121.9, 123.3, 123.7, 126.3, 126.9, 127.0, 128.1, 129.2, 129.3, 129.8, 130.3, 130.78, 130.82, 130.9, 131.9, 132.45, 132.53, 133.3, 136.8, 137.0, 137.1, 149.3, 164.2. <sup>19</sup>F NMR (376 MHz, CDCl<sub>3</sub>, trifluoroacetic acid ( $\delta$  –79.0) as an external standard)  $\delta$  –75.5 (3F, s).

4-methyl-2-(2-methylpropyl)-pentanoxycarbonyl with chains, (P)-bD-2. Under an argon atmosphere, a mixture of tris(dibenzylideneacetone)dipalladium(0) chloroform adduct 8.52 mg, 0.00823 mmol), cuprous iodide (18.8 mg, 0.0988 mmol), tris(2,4,6-trimethylphenyl)phosphine (19.2 mg, 0.0494 mmol), triphenylphosphine (13.0 mg, 0.494 mmol), tetrabutylammonium iodide (243 mg, 0.648 mmol), triethylamine (0.11 mL), N,N-dimethylformamide (1.1 mL), and THF (0.2 mL) was freeze-evacuated three times in flask A. In flask B, a mixture of monosilylated ethynylhelicene (P)-17 (56.7 mg, 0.151 mmol) and 16 (42.1 mg, 0.0753 mmol) in THF (4.0 mL) was freeze-evacuated three times, and the mixture was slowly added to flask A. The mixture was stirred at 45 °C for 4 h. The reaction was quenched by adding saturated aqueous ammonium chloride, and the organic materials were extracted with toluene. The organic layer was washed with water, brine, and dried over magnesium sulfate. The solvents were evaporated under reduced pressure, and separation by silica gel chromatography and recycling GPC gave (P)-bD-2 as yellow solid (72.4 mg, 0.715 mmol, 95 %). Mp 158–160 °C (toluene-methanol).  $\left[\alpha\right]_{D}^{27}$  –591 (c 0.50, CHCl<sub>3</sub>). MALDI-TOF MS m/z Calcd for  $C_{71}H_{70}O_2Si_2$ : 1010.5. Found: 1010.4. UV-Vis (CHCl<sub>3</sub>,  $5.0 \times 10^{-6} \text{ M}$ )  $\lambda_{\text{max}}$  ( $\epsilon$ ) 334 nm (1.6 × 10<sup>5</sup>). CD (CHCl<sub>3</sub>, 5.0 × 10<sup>-6</sup> M)  $\lambda(\Delta \epsilon)$ 262 nm (115), 296 nm (-35), 333 nm (67), 385 nm (-87). IR (KBr) 2954, 2147, 1724, 1247 cm<sup>-1</sup>. Anal. (C<sub>71</sub>H<sub>70</sub>O<sub>2</sub>Si<sub>2</sub>) Calcd: C, 84.31; H, 6.98. Found: C, 84.43; H, 7.24. <sup>1</sup>H NMR (400 MHz, CDCl<sub>3</sub>)  $\delta$  0.40 (18H, s), 0.98 (6H, d, J = 6.8 Hz), 0.99 (6H, d, J = 6.8 Hz), 1.26 (6H, quin, J = 6.8 Hz), 1.38 (2H, quin,

J=6.8 Hz), 1.79 (2H, sep, J=6.4 Hz), 1.92 (6H, s), 1.98–2.05 (1H, m), 4.31 (2H, d, J=5.6 Hz), 7.43 (2H, d, J=7.2 Hz), 7.46 (2H, d, J=7.2 Hz), 7.65 (2H, dd, J=8.0, 7.2 Hz), 7.70 (2H, dd, J=8.0, 7.2 Hz), 8.01 (2H, s), 8.05 (2H, s), 8.19 (2H, t, J=1.2 Hz), 8.35 (2H, d, J=1.2 Hz), 8.44 (2H, d, J=8.0 Hz), 8.54 (2H, d, J=8.0 Hz). <sup>13</sup>C NMR (100 MHz, CDCl<sub>3</sub>)  $\delta$  0.14, 22.8, 23.16, 23.18, 25.4, 33.1, 41.8, 69.0, 89.4, 92.9, 100.2, 103.1, 119.6, 120.3, 123.5, 123.6, 124.3, 126.6, 126.9, 129.1, 129.8, 130.8, 130.9, 131.5, 132.1, 132.31, 132.35, 136.7, 136.8, 138.2, 165.5.

Deprotected (P)-dimer with 4-methyl-2-(2-methylpropyl)-pentanoxycarbonyl side chains, (P)-bD-2H (Typical procedure for desilylation of (P)-bD-n). To a solution of (P)-bD-2 (60.2 mg, 0.0595 mmol) in THF (0.9 mL) was added 1.0 M tetrabutylammonium fluoride in THF (0.18 mL, 0.18 mmol) at 0 °C. After being stirred for 30 min at the temperature, saturated aqueous ammonium chloride was added. The organic materials were extracted with toluene. The organic layer was washed with water, brine, and dried over magnesium sulfate. The solvents were evaporated under reduced pressure, and silica gel chromatography gave (P)bD-2H (51.6 mg, 0.0595 mmol, quant.). Mp 145-149 °C, decomp. (toluenemethanol).  $\left[\alpha\right]_{D}^{27}$  -582 (c 0.50, CHCl<sub>3</sub>). MALDI-TOF MS m/z Calcd for  $C_{65}H_{54}O_2$ : 866.4. Found: 866.6. UV–Vis (CHCl<sub>3</sub>, 5.0 × 10<sup>-6</sup> M)  $\lambda_{max}$  ( $\epsilon$ ) 330 nm  $(1.5 \times 10^5)$ . CD (CHCl<sub>3</sub>,  $5.0 \times 10^{-6}$  M)  $\lambda(\Delta \varepsilon)$  264 nm (112), 297 nm (-37), 329 nm (64), 383 nm (-84). IR (KBr) 2952, 2205, 1719, 1240 cm<sup>-1</sup>. Anal.  $(C_{65}H_{54}O_2)$  Calcd for: C, 90.03; H, 6.28. Found: C, 89.88; H, 6.56. <sup>1</sup>H NMR (400 MHz, CDCl<sub>3</sub>)  $\delta$  0.98 (6H, d, J = 6.4 Hz), 0.99 (6H, d, J = 6.4 Hz), 1.26 (6H, quin, J = 6.8 Hz), 1.38 (2H, quin, J = 6.8 Hz), 1.79 (2H, sep, J = 6.4 Hz), 1.94 (12H, s), 1.98-2.05 (1H, m), 3.56 (2H, s), 4.31 (2H, d, J = 5.6 Hz), 7.45 (2H, d, J = 5.6 Hz)d, J = 7.2 Hz), 7.49 (2H, d, J = 7.2 Hz), 7.65 (2H, dd, J = 8.0, 7.2 Hz), 7.71 (2H, dd, J = 8.0, 7.2 Hz), 8.04 (2H, s), 8.07 (2H, s), 8.17 (2H, t, J = 1.6 Hz), 8.34(2H, d, J = 1.6 Hz), 8.44 (2H, d, J = 8.0 Hz), 8.53 (2H, d, J = 8.0 Hz). <sup>13</sup>C NMR (100 MHz, CDCl<sub>3</sub>)  $\delta$  22.8, 23.16, 23.18, 25.4, 33.1, 41.8, 69.0, 81.8, 82.4, 89.3, 93.0, 119.4, 119.7, 123.5, 124.3, 126.8, 126.9, 127.0, 129.19, 129.24, 129.8, 130.4, 130.8, 130.9, 131.5, 132.1, 132.3, 132.4, 136.8, 136.9, 138.2, 165.5.

(P)-Trimer with 4-methyl-2-(2-methylpropyl)-pentanoxycarbonyl side chains, (P)-bD-3 (Typical procedure for the Sonogashira coupling reaction of (P)-bD-n). Under an argon atmosphere, a mixture of tris(dibenzylideneacetone)dipalladium(0) chloroform adduct 13.2 mg, 0.0127 mmol), cuprous iodide (29.1 mg, 0.1529 mmol), tris(2,4,6-trimethylphenyl)phosphine 0.764 mmol), triphenylphosphine (20.1 mg, 0.0764 mmol), tetrabutylammonium iodide (376 mg, 0.255 mmol), triethylamine (0.12 mL), N,N-dimethylformamide (1.2 mL), and THF (0.2 mL) was freeze-evacuated three times in flask A. In flask B, a mixture of diethynylhelicene (P)-18 (38.8 mg, 0.127 mmol) and (P)-bD-1 (200 mg, 0.255 mmol) in THF (1.0 mL) was freeze-evacuated three times, and the mixture was slowly added to flask A. The mixture was stirred at 45 °C for 4 h. The reaction was quenched by adding saturated aqueous ammonium chloride, and the organic materials were extracted with toluene three times. The combined organic layer was washed with water, brine, and dried over magnesium sulfate. The

solvents were evaporated under reduced pressure, and separation by silica gel chromatography and recycling GPC gave (P)-bD-3 as yellow solid (182 mg, 0.116 mmol, 91 %). Mp 175–177 °C (toluene-methanol).  $[\alpha]_D^{27}$  –592 (c 0.50, CHCl<sub>3</sub>). MALDI-TOF MS *m/z* Calcd for C<sub>112</sub>H<sub>108</sub>O<sub>4</sub>Si<sub>2</sub>: 1572.8. Found: 1572.4. UV-Vis (CHCl<sub>3</sub>,  $5.0 \times 10^{-6}$  M)  $\lambda_{\text{max}}$  ( $\epsilon$ ) 335 nm ( $2.5 \times 10^{5}$ ). CD (CHCl<sub>3</sub>,  $5.0 \times 10^{-6} \,\mathrm{M}$ )  $\lambda(\Delta\varepsilon)$  264 nm (174), 296 nm (-52), 333 nm (81), 387 nm (-146). IR (KBr) 2954, 2148, 1724, 1242 cm<sup>-1</sup>, Anal. (C<sub>112</sub>H<sub>108</sub>O<sub>4</sub>Si<sub>2</sub>) Calcd: C, 85.45; H, 6.91. Found: C, 85.56; H, 6.90. <sup>1</sup>H NMR (400 MHz, CDCl<sub>3</sub>)  $\delta$  0.40 (18H, s), 0.99 (12H, d, J = 6.4 Hz), 1.00 (12H, d, J = 6.4 Hz), 1.26 (4H, quin. J = 6.4 Hz), 1.39 (4H, quin, J = 6.4 Hz), 1.80 (4H, sep, J = 6.4 Hz), 1.93 (6H, s), 1.95 (6H, s), 1.99 (6H, s), 1.99–2.05 (2H, m), 4.32 (4H, d, J = 5.6 Hz), 7.44 (2H, d, J = 7.2 Hz), 7.47 (2H, d, J = 7.2 Hz), 7.50 (2H, d, J = 7.2 Hz), 7.66 (2H,dd, J = 8.0, 7.2 Hz), 7.71 (2H, dd, J = 8.0, 7.2 Hz), 7.73 (2H, dd, J = 8.0, 7.2 Hz), 8.02 (2H, s), 8.06 (2H, s), 8.11 (2H, s), 8.20 (2H, dd, J = 1.6, 1.2 Hz), 8.35 (2H, t, J = 1.2 Hz), 8.36 (2H, t, J = 1.6 Hz), 8.44 (2H, d, J = 8.0 Hz), 8.54 (2H, d, J = 8.0 Hz), 8.56 (2H, d, J = 8.0 Hz). <sup>13</sup>C NMR (100 MHz, CDCl<sub>3</sub>)  $\delta$ 0.13, 22.8, 23.16, 23.23, 25.4, 33.1, 41.9, 69.0, 89.3, 89.4, 92.9, 93.0, 100.2, 103.1, 119.6, 119.8, 120.3, 123.5, 123.6, 123.7, 124.3, 124.4, 126.6, 126.8, 126.9, 127.0, 129.1, 129.2, 129.3, 129.9, 130.8, 130.9, 131.0, 131.5, 132.1, 132.2, 132.4, 136.7, 136.86, 136.92, 138.3, 165.5.

Deprotected (P)-trimer with 4-methyl-2-(2-methylpropyl)-pentanoxycarbonyl side chains, (P)-bD-3H. The compound (76.7 mg, 0.0536 mmol, quant.) was prepared from (*P*)-bD-3 (84.5 mg, 0.0536 mmol). Mp 167–170 °C, decomp. (toluene-methanol).  $\left[\alpha\right]_{D}^{21}$  -603 (c 0.50, CHCl<sub>3</sub>). MALDI-TOF MS m/z Calcd for  $C_{106}H_{92}O_4$ : 1428.7. Found: 1428.9. UV–Vis (CHCl<sub>3</sub>, 5.0 × 10<sup>-6</sup> M)  $\lambda_{max}$  (ε) 331 nm (2.1 × 10<sup>5</sup>). CD (CHCl<sub>3</sub>, 5.0 × 10<sup>-6</sup> M)  $\lambda(\Delta\varepsilon)$  264 nm (175), 297 nm (– 51), 330 nm (71), 387 nm (-136). IR (KBr) 2954, 2208, 1724, 1240 cm<sup>-1</sup>. Anal. (C<sub>106</sub>H<sub>92</sub>O<sub>4</sub>) Calcd: C, 89.04; H, 6.49. Found: C, 89.04; H, 6.43. <sup>1</sup>H NMR (400 MHz, CDCl<sub>3</sub>)  $\delta$  0.98 (12H, d, J = 6.8 Hz), 0.99 (12H, d, J = 6.4 Hz), 1.26 (4H, quin, J = 7.0 Hz), 1.39 (4H, quin, J = 6.8 Hz), 1.80 (4H, sep, J = 6.4 Hz), 1.95 (12H, s), 1.99 (6H, s), 1.99-2.05 (2H, m), 3.56 (2H, s), 4.31 (4H, d, J = 5.6 Hz), 7.45–7.51 (6H, m), 7.66 (2H, dd, J = 8.0, 7.2 Hz), 7.72 (2H, dd, J = 8.0, 7.2 Hz, 7.73 (2H, dd, J = 8.0, 7.2 Hz), 8.05 (2H, s), 8.08 (2H, s), 8.12 (2H, s), 8.19 (2H, t, J = 1.6 Hz), 8.34 (2H, t, J = 1.6 Hz), 8.36 (2H, t, J = 1.6 Hz)J = 1.6 Hz), 8.44 (2H, d, J = 8.0 Hz), 8.54 (2H, d, J = 8.0 Hz), 8.55 (2H, d, J = 8.0 Hz). <sup>13</sup>C NMR (100 MHz, CDCl<sub>3</sub>)  $\delta$  22.8, 23.17, 23.19, 23.24, 25.4, 33.1, 41.9, 69.0, 81.8, 82.4, 89.3, 92.96, 93.01, 119.4, 119.75, 119.83, 123.5, 124.3, 126.8, 126.86, 126.94, 126.99, 127.03, 129.2, 129.25, 129.31, 129.8, 129.9, 130.4, 130.8, 130.9, 131.0, 131.1, 131.5, 132.1, 132.2, 132.4, 136.8, 136.9, 137.0, 138.3, 165.5.

(*P*)-Tetramer with 4-methyl-2-(2-methylpropyl)-pentanoxycarbonyl side chains, (*P*)-bD-4. The compound (86.2 mg, 0.0403 mmol, 92 %) was prepared from (38.0 mg, 0.0438 mmol) and (*P*)-bD-1 (68.8 mg, 0.0877 mmol) as yellow solid. Mp 187–189 °C (toluene-methanol). [ $\alpha$ ]<sub>D</sub><sup>27</sup> –566 (c 0.50, CHCl<sub>3</sub>). MALDITOF MS m/z Calcd for C<sub>153</sub>H<sub>146</sub>O<sub>6</sub>Si<sub>2</sub>: 2135.1. Found: 2135.6. UV–Vis (CHCl<sub>3</sub>,

 $5.0 \times 10^{-6}$  M)  $\lambda_{\rm max}$  ( $\varepsilon$ ) 335 nm ( $2.9 \times 10^{5}$ ). CD (CHCl<sub>3</sub>,  $5.0 \times 10^{-6}$  M)  $\lambda(\varDelta\varepsilon)$  264 nm (237), 296 nm (-66), 333 nm (87), 387 nm (-193). IR (KBr) 2953, 2146, 1724, 1239 cm<sup>-1</sup>. Anal. (C<sub>153</sub>H<sub>146</sub>O<sub>6</sub>Si<sub>2</sub>) Calcd: C, 85.99; H, 6.89. Found: C, 85.97; H, 7.00. <sup>1</sup>H NMR (400 MHz, CDCl<sub>3</sub>)  $\delta$  0.40 (18H, s), 0.98–1.02 (36H, m), 1.23–1.31 (6H, m), 1.36–1.44 (6H, m), 1.75–1.84 (6H, m), 1.94 (6H, s), 1.95 (6H, m), 2.00 (12H, s), 2.00–2.05 (3H, m), 4.32–4.34 (6H, m), 7.45 (2H, d, J=7.2 Hz), 7.48 (2H, d, J=7.2 Hz), 7.51 (4H, d, J=7.2 Hz), 7.66 (2H, dd, J=8.0, 7.2 Hz), 7.70–7.76 (6H, m), 8.02 (2H, s), 8.06 (2H, s), 8.12 (4H, s), 8.21 (2H, t, J=1.6 Hz), 8.22 (1H, t, J=1.6 Hz), 8.35 (2H, t, J=1.6 Hz), 8.37 (4H, t, J=1.6 Hz), 8.44 (2H, d, J=7.2 Hz), 8.54–8.58 (6H, m). <sup>13</sup>C NMR (100 MHz, CDCl<sub>3</sub>)  $\delta$  0.13, 22.8, 23.15, 23.25, 25.4, 33.1, 41.8, 69.0, 89.3, 89.4, 92.9, 93.0, 100.2, 103.1, 119.6, 119.8, 120.3, 123.5, 123.59, 123.64, 124.3, 124.34, 124.4, 126.6, 126.8, 126.9, 127.0, 129.1, 129.2, 129.3, 129.8, 130.8, 130.9, 130.93, 131.0, 131.5, 132.1, 132.2, 132.3, 136.7, 136.86, 136.92, 138.2, 165.5.

Deprotected (P)-tetramer with 4-methyl-2-(2-methylpropyl)-pentanoxycarbonyl side chains, (P)-bD-4H. The compound (45.5 mg, 0.0228 mmol, 98 %) was prepared from (P)-bD-4 (50.0 mg, 0.0234 mmol) as yellow solid. Mp 205–208 °C, decomp. (toluene-methanol).  $[\alpha]_D^{27}$  –572 (c 0.50, CHCl<sub>3</sub>). MALDI-TOF MS m/z Calcd for C<sub>147</sub>H<sub>130</sub>O<sub>6</sub>: 1991.0. Found: 1990.3. UV-Vis (CHCl<sub>3</sub>,  $5.0 \times 10^{-6} \text{ M}$ )  $\lambda_{\text{max}}$  ( $\epsilon$ ) 332 nm (2.7 × 10<sup>5</sup>). CD (CHCl<sub>3</sub>, 5.0 × 10<sup>-6</sup> M)  $\lambda(\Delta \epsilon)$ 265 nm (235), 297 nm (-51), 330 nm (83), 387 nm (-184). IR (KBr) 2953, 2205, 1724, 1240 cm<sup>-1</sup>. Anal.  $(C_{147}H_{130}O_6)$  Calcd: C, 88.61; H, 6.58. Found: C, 88.33; H, 6.83. <sup>1</sup>H NMR (400 MHz, CDCl<sub>3</sub>)  $\delta$  0.97–1.01 (36H, m), 1.23–1.30 (6H, m), 1.35–1.43 (6H, m), 1.76–1.83 (6H, m), 1.94 (12H, s), 1.99 (12H, s), 1.99–2.04 (3H, m), 3.56 (2H, s), 4.31–4.33 (6H, m), 7.45 (2H, d, J = 6.8 Hz), 7.48 (2H, d, J = 7.2 Hz), 7.51 (4H, d, J = 6.8 Hz), 7.66 (2H, dd, J = 8.0, 7.2 Hz), 7.69–7.76 (6H, m), 8.05 (2H, s), 8.08 (2H, s), 8.13 (4H, s), 8.19 (2H, t, J = 1.6 Hz), 8.22 (1H, t, J = 1.6 Hz), 8.34 (2H, t, J = 1.6 Hz), 8.35–8.36 (4H, m), 8.44 (2H, d, J = 8.0 Hz), 8.53–8.57 (6H, m). <sup>13</sup>C NMR (100 MHz, CDCl<sub>3</sub>)  $\delta$  22.8, 23.16, 23.24, 25.4, 33.1, 41.9, 69.0, 81.8, 82.4, 89.3, 92.95, 93.01, 119.4, 119.7, 119.8, 123.5, 123.6, 124.3, 126.8, 126.87, 126.94, 126.99, 127.04, 129.19, 129.24, 129.3, 129.8, 129.9, 130.4, 130.82, 130.84, 130.9, 131.0, 131.1, 131.5, 132.1, 132.2, 132.4, 136.8, 136.9, 137.0, 138.3, 165.5.

(*P*)-Pentamer with 4-methyl-2-(2-methylpropyl)-pentanoxycarbonyl side chains, (*P*)-bD-5. The compound (133 mg, 0.0494 mmol, 92 %) was prepared from (*P*)-bD-3H (76.7 mg, 0.0536 mmol) and (*P*)-bD-1 (84.2 mg, 0.107 mmol) as yellow solid. Mp 189–191 °C (toluene-methanol). [α]<sub>D</sub><sup>21</sup> –550 (c 0.50, CHCl<sub>3</sub>). MALDI-TOF MS *m/z* Calcd for C<sub>194</sub>H<sub>184</sub>O<sub>8</sub>Si<sub>2</sub>: 2697.4. Found: 2696.9. UV–Vis (CHCl<sub>3</sub>, 5.0 × 10<sup>-6</sup> M)  $\lambda_{\text{max}}$  (ε) 336 nm (3.7 × 10<sup>5</sup>). CD (CHCl<sub>3</sub>, 5.0 × 10<sup>-6</sup> M)  $\lambda(\Delta\epsilon)$  264 nm (304), 297 nm (–83), 334 nm (101), 389 nm (–248). IR (KBr) 2954, 2150, 1726, 1240 cm<sup>-1</sup>. Anal. (C<sub>194</sub>H<sub>184</sub>O<sub>8</sub>Si<sub>2</sub>) Calcd: C, 86.31; H, 6.87. Found: C, 86.37; H, 7.10. <sup>1</sup>H NMR (400 MHz, CDCl<sub>3</sub>) δ 0.39 (18H, s), 0.97–1.01 (48H, m), 1.22–1.30 (8H, m), 1.35–1.43 (8H, m), 1.74–1.83 (8H, m), 1.93 (6H, s), 1.94 (6H, s), 1.99 (12H, s), 2.00 (6H, s), 2.00–2.04 (4H, m), 4.30–4.33 (8H, m), 7.44 (2H, d, J = 6.8 Hz), 7.47 (2H, d, J = 7.2 Hz), 7.49–7.52 (6H, m), 7.66 (2H,

dd, J = 8.0, 7.2 Hz), 7.69–7.76 (8H, m), 8.01 (2H,s), 8.06 (2H, s), 8.11–8.12 (6H, m), 8.20 (2H, dd, J = 1.6, 1.2 Hz), 8.21 (2H, dd, J = 1.6, 1.2 Hz), 8.34 (2H, dd, J = 1.6, 1.2 Hz), 8.35–8.36 (6H, m), 8.43 (2H, d, J = 7.6 Hz), 8.53–8.57 (8H, m). <sup>13</sup>C NMR (100 MHz, CDCl<sub>3</sub>)  $\delta$  0.12, 22.8, 23.16, 23.23, 25.4, 33.1, 41.9, 69.0, 89.3, 89.4, 92.9, 93.0, 100.2, 103.1, 119.6, 119.8, 120.3, 123.5, 123.58, 123.65, 124.3, 126.6, 126.8, 126.9, 127.0, 129.1, 129.2, 129.3, 129.9, 130.8, 130.9, 131.0, 131.47, 131.48, 132.1, 132.2, 132.3, 136.7, 136.86, 136.93, 138.2, 165.5.

(P)-Hexamer with 4-methyl-2-(2-methylpropyl)-pentanoxycarbonyl side chains, (P)-bD-6. The compound (147 mg, 0.0451 mmol, 94 %) was prepared from (P)-bD-**4H** (96.0 mg, 0.0482 mmol) and (P)-bD-**1** (75.6 mg, 0.0964 mmol) as yellow solid. Mp 190–193 °C (toluene-methanol).  $\left[\alpha\right]_{D}^{27}$  –506 (c 0.50, CHCl<sub>3</sub>). MALDI-TOF MS m/z Calcd for C<sub>235</sub>H<sub>222</sub>O<sub>10</sub>Si<sub>2</sub>: 3259.6. Found: 3260.5. UV-Vis (CHCl<sub>3</sub>, 5.0 ×  $10^{-6}$  M)  $\lambda_{\text{max}}$  ( $\epsilon$ ) 336 nm (4.3 ×  $10^{5}$ ). CD (CHCl<sub>3</sub>, 5.0 ×  $10^{-6}$  M)  $\lambda(\Delta \varepsilon)$  264 nm (354), 297 nm (-88), 336 nm (111), 389 nm (-295). IR (KBr) 2954, 2148, 1724, 1239 cm<sup>-1</sup>. Anal. (C<sub>235</sub>H<sub>222</sub>O<sub>10</sub>Si<sub>2</sub>) Calcd: C, 86.52; H, 6.86. Found: C, 86.35; H, 7.11. <sup>1</sup>H NMR (400 MHz, CDCl<sub>3</sub>)  $\delta$  0.39 (18H, s), 0.97–1.01 (60H, m), 1.23–1.35 (10H, m), 1.36–1.43 (10H, m), 1.74–1.85 (10H, m), 1.92 (6H, s), 1.94 (6H, s), 1.98-2.06 (29H, m), 4.30-4.32 (10H, m), 7.44 (2H, d, J = 7.2 Hz, 7.46-7.51 (10H, m), 7.66 (2H, dd, J = 8.0, 7.2 Hz), 7.69-7.75 (10H, m)m), 8.01 (2H,s), 8.05 (2H, s), 8.10 (4H, s), 8.11 (4H, m), 8.19 (1H, t, J = 1.6 Hz), 8.20-8.22 (4H, m), 8.33 (2H, t, J = 1.6 Hz), 8.34-8.36 (8H, m), 8.43 (2H, d, J = 8.0 Hz), 8.53–8.57 (10H, m). <sup>13</sup>C NMR (100 MHz, CDCl<sub>3</sub>)  $\delta$  0.12, 22.8, 23.16, 23.25, 25.4, 29.7, 33.1, 41.8, 69.0, 89.3, 89.4, 92.9, 93.0, 100.2, 103.0, 119.6, 119.8, 120.3, 123.5, 123.57, 123.64, 124.3, 126.6, 126.8, 126.9, 127.0, 129.1, 129.2, 129.3, 129.8, 130.8, 130.9, 131.0, 131.4, 132.1, 132.2, 132.3, 136.7, 136.87, 136.92, 138.2, 165.5.

(*M*)-Dimer with 4-methyl-2-(2-methylpropyl)-pentanoxycarbonyl side chains, (*M*)-bD-2. [ $\alpha$ ]<sub>D</sub><sup>27</sup> +548 (c 0.50, CHCl<sub>3</sub>). Anal. (C<sub>71</sub>H<sub>76</sub>O<sub>2</sub>Si<sub>2</sub>) Calcd: C, 84.21; H, 6.98. Found: C, 84.59; H, 7.24.

**Deprotected** (*M*)-Dimer with 4-methyl-2-(2-methylpropyl)-pentanoxycarbonyl side chains, (*M*)-bD-2H.  $[\alpha]_D^{27}$  +543 (*c* 0.50, CHCl<sub>3</sub>). Anal. (C<sub>65</sub>H<sub>54</sub>O<sub>2</sub>) Calcd: C, 90.03; H, 6.28. Found: C, 90.13; H, 6.62.

(*M*)-Tetramer with 4-methyl-2-(2-methylpropyl)-pentanoxycarbonyl side chains, (*M*)-bD-4.  $[\alpha]_D^{27}$  +505 (*c* 0.25, CHCl<sub>3</sub>). Anal. (C<sub>153</sub>H<sub>146</sub>O<sub>6</sub>Si<sub>2</sub>) Calcd: C, 85.99; H, 6.89. Found: C, 86.18; H, 7.09.

**Deprotected** (*M*)-**Tetramer with 4-methyl-2-(2-methylpropyl)-pentanoxy-carbonyl side chains,** (*M*)-**bD-4H.**  $[\alpha]_D^{27}$  +566 (*c* 0.50, CHCl<sub>3</sub>). Anal. (C<sub>147</sub>H<sub>130</sub>O<sub>6</sub>) Calcd: C, 88.61; H, 6.58. Found: C, 88.68; H, 6.87.

- (*M*)-Hexamer with 4-methyl-2-(2-methylpropyl)-pentanoxycarbonyl side chains, (*M*)-bD-6. [ $\alpha$ ]<sub>D</sub><sup>27</sup> +520 (c 0.25, CHCl<sub>3</sub>). Anal. ( $C_{235}H_{222}O_{10}Si_2$ ) Calcd: C, 86.52; H, 6.86. Found: C, 86.14; H, 7.10.
- **3,5-Bis(trifluoromethanesulfonyloxy)iodobenzene, 20.** To a solution of 1,3-dihydroxy-5-iodobenzene **19** (1.73 g, 7.33 mmol) in pyridine (16 mL), trifluoromethanesulfonic anhydride (4.4 mL, 25.7 mmol) was added dropwise at -40 °C. Then the mixture was warmed to room temperature, and stirred 2 h. Water was

added, and the organic materials were extracted with ethyl acetate. The organic layer was washed with saturated aqueous ammonium chloride, saturated aqueous sodium hydroxyl carbonate, brine, and dried over magnesium sulfate. The solvent was evaporated under a reduced pressure, and separation by silica gel chromatography gave **20** (3.49 g, 6.98 mmol, 95 %). Mp 32–33 °C (ethyl acetate). MS (EI) m/z 500 (M<sup>+</sup>, 100 %), 113 (C<sub>6</sub>H<sub>3</sub>F<sub>2</sub>), 69 (CF<sub>3</sub>). HRMS Calcd for C<sub>8</sub>H<sub>3</sub>F<sub>6</sub>IO<sub>6</sub>S<sub>2</sub>: 499.8320.Found: 499.8319. IR (KBr) 1585, 1434, 1214, 1137, 973 cm<sup>-1</sup>. <sup>1</sup>H NMR (600 MHz, CDCl<sub>3</sub>)  $\delta$  7.25 (1H, t, J = 1.8 Hz), 7.70 (2H, d, J = 1.8 Hz). <sup>13</sup>C NMR (150 MHz, CDCl<sub>3</sub>)  $\delta$  93.5, 115.3,118.6 (q, J<sub>C-F</sub> = 319.3 Hz), 130.8, 149.1. <sup>19</sup>F NMR (565 MHz, CDCl<sub>3</sub>)  $\delta$  -73.6 (6F, s).

1-Heptadecafluorooctyl-3,5-bis(trifluoromethanesulfonyloxy)benzene, Under an argon atmosphere, a mixture of 20 (3.49 g, 6.98 mmol), heptadecafluoro-1-iodooctane (6.0 mL, 22.4 mmol), Cu powder (3.57 g, 56.1 mmol), and 2,2'bipyridyl (224 mg, 1.44 mmol) in N,N-dimethylformamide (35 mL) was stirred at 100 °C for 5 h. After being cooled to room temperature, the mixture was diluted with diethyl ether. Solids were removed by filtration, and washed with diethyl ether. The filtrate was poured to water, and the diethyl ether layer was separated. The organic layer was washed with 4 M HCl, water, brine, and dried over magnesium sulfate. The solvent was evaporated under reduced pressure, and silica gel chromatography gave **21** (4.24 g, 5.35 mmol, 77 %). Mp 49–50 °C (ethyl acetate). MS (EI) m/z 792 (M<sup>+</sup>, 19 %), 295 (C<sub>0</sub>H<sub>3</sub>O<sub>2</sub>F<sub>9</sub>, 100 %), 69 (CF<sub>3</sub>, 56 %). HRMS Calcd for C<sub>16</sub>H<sub>3</sub>F<sub>23</sub>O<sub>6</sub>S<sub>2</sub>: 791.9004. Found: 791.9018. IR (KBr) 1604, 1209, 1151 cm<sup>-1</sup>. <sup>1</sup>H NMR (600 MHz, CDCl<sub>3</sub>)  $\delta$  7.54 (1H, t, J = 1.8 Hz), 7.60 (2H, d, J = 1.8 Hz). <sup>13</sup>C NMR (150 MHz, CDCl<sub>3</sub>)  $\delta$  106.5–114.0 (m, br, CF<sub>2</sub>CF<sub>2</sub>CF<sub>2</sub>CF<sub>2</sub>CF<sub>2</sub>CF<sub>2</sub>CF<sub>2</sub>CF<sub>3</sub>), 117.3 (tq,  $J_{C-1}$  $_{\rm F} = 32.5 \text{ Hz}, 289.0 \text{ Hz}), 118.9 \text{ (q, } J_{\rm C-F} = 321.6 \text{ Hz}), 119.6, 120.7, 133.4 \text{ (t, } J_{\rm C-F} = 321.6 \text{ Hz})$  $_{\rm F} = 25.8 \text{ Hz}$ ), 150.0. <sup>19</sup>F NMR (559 MHz, CDCl<sub>3</sub>)  $\delta - 126.8$ , -126.7 (2F, m), -123.2 (2F, s, br), -122.4 (2F, s, br), -122.3 (2F, s, br), -122.0 (2F, s, br), -121.6(2F, s, br), -111.6 (2F, t, J = 14.3 Hz), -81.7 (3F, t, J = 10.0 Hz), -73.1 (6F, s).

Building block with perfluorooctyl side chains, (P)-F-1. Under an argon atmosphere, a mixture of 21 (1.00 g, 1.26 mmol), tris(dibenzylideneacetone)dipalladium(0) chloroform adduct (8.17 mg,  $7.89 \times 10^{-3}$  mmol), cuprous iodide (18.0 mg, 0.0947 mmol), tris(2,4,6-trimethylphenyl)phosphine (18.4 mg, 0.0473 mmol), triphenylphosphine (12.4 mg, 0.0473 mmol), tetrabutylammonium iodide (233 mg, 0.631 mmol), triethylamine (0.54 mL), N,N-dimethylformamide (2.6 mL), and THF (3.0 mL) was freeze-evacuated three times in flask A. In flask B, a solution of (P)-17 (119 mg, 0.316 mmol) in THF (4.8 mL) was freeze-evacuated three times, and was added dropwise to flask A. The mixture was stirred for 1.5 h at room temperature. The reaction was quenched by adding saturated aqueous ammonium chloride, and the organic materials were extracted with toluene and ethyl acetate. The organic layer was washed with brine and dried over magnesium sulfate. The solvent was evaporated under a reduced pressure, and separation by silica gel chromatography and recycling GPC gave (P)-F-1 (258 mg, 0.253 mmol, 80 % from (*P*)-17). Mp 169–171 °C (toluene-methanol).  $[\alpha]_D^{21}$  –233 (*c* 0.50, CHCl<sub>3</sub>). MS (FAB, NBA) m/z Calcd for C<sub>42</sub>H<sub>26</sub>F<sub>20</sub>O<sub>3</sub>SSi: 1018.1036. Found: 1018.1053. UV-Vis (CHCl<sub>3</sub>, 5.0 ×  $10^{-6}$  M)  $\lambda_{max}$  ( $\epsilon$ ) 336 nm (6.8 ×  $10^{4}$ ). CD (CHCl<sub>3</sub>, 5.0 ×  $10^{-6}$ 

M)  $\lambda(\Delta\varepsilon)$  297 nm (-18), 335 nm (21), 382 nm (-40). IR (KBr) 2152, 1433, 1249, 1215, 1144 cm<sup>-1</sup>. Anal. ( $C_{42}H_{26}F_{20}$  O<sub>3</sub>SSi) Calcd for: C, 49.52; H, 2.57; F, 37.30 %. Found: C, 49.48; H, 2.53; F, 37.10 %. <sup>1</sup>H NMR (600 MHz, CDCl<sub>3</sub>)  $\delta$  0.39 (9H, s), 1.93 (6H, s), 7.46 (1H, d, J = 7.2 Hz), 7.48 (1H, d, J = 7.2 Hz), 7.50 (1H, s), 7.68 (1H, dd, J = 7.8, 7.2 Hz), 7.70 (1H, dd, J = 7.8, 7.2 Hz), 7.80 (1H, s), 7.92 (1H, s), 8.01 (1H, s), 8.08 (1H, s), 8.41 (1H, d, J = 7.8 Hz), 8.43 (1H, d, J = 7.8 Hz). <sup>13</sup>C NMR (150 MHz, CDCl<sub>3</sub>)  $\delta$  0.086, 23.1, 90.7, 92.1, 100.4, 102.9, 105.0–117.0 (m, br, CF<sub>2</sub>CF<sub>2</sub>CF<sub>2</sub>CF<sub>2</sub>CF<sub>2</sub>CF<sub>2</sub>CF<sub>2</sub>CF<sub>3</sub>), 117.7, 118.1, 118.6, 119.78, 119.82, 120.6, 122.0, 123.2, 123.8, 127.07, 127.14, 127.8, 129.3, 129.4, 129.7, 129.8, 129.9, 130.6, 130.8, 131.0, 131.7, 131.8, 131.9, 132.0, 132.6, 136.9, 137.1, 149.3. <sup>19</sup>F NMR (565 MHz, CDCl<sub>3</sub>)  $\delta$  –127.3, –127.2 (2F, m), –123.9 (2F, s, br), –123.1 (2F, s, br), –122.9 (2F, s, br), –122.7 (2F, s, br), –122.3 (2F, s, br), –122.1 (2F, t, J = 13.3 Hz), –81.9 (3F, t, J = 9.6 Hz), –73.3 (3F, s).

(P)-Dimer with perfluorooctvl side chains, (P)-F-2. Under an argon atmosphere, a mixture of 21 (210 mg, 0.266 mmol), tris(dibenzylideneacetone)dipalladium(0) chloroform adduct (28.8 mg, 0.0266 mmol), cuprous iodide (60.7 mg, 0.319 mmol), tris(2,4,6-trimethylphenyl)phosphine (61.9 mg, 0.159 mmol), triphenylphosphine (41.8 mg, 0.159 mmol), tetrabutylammonium iodide (785 mg, 2.13 mmol), triethylamine (1.4 mL), N,N-dimethylformamide (4.6 mL), and THF (8.0 mL) was freeze-evacuated three times in flask A. In flask B, a solution of (P)-17 (200 mg, 0.531 mmol) in THF (15 mL) was freeze-evacuated three times, and was added dropwise to flask A. The mixture was stirred for 6 h at room temperature. The reaction was quenched by adding saturated aqueous ammonium chloride, and the organic materials were extracted with toluene and ethyl acetate. The organic layer was washed with brine and dried over magnesium sulfate. The solvent was evaporated under a reduced pressure, and separation by silica gel chromatography and recycling GPC gave (P)-F-2 (269 mg, 0.216 mmol, 81 % from 21). Mp 188–190 °C (toluene-methanol).  $[\alpha]_D^{20}$  –450 (c 0.25, CHCl<sub>3</sub>). MS (FAB, NBA) m/z Calcd for  $C_{68}H_{49}F_{17}Si_2$ : 1244.3101. Found: 1244.3121. UV–Vis (CHCl<sub>3</sub>, 5.0 × 10<sup>-6</sup> M)  $\lambda_{max}$ (ε) 335 nm (1.6 × 10<sup>5</sup>). CD (CHCl<sub>3</sub>, 5.0 × 10<sup>-6</sup> M)  $\lambda(\Delta \varepsilon)$  296 nm (-37), 335 nm (58), 383 nm (-85). IR (KBr) 2149, 1243, 1214, 1151, 845 cm<sup>-1</sup>. Anal. (C<sub>68</sub>H<sub>49</sub>F<sub>17</sub>Si<sub>2</sub>) Calcd for: C, 65.59; H, 3.97; F, 25.94 %. Found: C, 65.39; H, 4.09; F, 25.88 %. <sup>1</sup>H NMR (600 MHz, CDCl<sub>3</sub>) δ 0.39 (18H, s), 1.93 (6H, s), 1.94 (6H, s), 7.44 (2H, d, J = 7.2 Hz), 7.47 (2H, d, J = 7.2 Hz), 7.65 (2H, dd, J = J = 7.8, 7.2 Hz), 7.70 (2H, dd, J = 7.8, 7.2 Hz), 7.91 (2H, s), 8.00 (2H, s), 8.05 (2H, s), 8.19 (1H, s), 8.44 (2H, d, J = 7.8 Hz), 8.50 (2H, d, J = 7.8 Hz). <sup>13</sup>C NMR (150 MHz,  $CDCl_3$ )  $\delta$  0.12, 23.15, 23.17, 90.2, 92.2, 100.3, 103.1, 105–119 (m, br, CF<sub>2</sub>CF<sub>2</sub>CF<sub>2</sub>CF<sub>2</sub>CF<sub>2</sub>CF<sub>2</sub>CF<sub>2</sub>CF<sub>3</sub>), 119.3, 120.4, 123.5, 123.7, 125.0, 126.8, 127.0, 129.2, 129.3, 129.39, 129.43, 129.47, 129.8, 130.1, 130.8, 130.9, 131.0, 132.0, 132.5, 136.8, 137.0, 137.8. <sup>19</sup>F NMR (565 MHz, CDCl<sub>3</sub>)  $\delta$  –127.3, –127.2 (2F, m), -123.8 (2F, s, br), -123.0 (2F, s, br), -122.9 (2F, s, br), -122.5 (2F, s, br), -122.3(2F, s, br), -112.2 (2F, t, J = 13.3 Hz), -81.9 (3F, t, J = 9.6 Hz).

**Deprotected** (*P*)-**Dimer with perfluorooctyl side chains,** (*P*)-**F-2H.** To a solution of (*P*)-F-**2** (49.0 mg, 0.0394 mmol) in THF (2.9 mL) was added 1.0 M tetrabutylammonium fluoride in tetrahydrofran (0.10 mL, 0.10 mmol) at 0 °C. The

mixture was warmed to room temperature, and after being stirred for 1 h at the temperature, satured aqueous ammonium chloride was added. The organic materials were extracted with ethyl acetate and toluene. The organic layer was washed with brine, and dried over magnesium sulfate. The solvents were evaporated under reduced pressure, and silica gel chromatography gave (P)-F-2H (43.1 mg, 0.0392 mmol, 99 %). Mp 197 °C dec. (toluene-methanol).  $[\alpha]_D^{21}$  -418 (c 0.25, CHCl<sub>3</sub>). MS (FAB, NBA) m/z Calcd for  $C_{62}H_{33}F_{17}$ : 1100.2277. Found: 1100.2311. UV-Vis (CHCl<sub>3</sub>,  $5.0 \times 10^{-6}$  M)  $\lambda_{\text{max}}$  ( $\epsilon$ ) 330 nm (1.4 × 10<sup>5</sup>). CD (CHCl<sub>3</sub>,  $5.0 \times 10^{-6} \,\mathrm{M}$ )  $\lambda(\Delta\varepsilon)$  296 nm (-43), 329 nm (53), 382 nm (-77). IR (KBr) 3310, 1243, 1213, 1150 cm<sup>-1</sup>. Anal.  $(C_{62}H_{33}F_{17})$  Calcd for: C, 67.64; H, 3.02; F, 29.34 %. Found: C, 67.37; H, 3.14; F, 29.34 %.  $^{1}$ H NMR (600 MHz, CDCl<sub>3</sub>)  $\delta$ 1.69 (12H, s), 3.57 (2H, s), 7.47 (2H, d, J = 7.2 Hz), 7.49 (2H, d, J = 7.2 Hz), 7.68 (2H, dd, J = 7.8, 7.2 Hz), 7.73 (2H, dd, J = 7.8, 7.2 Hz), 7.90 (2H, s), 8.07 (2H, s), 8.11 (2H, s), 8.20 (1H, s), 8.46 (2H, d, J = 7.8 Hz), 8.51 (2H, d, J = 7.8 Hz)J = 7.8 Hz). <sup>13</sup>C NMR (150 MHz, CDCl<sub>3</sub>)  $\delta$  23.2, 81.8, 82.5, 90.1, 92.2, 105–119 (m, br, CF<sub>2</sub>CF<sub>2</sub>CF<sub>2</sub>CF<sub>2</sub>CF<sub>2</sub>CF<sub>2</sub>CF<sub>2</sub>CF<sub>3</sub>), 119.4, 119.5, 123.5, 123.6, 124.9, 127.0, 127.05, 127.07, 129.2, 129.3, 129.4, 129.45, 129.48, 130.1, 130.2, 130.4, 130.83, 130.85, 130.9, 132.1, 132.4, 136.9, 137.0, 137.7.  $^{19}$ F NMR (565 MHz, CDCl<sub>3</sub>)  $\delta$  – 127.3, -127.2 (2F, m), -123.8 (2F, s, br), -123.0 (2F, s, br), -122.9 (2F, s, br), -122.5 (2F, s, br), -122.3 (2F, s, br), -122.2 (2F, t, J = 13.8 Hz), -81.9 (2F, t, J = 9.6 Hz).

(P)-Trimer with perfluorooctyl side chains, (P)-F-3. Under an argon atmosphere, a mixture of (P)-F-1 (669 mg, 0.657 mmol), tris(dibenzylideneacetone)dipalladium(0) chloroform adduct (68.0 mg, 0.0657 mmol), cuprous iodide tris(2,4,6-trimethylphenyl)phosphine 0.789 mmol), 0.394 mmol), triphenylphosphine (103 mg, 0.394 mmol), tetrabutylammonium iodide (1.94 g, 5.26 mmol), triethylamine (1.7 mL), N,N-dimethylformamide (5.7 mL), and THF (13.5 mL) was freeze-evacuated three times in flask A. In flask B, a solution of (P)-18 (100 mg, 0.329 mmol) in THF (15 mL) was freezeevacuated three times, and was added dropwise to flask A. The mixture was stirred for 4 h at room temperature. The reaction was quenched by adding saturated aqueous ammonium chloride, and the organic materials were extracted with chloroform. The organic layer was washed with brine and dried over magnesium sulfate. The solvent was evaporated under a reduced pressure, and separation by silica gel chromatography and recycling GPC gave (P)-F-3 (517 mg, 0.253 mmol, 77 % from (P)-18). Mp higher than 250 °C (toluene-methanol).  $[\alpha]_D^{21}$  -462 (c 0.10, CHCl<sub>3</sub>). MALDI TOF-MS m/z Calcd for  ${}^{12}C_{105}{}^{13}CH_{66}F_{34}Si_2$ : 2041.6. Found: 2042.2. UV–Vis (CHCl<sub>3</sub>,  $5.0 \times 10^{-6}$  M)  $\lambda_{\text{max}}$  ( $\epsilon$ ) 335 nm (2.2 × 10<sup>5</sup>). CD  $(CHCl_3, 5.0 \times 10^{-6} \text{ M}) \lambda(\Delta \varepsilon)$  296 nm (-59), 335 nm (59), 386 nm (-132). IR (KBr) 2148, 1241, 1211, 1150 cm $^{-1}$ . Anal. ( $C_{106}H_{66}F_{34}Si_2$ ) Calcd for: C, 62.35; H, 3.26; F, 31.64 %. Found: C, 62.34; H, 3.40; F, 31.59 %. <sup>1</sup>H NMR (600 MHz, CDCl<sub>3</sub>)  $\delta$  0.39 (18H, s), 1.94 (6H, s), 1.95 (6H, s), 2.00 (6H, s), 7.46 (2H, d, J = 7.2 Hz, 7.49 (2H, d, J = 7.2 Hz), 7.52 (2H, d, J = 7.2 Hz), 7.68 (2H, dd, J = 7.8, 7.2 Hz, 7.72 (2H, dd, J = 7.8, 7.2 Hz), 7.75 (2H, dd, J = 7.8, 7.2 Hz), 7.91 (4H,s), 8.03 (2H, s), 8.10 (2H, s), 8.16 (2H, s), 8.22 (2H, s), 8.43 (2H, d,

Deprotected (P)-Trimer with perfluorooctyl side chains, (P)-F-3H. To a solution of (P)-F-3 (100 mg, 0.0490 mmol) in THF (10 mL) was added 1.0 M tetrabutylammonium fluoride in tetrabydrofran (0.15 mL, 0.15 mmol) at 0 °C. The mixture was warmed to room temperature, and after being stirred for 1 h at the temperature, satured aqueous ammonium chloride was added. The organic materials were extracted with chloroform. The organic layer was washed with brine, and dried over magnesium sulfate. The solvents were evaporated under reduced pressure, and silica gel chromatography gave (P)-F-3H (93.0 mg, 0.0490 mmol, quant.). Mp 210 °C dec. (toluene-methanol).  $\left[\alpha\right]_{D}^{21}$  -437 (c 0.10, CHCl<sub>3</sub>). MALDI TOF-MS m/z Calcd for C<sub>100</sub>H<sub>50</sub>F<sub>34</sub>: 1896.3. Found: 1896.7. UV-Vis (CHCl<sub>3</sub>, 5.0 ×  $10^{-6}$  M)  $\lambda_{\text{max}}$  ( $\epsilon$ ) 332 nm (2.0 ×  $10^{5}$ ). CD (CHCl<sub>3</sub>, 5.0 ×  $10^{-6}$  M)  $\lambda(\Delta \varepsilon)$  296 nm (-61), 331 nm (57), 386 nm (-119). IR (KBr) 3291, 1241, 1203, 1151 cm<sup>-1</sup>. Anal. ( $C_{100}H_{50}F_{34}$ ) Calcd for: C, 63.30; H, 2.66; F, 34.04 %. Found: C, 62.89; H, 2.67; F, 34.20 %. <sup>1</sup>H NMR (600 MHz, CDCl<sub>3</sub>, observed at 45 °C)  $\delta$ 1.96 (12H, s), 2.00 (6H, s), 3.55 (2H, s), 7.46 (2H, d, J = 7.2 Hz), 7.49 (2H, d, J = 7.2 Hz), 7.51 (2H, d, J = 7.2 Hz), 7.67 (2H, dd, J = 7.4, 7.2 Hz), 7.72 (2H, dd, J = 7.8, 7.2 Hz), 7.74 (2H, dd, J = 7.8, 7.2 Hz), 7.90–7.91 (4H, m), 8.06 (2H, s), 8.11 (2H, s), 8.15 (2H, s), 8.21 (2H, s), 8.45 (2H, d, J = 7.8 Hz), 8.51 (2H, d, J = 7.8 Hz), 8.53 (2H, d, J = 8.4 Hz). <sup>13</sup>C NMR (150 MHz, CDCl<sub>3</sub>, observed at 45 °C)  $\delta$  23.11, 23.13, 23.2, 81.8, 82.4, 90.2, 90.3, 92.3, 92.4, 105–119 (m, br, CF<sub>2</sub>CF<sub>2</sub>CF<sub>2</sub>CF<sub>2</sub>CF<sub>2</sub>CF<sub>2</sub>CF<sub>3</sub>), 119.5, 119.6, 119.7, 123.5, 123.6, 123.7, 125.0, 125.1, 127.08, 127.10, 127.2, 127.26, 127.28, 129.2, 129.3, 129.4, 129.50, 129.53, 130.1, 130.3, 130.4, 130.91, 130.94, 131.05, 131.08, 132.2, 132.3, 132.6, 136.9, 137.09. 137.13, 137.8. <sup>19</sup>F NMR (565 MHz, CDCl<sub>3</sub>)  $\delta$  –127.3, –127.2 (4F, m), – 123.8 (4F, s, br), -123.0 (4F, s, br), -122.9 (4F, s, br), -122.5 (4F, s, br), -122.3(4F, s, br), -112.2 (4F, t, J = 13.0 Hz), -81.9 (6F, t, J = 9.6 Hz).

(*P*)-Tetramer with perfluorooctyl side chains, (*P*)-F-4. Under an argon atmosphere, a mixture of (*P*)-F-1 (35.5 mg, 0.0349 mmol), tris(dibenzylidene-acetone)dipalladium(0) chloroform adduct (3.79 mg,  $3.49 \times 10^{-3}$  mmol), cuprous iodide (7.97 mg, 0.0419 mmol), tris(2,4,6-trimethylphenyl)phosphine (8.13 mg, 0.0209 mmol), triphenylphosphine (5.49 mg, 0.0209 mmol), tetrabutylammonium iodide (103 mg, 0.279 mmol), triethylamine (0.10 mL), *N*,*N*-dimethylformamide (0.30 mL), and THF (0.50 mL) was freeze-evacuated three times in flask A. In flask B, a solution of (*P*)-F-2H (19.2 mg, 0.0174 mmol) in THF (1.0 mL) was freeze-evacuated three times, and was added dropwise to flask A. The mixture was stirred for 6 h at room temperature. The reaction was quenched by adding

saturated aqueous ammonium chloride, and the organic materials were extracted with chloroform. The organic layer was washed with brine and dried over magnesium sulfate. The solvent was evaporated under a reduced pressure, and separation by silica gel chromatography and recycling GPC gave (P)-F-4 (24.3 mg,  $8.56 \times 10^{-3}$  mmol, 50 % from (P)-F-2H). Mp 240 °C dec. (toluene-methanol).  $[\alpha]_{\rm D}^{21}$  –532 (c 0.050, CHCl<sub>3</sub>). MALDI TOF–MS m/z Calcd for  $^{12}C_{143}^{13}CH_{83}F_{51}Si_2$ : 2837.8. Found: 2838.4. UV–Vis (CHCl<sub>3</sub>,  $5.0 \times 10^{-6}$  M)  $\lambda_{\text{max}}$  ( $\epsilon$ ) 336 nm  $(2.8 \times 10^5)$ . CD (CHCl<sub>3</sub>,  $5.0 \times 10^{-6}$  M)  $\lambda(\Delta \varepsilon)$  297 nm (-72), 336 nm (73), 389 nm (-174). IR (KBr) 2150, 1241, 1212, 1150 cm<sup>-1</sup>. Anal. (C<sub>144</sub>H<sub>83</sub>F<sub>51</sub>Si<sub>2</sub>) Calcd for: C, 60.94; H, 2.95; F, 34.14 %. Found: C, 60.75; H, 3.01; F, 33.70 %. <sup>1</sup>H NMR (600 MHz, CDCl<sub>3</sub>, observed at 50 °C)  $\delta$  0.38 (18H, s), 1.94 (6H, s), 1.95 (6H, s), 2.00 (12H, s), 7.44 (2H, d, J = 7.2 Hz), 7.47 (2H, d, J = 7.2 Hz), 7.51 (4H, d, J = 7.2 Hz), 7.66 (2H, dd, J = 7.8, 7.2 Hz), 7.70 (2H, dd, J = 7.8, 7.2 Hz), 7.74 (4H, dd, J = 7.8, 7.2 Hz) 7.90 (4H, s), 7.92 (2H, s), 8.01 (2H, s), 8.08 (2H, s), 8.14 (4H, s), 8.20 (2H, s), 8.22 (1H, s), 8.43 (2H, d, J = 7.8 Hz), 8.50(2H, d, J = 7.8 Hz), 8.53 (4H, d, J = 7.8 Hz). <sup>13</sup>C NMR (150 MHz, CDCl<sub>3</sub>, observed at 50 °C) δ 0.11, 23.1, 23.2, 90.18, 90.24, 90.3, 92.2, 92.42, 92.44, 100.4, 103.2, 105-119 (m, br, CF<sub>2</sub>CF<sub>2</sub>CF<sub>2</sub>CF<sub>2</sub>CF<sub>2</sub>CF<sub>2</sub>CF<sub>2</sub>CF<sub>3</sub>), 119.4, 119.7, 119.8, 120.6, 123.5, 123.6, 123.8, 125.0, 125.06, 125.11, 126.9, 127.0, 127.2, 127.3, 129.2, 129.3, 129.4, 129.48, 129.53, 129.6, 129.9, 130.1, 130.2, 130.4, 130.96, 131.03, 131.1, 132.2, 132.3, 132.6, 136.9, 137.1, 137.2, 137.8. <sup>19</sup>F NMR  $(565 \text{ MHz}, \text{CDCl}_3) \delta -127.3 (6\text{F}, \text{s}, \text{br}), -123.8 (6\text{F}, \text{s}, \text{br}), -123.0 (6\text{F}, \text{s}, \text{br}), -$ 122.9 (6F, s, br), -122.5 (6F, s, br), -122.3 (6F, s, br), -112.2 (6F, t, J = 12.4 Hz, -81.9 (9F, t, J = 9.6 Hz).

(P)-Pentamer with perfluorooctyl side chains, (P)-F-5. Under an argon atmosphere, a mixture of (P)-F-1 (59.3 mg, 0.0582 mmol), tris(dibenzylideneacetone)dipalladium(0) chloroform adduct (6.03 mg,  $5.82 \times 10^{-3}$  mmol), cuprous iodide (13.3 mg, 0.0698 mmol), tris(2.4.6-trimethylphenyl)phosphine (13.6 mg, 0.0349 mmol), triphenylphosphine (9.16 mg, 0.0349 mmol), tetrabutylammonium iodide (172 mg, 0.466 mmol), triethylamine (0.48 mL), N.N-dimethylformamide (1.6 mL), and THF (2.0 mL) was freeze-evacuated three times in flask A. In flask B, a solution of (P)-F-**3H** (55.2 mg, 0.0291 mmol) in THF (7.0 mL) was freezeevacuated three times, and was added dropwise to flask A. The mixture was stirred for 24 h at room temperature, and insoluble materials appeared. The reaction was quenched by adding saturated aqueous ammonium chloride. The solid was filtrated and washed with water, methanol, ethyl acetate, and hexane on the filter. The organic materials in the residual solution were extracted with toluene. The organic layer was washed with brine and dried over magnesium sulfate. The filtered solid was dissolved in toluene and was mixed with the organic layer. The solvent was evaporated under a reduced pressure, and separation by silica gel chromatography and recycling gel permeation chromatography gave (P)-F-5 (37.8 mg, 0.0104 mmol, 36 % from (P)-F-3H). Mp 230 °C dec. (toluene-methanol).  $\left[\alpha\right]_{D}^{21}$ -335 (c 0.05, CHCl<sub>3</sub>). MALDI TOF-MS m/z Calcd for  ${}^{12}C_{180}^{13}C_2H_{100}F_{68}Si_2$ : 3634.9. Found: 3635.6. UV-Vis (CHCl<sub>3</sub>,  $5.0 \times 10^{-6}$  M)  $\lambda_{max}$  ( $\epsilon$ ) 336 nm  $(3.5 \times 10^5)$ . CD (CHCl<sub>3</sub>,  $5.0 \times 10^{-6}$  M)  $\lambda(\Delta \varepsilon)$  297 nm (-96), 337 nm (89),

389 nm (-245). IR (KBr) 2209, 2151, 1242, 1211, 1150 cm<sup>-1</sup>. Anal. ( $C_{182}H_{100}F_{68}Si_2$ ) Calcd for: C, 60.14; H, 2.77; F, 35.54 %. Found: C, 59.85; H, 3.08; F, 35.28 %. <sup>1</sup>H NMR (600 MHz, CDCl<sub>3</sub>)  $\delta$  0.36 (18H, s), 1.92 (6H, s), 1.93 (6H, s), 1.97 (12H, s), 1.98 (6H, s), 7.44 (2H, d, J = 7.2 Hz), 7.46 (2H, d, J = 7.2 Hz), 7.49–7.51 (6H, m), 7.65 (2H, dd, J = 7.8, 7.2 Hz), 7.70 (2H, dd, J = 7.8, 7.2 Hz), 7.72–7.75 (6H, m), 7.88–7.90 (4H, m), 7.91 (4H, s), 8.01 (2H, s), 8.08 (2H, s), 8.15 (4H, s), 8.16 (2H, s), 8.20 (2H, s), 8.22 (2H, s), 8.41 (2H, d, J = 7.8 Hz), 8.49 (2H, d, J = 7.8 Hz), 8.52–8.53 (6H, m). <sup>13</sup>C NMR (150 MHz, CDCl<sub>3</sub>, observed at 50 °C)  $\delta$  1.00, 23.1, 23.2, 23.3, 29.7, 105–119 (m, br), 119.4, 119.7, 119.8, 120.6, 123.5, 123.6, 123.8, 124.7, 125.0, 125.1, 127.0, 127.20, 127.22, 127.3, 129.2, 129.3, 129.4, 129.8, 129.9, 130.1, 130.2, 131.0, 131.1, 131.3, 132.2, 132.3, 137.8. <sup>19</sup>F NMR (565 MHz, CDCl<sub>3</sub>)  $\delta$  –127.3 (8F, s, br), –123.0 (8F, s, br), –122.9 (8F, s, br), –122.5 (8F, s, br), –122.3 (8F, s, br), –112.2 (8F, t, J = 12.4 Hz), –81.9 (12F, t, J = 9.6 Hz).

(P)-Tetramer with alternating decyloxycarbonyl/perfluorooctyl side chains, (P)-DF-4 (Typical procedure for the Sonogashira coupling reaction of (P)-DF**n and** (P)-FD-n). Under an argon atmosphere, a mixture of (P)-D-1 [1] (114 mg, tris(dibenzylideneacetone)dipalladium(0) chloroform (15.1 mg, 0.0145 mmol), cuprous iodide (33.2 mg, 0.174 mmol), tris(2,4,6-trimethylphenyl)phosphine (33.9 mg, 0.0872 mmol), triphenylphosphine (22.9 mg, 0.0872 mmol), tetrabutylammonium iodide (429 mg, 1.16 mmol), triethylamine (0.26 mL), N,N-dimethylformamide (1.3 mL), and THF (1.0 mL) was freezeevacuated three times in flask A. In flask B, a solution of (P)-F-2H (80.0 mg, 0.0727 mmol) in THF (2.9 mL) was freeze-evacuated three times, and the mixture was slowly added to flask A. The mixture was stirred at 45 °C for 2 h. The reaction was quenched by adding saturated aqueous ammonium chloride, and the organic materials were extracted with toluene three times. The combined organic layer was washed with water, brine, and dried over magnesium sulfate. The solvents were evaporated under reduced pressure, and separation by silica gel chromatography and recycling GPC gave (P)-DF-4 as yellow solid (153 mg, 0.0646 mmol, 89 %). Mp 228–230 °C (toluene-methanol).  $\left[\alpha\right]_{D}^{22}$  –473 (c 0.10, CHCl<sub>3</sub>). MALDI-TOF MS m/z Calcd for  ${}^{12}C_{149}^{13}CH_{125}F_{17}O_4Si_2$ : 2369.9. Found: 2370.3. UV–Vis (CHCl<sub>3</sub>,  $5.0 \times 10^{-6} \text{ M}$ )  $\lambda_{\text{max}}$  ( $\epsilon$ ) 336 nm (2.8 × 10<sup>5</sup>). CD (CHCl<sub>3</sub>, 5.0 × 10<sup>-6</sup> M)  $\lambda(\Delta \epsilon)$ 297 nm (-54), 333 nm (89), 387 nm (-175). IR (KBr) 2924, 2148, 1724, 1240,  $1207 \text{ cm}^{-1}$ . Anal. ( $C_{150}H_{125}F_{17}O_4Si_2$ ) Calcd: C, 75.99; H, 5.31; F, 13.62. Found: C, 75.77; H, 5.48; F, 13.58. <sup>1</sup>H NMR (600 MHz, CDCl<sub>3</sub>) δ 0.39 (18H, s), 0.86 (6H, t, J = 6.6 Hz), 1.26–1.42 (24H, m), 1.50 (4H, quin, J = 7.2 Hz), 1.85 (4H, quin, J = 7.2 Hz, 1.93 (6H, s), 1.95 (6H, s), 2.00 (12H, s), 4.42 (4H, t, J = 6.6 Hz), 7.44 (2H, d, J = 7.2 Hz), 7.47 (2H, d, J = 7.2 Hz), 7.50–7.52 (4H, m), 7.65 (2H, t, J = 7.2 Hz), 7.70–7.75 (6H, m), 7.92 (2H, s), 8.00 (2H, s), 8.05 (2H, s), 8.08 (2H, s), 8.09 (2H, s), 8.18 (2H, s), 8.22 (1H, s), 8.35 (2H, s), 8.36 (2H, s), 8.43 (2H, d, J = 7.8 Hz), 8.53–8.56 (6H, m). <sup>13</sup>C NMR (150 MHz, CDCl<sub>3</sub>)  $\delta$  0.12, 14.1, 22.7, 23.1, 23.17, 23.23, 26.1, 28.8, 29.31, 29.33, 29.6, 31.9, 65.8, 89.3, 89.4, 90.2, 92.3, 92.9, 93.1, 100.2, 103.1, 119.5, 119.7, 120.0, 120.4, 123.5, 123.6, 123.7, 124.3, 124.4, 124.9, 126.7, 126.9, 127.0, 127.108, 127.12, 129.1, 129.2, 129.36, 129.37, 129.5, 129.8, 129.9, 130.1, 130.9, 130.98, 131.02, 131.5, 132.1, 132.3, 132.38, 132.40, 136.8, 136.9, 136.97, 137.02, 137.8, 138.3, 165.4. <sup>19</sup>F NMR (565 MHz, CDCl<sub>3</sub>)  $\delta$  –127.4 (2F, s, br), –124.0 (2F, s, br), –123.1 (2F, s, br), –123.0 (2F, s, br), –122.6 (2F, s, br), –122.4 (2F, s, br), –122.3 (2F, t, J = 13.3 Hz), –82.1 (3F, t, J = 9.9 Hz).

Deprotected (P)-Tetramer with alternating decyloxycarbonyl/perfluorooctvl side chains, (P)-DF-4H (Typical procedure for desilvlation of (P)-DF-n). To a solution of (P)-DF-4 (150 mg, 0.0634 mmol) in THF (1.8 mL) was added 1.0 M tetrabutylammonium fluoride in THF (0.16 mL, 0.16 mmol) at 0 °C. After being stirred at the temperature for 30 min, the reaction was quenched by adding saturated aqueous ammonium chloride. The organic materials were extracted with toluene. The organic layer was washed with water, brine, and dried over magnesium sulfate. The solvents were evaporated under reduced pressure, and silica gel chromatography gave (P)-DF-4H as yellow solid (141 mg, 0.0634 mmol, quant.). Mp 175 °C, decomp. (chloroform–methanol).  $[\alpha]_D^{23}$  –523 (c 0.10, CHCl<sub>3</sub>). MALDI-TOF MS m/z Calcd for  $^{12}C_{143}^{13}CH_{109}F_{17}O_4$ : 2225.8. Found: 2226.3. UV– Vis (CHCl<sub>3</sub>,  $5.0 \times 10^{-6}$  M)  $\lambda_{max}$  ( $\epsilon$ ) 333 nm ( $2.4 \times 10^{5}$ ). CD (CHCl<sub>3</sub>,  $5.0 \times 10^{-6}$ M)  $\lambda(\Delta \varepsilon)$  297 nm (-73), 329 nm (62), 387 nm (-166). IR (KBr) 2924, 2207, 1723, 1240, 1207 cm<sup>-1</sup>. Anal. ( $C_{144}H_{109}F_{17}O_4$ ) Calcd: C, 77.68; H, 4.93; F, 14.51. Found: C, 77.44; H, 5.18; F, 14.24. <sup>1</sup>H NMR (600 MHz, CDCl<sub>3</sub>) δ 0.85 (6H, t, J = 7.2 Hz, 1.26–1.43 (24H, m), 1.50 (4H, quin, J = 7.2 Hz), 1.85 (4H, quin, J = 7.2 Hz, 1.95 (12H, s), 1.99 (12H, s), 3.56 (2H, s), 4.42 (4H, t, J = 7.2 Hz), 7.45 (2H, d, J = 7.2 Hz), 7.48 (2H, d, J = 7.2 Hz), 7.50–7.52 (4H, m), 7.66 (2H, t, J = 7.8 Hz), 7.70–7.76 (6H, m), 7.92 (2H, s), 8.04 (2H, s), 8.07 (2H, s), 8.11 (2H, s), 8.12 (2H, s), 8.18 (2H, t, J = 1.5 Hz), 8.22 (1H, s), 8.35 (2H, t, J = 1.5 Hz)J = 1.5 Hz), 8.36 (2H, t, J = 1.5 Hz), 8.44 (2H, d, J = 7.8 Hz), 8.53 (4H, d, J = 7.8 Hz), 8.55 (2H, d, J = 7.8 Hz). <sup>13</sup>C NMR (150 MHz, CDCl<sub>3</sub>)  $\delta$  14.1, 22.7, 23.17, 23.23, 26.1, 28.7, 29.3, 29.5, 29.6, 31.9, 65.8, 81.8, 82.4, 89.27, 89.31, 90.1, 92.3, 92.9, 93.1, 119.4, 119.5, 119.8, 119.9, 123.5, 123.55, 123.57, 123.6, 124.29, 124.32, 124.9, 126.8 126.95, 127.00, 127.10, 127.12, 129.0, 129.2, 129.25, 129.35, 129.4, 129.5, 129.8, 130.1, 130.4, 130.86, 130.94, 130.97, 130.99, 131.02, 131.5, 132.1, 132.2, 132.3, 132.4, 136.8, 136.9, 136.98, 137.02, 137.8, 138.3, 165.4. <sup>19</sup>F NMR (565 MHz, CDCl<sub>3</sub>)  $\delta$  -127.2 (2F, s, br), -123.8 (2F, s, br), -123.0 (2F, s, br), -122.9 (2F, s, br), -122.4 (2F, s, br), -122.2 (2F, s, br), -122.1 (2F, t, J = 13.6 Hz), -81.9 (3F, t, J = 9.9 Hz).

(*P*)-Hexamer with alternating perfluorooctyl/decyloxycarbonyl side chains, (*P*)-FD-6. The compound (214 mg, 0.0539 mmol, 80 %) was prepared from (*P*)-DF-4H (150 mg, 0.0674 mmol) and (*P*)-F-1 (137 mg, 0.135 mmol) as yellow solid. Mp > 240 °C (chloroform–methanol). [α]<sub>D</sub><sup>22</sup> –433 (*c* 0.10, CHCl<sub>3</sub>). MALDI-TOF MS m/z Calcd for  $^{12}\text{C}_{225}^{13}\text{CH}_{159}\text{F}_{51}\text{O}_4\text{Si}_2$ : 3962.1. Found: 3962.2. UV–Vis (CHCl<sub>3</sub>, 2.5 × 10<sup>-6</sup> M)  $\lambda_{\text{max}}$  (ε) 338 nm (4.2 × 10<sup>5</sup>). CD (CHCl<sub>3</sub>, 5.0 × 10<sup>-6</sup> M)  $\lambda(\Delta\varepsilon)$  297 nm (–85), 336 nm (118), 388 nm (–265). IR (KBr) 2925, 2205, 1726, 1241, 1207 cm<sup>-1</sup>. Anal. (C<sub>226</sub>H<sub>159</sub>F<sub>51</sub>O<sub>4</sub>Si<sub>2</sub>) Calcd: C, 68.48; H, 4.04; F, 24.44. Found: C, 68.12; H, 4.26; F, 24.51.  $^{1}$ H NMR (600 MHz, CDCl<sub>3</sub>)  $\delta$  0.39 (18H, s), 0.85 (6H, t, J = 7.2 Hz), 1.26–1.42 (24H, m), 1.49 (4H, quin,

J = 7.2 Hz), 1.85 (4H, quin, J = 7.2 Hz), 1.93 (6H, s), 1.94 (6H, s), 1.99 (24H, s), 4.42 (4H, t, J = 7.2 Hz), 7.45 (2H, d, J = 7.2 Hz), 7.48 (2H, d, J = 7.2 Hz), 7.50–7.51 (8H, m), 7.66 (2H, dd, J = 7.8, 7.2 Hz), 7.70–7.75 (10H, m), 7.90–7.92 (6H, m), 8.00 (2H, s), 8.06 (2H, s), 8.09 (4H, s), 8.10 (4H, s), 8.19 (2H, s), 8.20 (2H, s), 8.22 (1H, s), 8.36 (4H, s), 8.43 (2H, d, J = 7.8 Hz), 8.53–8.56 (10H, m). <sup>13</sup>C NMR (150 MHz, CDCl<sub>3</sub>) δ 0.19, 14.2, 22.8, 23.23, 23.25, 23.32, 26.2, 28.8, 29.4, 29.7, 29.8, 32.0, 65.9, 89.4, 90.22, 90.23, 90.3, 92.3, 92.4, 93.1, 100.4, 103.1, 115.5–118.4 (m, br), 119.4, 119.6, 120.0, 120.5, 123.5, 123.6, 123.7, 123.8, 124.4, 124.98, 125.00, 125.02, 126.9, 127.06, 127.10, 127.2, 129.3, 129.4, 129.5, 129.46, 129.54, 129.9, 130.2, 130.3, 130.4, 130.9, 131.0, 130.07, 131.10, 131.6, 132.1, 132.2, 132.4, 132.5, 136.9, 137.0, 137.07, 137.10, 137.8, 138.4, 165.5. <sup>19</sup>F NMR (565 MHz, CDCl<sub>3</sub>) δ −127.3 (6F, s, br), −123.9 (6F, s, br), −123.0 (6F, s, br), −122.9 (6F, s, br), −122.5 (6F, s, br), −122.3 (6F, s, br), −122.2 (6F, t, J = 14.1 Hz), −82.1 (9F, t, J = 9.3 Hz).

Deprotected (P)-hexamer with alternating perfluorooctyl/decyloxycarbonyl side chains, (P)-FD-6H. The compound (92.0 mg, 0.0241 mmol, 99 %) was prepared from (P)-FD-6 (96.1 mg, 0.0242 mmol) as yellow solid. Mp 185 °C, decomp. (chloroform–methanol).  $\left[\alpha\right]_{D}^{23}$  –437 (c 0.10, CHCl<sub>3</sub>). MALDI-TOF MS m/z Calcd for  ${}^{12}C_{218}^{13}C_2H_{143}F_{51}O_4$ : 3819.0. Found: 3818.7. UV-Vis (CHCl<sub>3</sub>,  $2.5 \times 10^{-6} \text{ M}$ )  $\lambda_{\text{max}}$  ( $\epsilon$ ) 336 nm (3.8 × 10<sup>5</sup>). CD (CHCl<sub>3</sub>, 5.0 × 10<sup>-6</sup> M)  $\lambda(\Delta \epsilon)$ 296 nm (-104), 332 nm (88), 389 nm (-259). IR (KBr) 2925, 2207, 1725, 1241,  $1208 \text{ cm}^{-1}$ . Anal. ( $C_{220}H_{143}F_{51}O_4$ ) Calcd: C, 69.18; H, 3.77; F, 25.37. Found: C, 68.86; H, 4.17; F, 25.29. <sup>1</sup>H NMR (600 MHz, CDCl<sub>3</sub>, observed at 40 °C)  $\delta$  0.85 (6H, t, J = 7.2 Hz), 1.26–1.36 (24H, m), 1.41 (4H, quin, J = 7.2 Hz), 1.85 (4H, quin, J = 7.2 Hz), 1.95 (12H, s), 1.99 (24H, s), 3.54 (2H, s), 4.42 (4H, t, J = 7.2 Hz), 7.45 (2H, d, J = 7.2 Hz), 7.48 (2H, d, J = 7.2 Hz), 7.49–7.51 (8H, m), 7.65 (2H, t, J = 7.8 Hz), 7.70–7.74 (10H, m), 7.89 (2H, s), 7.90 (2H, s), 7.91(2H, s), 8.04 (2H, s), 8.08 (2H, s), 8.11 (4H, m), 8.12 (4H, m), 8.19 (4H, s), 8.22 (1H, s), 8.35–8.36 (4H, m), 8.44 (2H, d, J = 7.8 Hz), 8.50–8.56 (10H, m). <sup>13</sup>C NMR (150 MHz, CDCl<sub>3</sub>, observed at 40 °C)  $\delta$  14.0, 22.7, 23.1, 23.2, 26.1, 28.8, 29.31, 29.34, 29.6, 31.9, 65.9, 81.8, 82.4, 89.4, 90.2, 92.3, 92.4, 93.1, 105.0–119.0 (m, br), 119.5, 119.56, 119.59, 120.0, 123.5, 123.55, 123.62, 123.7, 124.4, 125.0, 127.03, 127.05, 127.07, 127.09, 127.12, 127.2, 129.25, 129.33, 129.36, 129.38, 129.4, 129.5, 129.9, 130.08, 130.14, 130.3, 130.4, 130.5, 130.87, 130.90, 131.0, 131.05, 131.08, 131.7, 132.1, 132.2, 132.4, 132.46, 132.52, 136.9, 137.0, 137.1, 137.8, 138.3, 165.4. <sup>19</sup>F NMR (565 MHz, CDCl<sub>3</sub>, observed at 40 °C)  $\delta$  -127.1 (6F, s, br), -123.7 (6F, s, br), -122.9 (6F, s, br), -122.7 (6F, s, br), -122.3 (6F, s, br), -122.1 (6F, s, br), -122.0 (6F, t, J = 12.7 Hz), -81.9 (9F, t, J = 8.5 Hz).

(*P*)-Octamer with alternating decyloxycarbonyl/perfluorooctyl side chains, (*P*)-DF-8. The compound (51.8 mg, 0.0102 mmol, 79 %) was prepared from (*P*)-FD-6H (49.0 mg, 0.0128 mmol) and (*P*)-D-1 (20.4 mg, 0.0259 mmol) as yellow solid. Mp > 240 °C (chloroform—methanol). [α]<sub>D</sub><sup>23</sup> -487 (*c* 0.10, CHCl<sub>3</sub>). MALDI-TOF MS m/z Calcd for  $^{12}$ C<sub>308</sub>H<sub>235</sub>F<sub>51</sub>O<sub>8</sub>Si<sub>2</sub>: 5085.7. Found: 5085.9. UV–Vis (CHCl<sub>3</sub>, 2.5 × 10<sup>-6</sup> M)  $\lambda_{max}$  (ε) 339 nm (5.4 × 10<sup>5</sup>). CD (CHCl<sub>3</sub>, 2.5 × 10<sup>-6</sup>

M)  $\lambda(\Delta \varepsilon)$  297 nm (-112), 336 nm (155), 389 nm (-374). IR (KBr) 2958, 2208, 1724, 1241, 1207 cm<sup>-1</sup>. Anal.  $(C_{308}H_{235}F_{51}O_8Si_2)$  Calcd: C, 72.69; H, 4.65; F, 19.04. Found: C, 72.37; H, 4.95; F, 18.78. <sup>1</sup>H NMR (600 MHz, CDCl<sub>3</sub>)  $\delta$  0.38 (18H, s), 0.85 (12H, t, J = 7.2 Hz), 1.26–1.34 (40H, m), 1.34–1.47 (8H, m), 1.49-1.53 (8H, m), 1.82-1.88 (8H, m), 1.93 (6H, s), 1.94 (6H, s), 1.98 (36H, s), 4.40-4.43 (8H, m), 7.44 (2H, d, J = 7.2 Hz), 7.47 (2H, d, J = 7.2 Hz), 7.50-7.51(12H, m), 7.66 (2H, t, J = 7.8 Hz), 7.70–7.75 (14H, m), 7.90–7.91 (6H, m), 8.01 (2H, s), 8.05 (2H, s), 8.10–8.11 (12H, m), 8.18 (2H, s), 8.19 (2H, s), 8.22 (3H, s), 8.33–8.35 (8H, m), 8.42 (2H, d, J = 7.8 Hz), 8.52–8.55 (14H, m), <sup>13</sup>C NMR (150 MHz, CDCl<sub>3</sub>)  $\delta$  0.11, 14.1, 22.6, 23.1, 23.16, 23.21, 26.1, 28.8, 29.31, 29.33, 29.6, 29.65, 29.70, 31.9, 65.8, 89.28, 89.30, 89.4, 90.2, 92.3, 92.9, 93.1, 100.2, 103.1, 108.3–118.1 (m, br), 119.5, 119.7, 119.9, 120.4, 123.5, 123.6, 123.66, 123.68, 124.3, 124.4, 124.9, 126.7, 126.9, 127.0, 127.1, 129.1, 129.2, 129.4, 129.5, 129.8, 129.9, 130.0, 130.1, 130.2, 130.9, 131.0, 131.5, 132.1, 132.3, 132.4, 136.8, 136.9, 136.98, 137.02, 137.8, 138.3, 165.4. <sup>19</sup>F NMR (565 MHz, CDCl<sub>3</sub>)  $\delta$  –127.3 (6F, s, br), -123.9 (6F, s, br), -123.0 (6F, s, br), -122.9 (6F, s, br), -122.4 (6F, s, br)br), -122.3 (6F, s, br), -122.2 (6F, t, J = 13.0 Hz), -82.1 (9F, t, J = 9.0 Hz).

Deprotected (P)-Octamer with alternating decyloxycarbonyl/perfluorooctvl side chains, (P)-DF-8H. The compound (61.7 mg, 0.0125 mmol, quant.) was prepared from (P)-DF-8 (63.5 mg, 0.0125 mmol) as yellow solid. Mp 212 °C, decomp. (chloroform–methanol).  $\left[\alpha\right]_{D}^{23}$  –453 (c 0.10, CHCl<sub>3</sub>). MALDI-TOF MS  $\it m/z$  Calcd for  $^{12}C_{301}^{13}CH_{219}F_{51}O_8$ : 4942.6. Found: 4942.5. UV–Vis (CHCl<sub>3</sub>,  $2.5 \times 10^{-6} \text{ M}$ )  $\lambda_{\text{max}}$  ( $\epsilon$ ) 337 nm (4.9 × 10<sup>5</sup>). CD (CHCl<sub>3</sub>, 2.5 × 10<sup>-6</sup> M)  $\lambda(\Delta \epsilon)$ 297 nm (-133), 337 nm (158), 389 nm (-374). IR (KBr) 2924, 2207, 1725, 1240, 1207 cm<sup>-1</sup>. Anal. (C<sub>302</sub>H<sub>219</sub>F<sub>51</sub>O<sub>8</sub>) Calcd: C, 73.35; H, 4.46; F, 19.59. Found: C. 73.10; H, 4.72; F, 19.34. <sup>1</sup>H NMR (600 MHz, CDCl<sub>3</sub>, observed at 50 °C)  $\delta$  0.85 (12H, t, J = 6.6 Hz), 1.26-1.35 (48H, m), 1.39-1.42 (8H, m), 1.82-1.87 (8H, m),1.95 (12H, s), 1.98 (36H, s), 3.53 (2H, s), 4.40-4.43 (8H, m), 7.44 (2H, d, J = 6.6 Hz), 7.46–7.50 (14H, m), 7.64 (2H, d, J = 7.2 Hz), 7.69–7.72 (14H, m), 7.90 (6H, s), 8.03 (2H, s), 8.06 (2H, s), 8.10–8.11 (12H, m), 8.16 (2H, s), 8.18 (2H, s), 8.21 (3H, s), 8.32 (2H, s), 8.35 (6H, m), 8.43 (2H, d, J = 7.8 Hz), 8.50–8.55 (14H, m).  $^{13}$ C NMR (150 MHz, CDCl<sub>3</sub>, observed at 50 °C)  $\delta$  15.4, 26.6, 33.5, 33.89, 33.92, 36.3, 38.5, 38.8, 38.9, 39.1, 40.9, 68.1, 80.9, 81.3, 86.92, 86.94, 87.6, 89.3, 89.8, 89.9, 95.4, 111.0, 111.1, 111.3, 111.5, 114.2, 114.3, 114.4, 114.9, 115.4, 116.9, 116.98, 117.02, 117.10, 117.12, 118.77, 118.81, 118.9, 118.98, 119.01, 119.3, 119.5, 119.7, 119.8, 120.2, 120.3, 120.8, 121.20, 121.24, 121.3, 121.37, 121.41, 124.9, 125.0, 125.05, 125.08, 125.6, 126.0, 147.7. <sup>19</sup>F NMR (565 MHz, CDCl<sub>3</sub>)  $\delta$  –127.3 (6F, s, br), –123.9 (6F, s, br), –123.1 (6F, s, br), -122.9 (6F, s, br), -122.5 (6F, s, br), -122.3 (6F, s, br), -112.2 (6F, s, br), -82.0(9F, t, J = 9.6 Hz).

(*P*)-Decamer with alternating perfluorooctyl/decyloxycarbonyl side chains, (*P*)-FD-10. The compound (17.4 mg, 0.00260 mmol, 40 %) was prepared from (*P*)-DF-8H (32.0 mg, 0.00647 mmol) and (*P*)-F-1 (13.2 mg, 0.0129 mmol) as yellow solid. Mp > 240 °C (chloroform–methanol).  $[\alpha]_D^{23}$  –394 (*c* 0.10, CHCl<sub>3</sub>). MALDI-TOF MS m/z Calcd for  $C_{384}H_{269}F_{85}O_8Si_2$ : 6677.9. Found: 6678.4. UV–

Vis (CHCl<sub>3</sub>,  $2.5 \times 10^{-6}$  M)  $\lambda_{\text{max}}$  ( $\epsilon$ ) 338 nm ( $6.9 \times 10^{5}$ ). CD (CHCl<sub>3</sub>,  $2.5 \times 10^{-6}$ M)  $\lambda(\Delta \varepsilon)$  296 nm (-147), 338 nm (158), 390 nm (-466). IR (KBr) 2924, 2208, 1725, 1241, 1208 cm<sup>-1</sup>. Anal.  $(C_{384}H_{269}F_{85}O_8Si_2)$  Calcd: C, 69.02; H, 4.06; F, 24.17. Found: C, 68.68; H, 4.37; F, 23.92. <sup>1</sup>H NMR (600 MHz, CDCl<sub>3</sub>, observed at 50 °C)  $\delta$  0.38 (18H, s), 0.85 (12H, t, J = 6.6 Hz), 1.26–1.34 (48H, m), 1.38–1.43 (8H, m), 1.82–1.87 (8H, m), 1.93 (6H, s), 1.94 (6H, s), 1.98–1.99 (48H, s), 4.42 (8H, t, J = 6.6 Hz), 7.44 (2H, d, J = 7.2 Hz), 7.46–7.50 (18H, m), 7.65 (2H, t, J = 7.2 Hz), 7.69-7.73 (18H, m), 7.89-7.90 (10H, m), 8.00 (2H, s), 8.07(2H, s), 8.11–8.13 (16H, m), 8.18–8.21 (9H, m), 8.34–8.35 (6H, m), 8.35 (2H, s), 8.42 (2H, d, J = 7.8 Hz), 8.49–8.55 (18H, m). <sup>13</sup>C NMR (150 MHz, CDCl<sub>3</sub>, observed at 55 °C) δ 0.12, 14.0, 22.6, 22.7, 23.0, 23.06, 23.08, 23.13, 23.9, 26.1, 28.8, 29.0, 29.29, 29.34, 29.4, 29.6, 29.67, 29.71, 30.5, 31.9, 32.0, 36.4, 39.0, 65.9, 89.4, 90.28, 90.30, 92.4, 93.2, 100.0, 103.2, 119.5, 119.7, 120.1, 120.6, 123.5, 123.6, 123.73, 123.74, 123.75, 123.81, 124.5, 125.08, 125.10, 125.13, 126.9, 127.0, 127.13, 127.14, 127.16, 127.17, 127.19, 129.2, 129.28, 129.29, 129.37, 129.39, 129.45, 129.47, 129.48, 129.87, 129.88, 130.17, 130.18, 130.19, 131.05, 131.12, 131.13, 131.14, 131.8, 132.2, 132.3, 132.46, 132.48, 132.50, 132.6, 136.6, 136.7, 136.8, 136.9, 137.02, 137.05, 137.07, 137.10, 137.13,, 137.76, 137.78, 137.80, 138.3, 165.4. <sup>19</sup>F NMR (565 MHz, CDCl<sub>3</sub>, observed at 40 °C)  $\delta$  –127.2 (10F, s, br), -123.8 (10F, s, br), -123.0 (10F, s, br), -122.9 (10F, s, br), -122.4(10F, s, br), -122.2 (10F, s, br), -112.1 (10F, s, br), -82.0 (15F, t, J = 8.8 Hz).(P)-Tetramer with alternating perfluorooctyl/decyloxycarbonyl side chains, (P)-FD-4. The compound (369 mg, 0.142 mmol, 78 %) was prepared from (P)-D-**2H** (158 mg, 0.182 mmol) and (P)-F-1 (289 mg, 0.364 mmol) as yellow solid. Mp > 240 °C (chloroform–methanol).  $[\alpha]_D^{22}$  –467 (c 0.10, CHCl<sub>3</sub>). MALDI-TOF MS m/z Calcd for  $C_{147}H_{104}F_{34}O_2Si_2$ : 2602.7. Found: 2603.2. UV–Vis (CHCl<sub>3</sub>,  $5.0 \times 10^{-6} \text{ M}$ )  $\lambda_{\text{max}}$  ( $\epsilon$ ) 336 nm (3.0 × 10<sup>5</sup>). CD (CHCl<sub>3</sub>, 5.0 × 10<sup>-6</sup> M)  $\lambda(\Delta\epsilon)$ 297 nm (-62), 335 nm (96), 388 nm (-188). IR (KBr) 2926, 2148, 1726, 1241,  $1212 \text{ cm}^{-1}$ . Anal.  $(C_{147}H_{104}F_{34}O_2Si_2)$  Calcd: C, 67.79; H, 4.02; F, 24.80. Found: C, 67.77; H, 4.37; F, 24.61. <sup>1</sup>H NMR (600 MHz, CDCl<sub>3</sub>) δ 0.39 (18H, s), 0.85 (6H, t, J = 7.0 Hz), 1.26–1.43 (12H, m), 1.50 (2H, quin, J = 7.6 Hz), 1.86 (2H, quin, J = 7.2 Hz, 1.93 (6H, s), 1.94 (6H, s), 2.00 (12H, s), 4.43 (4H, t, J = 6.8 Hz), 7.44 (2H, d, J = 7.0 Hz), 7.47 (2H, d, J = 6.7 Hz), 7.51 (4H, d, J = 7.2 Hz), 7.65 (2H, t, J = 7.6 Hz), 7.70-7.75 (6H, m), 7.91 (4H, s), 7.99 (2H, s), 8.05 (2H, s),8.06-8.07 (4H, m), 8.19 (1H, s), 8.20 (2H, s), 8.36 (1H, s), 8.37 (1H, s), 8.43 (2H, d, J = 8.1 Hz), 8.51 (2H, d, J = 8.6 Hz), 8.52 (2H, d, J = 8.6 Hz), 8.56 (2H, d, J = 8.6 Hz)J = 8.1 Hz). <sup>13</sup>C NMR (150 MHz, CDCl<sub>3</sub>)  $\delta$  0.11, 14.1, 22.7, 23.1, 23.17, 23.23,

124.3, 124.91, 124.95, 126.8, 126.96, 127.00, 127.10, 127.11, 129.1, 129.3, 129.37, 129.43, 129. 5, 129.8, 130.0, 130.1, 130.2, 130.3, 130.8, 130.9, 130.98, 131.01, 131.5, 132.0, 132.1, 132.3, 132.5, 136.8, 136.96, 136.98, 137.00, 137.7, 138.3, 165.4.  $^{19}\mathrm{F}$  NMR (565 MHz, CDCl<sub>3</sub>)  $\delta$  -129.4 (4F, s, br), -126.0 (4F, s, br), -125.1 (4F, s, br), -125.0 (4F, s, br), -124.6 (4F, s, br), -124.4 (4F, s, br), -114.3 (4F, t, J=13.4 Hz), -84.1 (6F, t, J=9.1 Hz).

26.1, 28.8, 29.32, 29.34, 29.6, 31.9, 65.9, 89.3, 90.1, 92.2, 92.3, 93.1, 100.3, 103.0, 108.0–118.3 (m, br), 119.3, 119.5, 119.9, 120.4, 123.4, 123.5, 123.66, 123.71,

Deprotected (P)-Tetramer with alternating perfluorooctyl/decyloxycarbonvl side chains, (P)-FD-4H. The compound (118 mg, 0.0480 mmol, 99 %) was prepared from (P)-FD-4 (100 mg, 0.0484 mmol) as yellow solid. Mp 187 °C, decomp. (chloroform–methanol).  $[\alpha]_D^{25}$  –476 (c 0.10, CHCl<sub>3</sub>). MALDI-TOF MS m/z Calcd for  $C_{141}H_{88}F_{34}O_2$ : 2458.6. Found: 2459.2. UV–Vis (CHCl<sub>3</sub>, 5.0 × 10<sup>-6</sup> M)  $\lambda_{\text{max}}$  (ε) 332 nm (2.6 × 10<sup>5</sup>). CD (CHCl<sub>3</sub>, 5.0 × 10<sup>-6</sup> M)  $\lambda(\Delta \epsilon)$  296 nm (-64), 332 nm (77), 387 nm (-162), IR (KBr) 2925, 2207, 1724, 1241, 1207 cm<sup>-1</sup>. Anal. (C<sub>141</sub>H<sub>88</sub>F<sub>34</sub>O<sub>2</sub>) Calcd: C, 68.84; H, 3.61; F, 26.26. Found: C, 68.77; H. 4.01; F. 25.96. <sup>1</sup>H NMR (600 MHz, CDCl<sub>3</sub>)  $\delta$  0.85 (3H, t, J = 7.0 Hz). 1.25–1.43 (12H, m), 1.50 (2H, quin, J = 7.5 Hz), 1.86 (2H, quin, J = 7.2 Hz), 1.94 (12H, s), 1.99 (12H, s), 3.55 (2H, s), 4.43 (2H, t, J = 6.7 Hz), 7.45 (2H, d, J = 7.0 Hz, 7.48 (2H, d, J = 7.0 Hz), 7.50–7.51 (4H, m), 7.65 (2H, t, J = 7.6 Hz, 7.70–7.74 (6H, m), 7.90 (2H, s), 7.91 (2H, s), 8.02 (2H, s), 8.06 (2H, s), 8.07 (2H, s), 8.08 (2H, s), 8.19–8.20 (3H, m), 8.36 (1H, s), 8.37 (1H, s), 8.44 (2H, d, J = 8.0 Hz), 8.51 (2H, d, J = 8.4 Hz), 8.52 (2H, d, J = 8.4 Hz), 8.55 (2H, d, J = 8.0 Hz)d, J = 8.2 Hz). <sup>13</sup>C NMR (150 MHz, CDCl<sub>3</sub>)  $\delta$  14.1, 22.7, 23.17, 23.24, 26.1, 28.8, 29.32, 29.34, 29.6, 29.66, 29.70, 31.88, 31.93, 65.9, 81.8, 82.5, 89.3, 90.1, 92.26, 92.32, 93.1, 108.3–118.3 (m, br), 119.4, 119.47, 119.51, 119.9, 123.47, 123.52, 123.6, 123.7, 124.3, 124.9, 126.96, 127.02, 127.04, 127.10, 127.12, 129.2, 129.3, 129.37, 129.44, 129.5, 129.8, 130.0, 130.1, 130.2, 130.4, 130.81, 130.84, 130.9, 130.99, 131.02, 131.5, 132.0, 132.1, 132.3, 132.4, 136.9, 136.99, 137.01, 137.8, 138.3, 165.5. <sup>19</sup>F NMR (565 MHz, CDCl<sub>3</sub>)  $\delta$  –129.4 (4F, s, br), –126.0 (4F, s, br), -125.1 (4F, s, br), -125.0 (4F, s, br), -124.6 (4F, s, br), -124.4 (4F, s, br)br), -114.3 (4F, t, J = 13.9 Hz), -84.1 (6F, t, J = 10.0 Hz).

(P)-Hexamer with alternating decyloxycarbonyl/perfluorooctyl side chains. (P)-DF-6. The compound (157 mg, 0.0420 mmol, 88 %) was prepared from (P)-FD-4H (117 mg, 0.0477 mmol) and (P)-D-1 (74.9 mg, 0.0954 mmol) as yellow solid. Mp > 240 °C (chloroform–methanol).  $[\alpha]_D^{25}$  -520 (c 0.10, CHCl<sub>3</sub>). MALDI-TOF MS m/z Calcd for C<sub>229</sub>H<sub>180</sub>F<sub>34</sub>O<sub>6</sub>Si<sub>2</sub>: 3727.3. Found: 3727.6. UV-Vis (CHCl<sub>3</sub>,  $5.0 \times 10^{-6}$  M)  $\lambda_{\text{max}}$  ( $\epsilon$ ) 336 nm (4.4 × 10<sup>5</sup>). CD (CHCl<sub>3</sub>,  $5.0 \times 10^{-6}$ M)  $\lambda(\Delta \varepsilon)$  297 nm (-100), 337 nm (148), 388 nm (-284). IR (KBr) 2925, 2206, 1724, 1240, 1207 cm<sup>-1</sup>. Anal.  $(C_{229}H_{180}F_{34}O_6Si_2)$  Calcd: C, 73.74; H, 4.86; F, 17.32. Found: C, 73.45; H, 4.95; F, 16.99. <sup>1</sup>H NMR (600 MHz, CDCl<sub>3</sub>)  $\delta$  0.39 (9H, s), 0.85-0.87 (9H, m), 1.26-1.41 (36H, m), 1.49 (6H, quin, J = 6.7 Hz), 1.84(6H, quin, J = 7.6 Hz), 1.93 (6H, s), 1.95 (6H, s), 2.00 (24H, s), 4.41 (6H, t, J = 6.1 Hz), 7.42 (2H, d, J = 7.0 Hz), 7.46 (2H, d, J = 7.0 Hz), 7.49–7.50 (8H, m), 7.63 (2H, t, J = 7.6 Hz), 7.68–7.73 (10H, m), 7.91 (4H, s), 7.94–7.99 (12H, m), 8.15 (3H, s), 8.18 (2H, s), 8.33–8.34 (6H, m), 8.43 (2H, d, J = 7.9 Hz), 8.51–8.54 (10H, m).  $^{13}$ C NMR (150 MHz, CDCl<sub>3</sub>)  $\delta$  0.12, 14.0, 22.6, 23.10, 23.12, 23.2, 26.1, 28.8, 29.30, 29.33, 29.4, 29.6, 29.7, 31.9, 65.8, 89.38, 89.41, 89.5, 90.3, 92.3, 93.0, 93.1, 100.2, 103.2, 108.4–118.4 (m, br), 119.5, 119.7, 119.98, 120.0, 120.4, 123.57, 123.61, 123.7, 124.35, 124.41, 125.0, 126.6, 126.86, 126.88, 127.0, 127.04, 127.08, 129.1, 129.2, 129.32, 129.35, 129.40, 129.43, 129.8, 129.9, 130.07, 130.8, 130.2, 130.4, 130.9, 130.99, 131.00, 131.6, 132.2, 132.3, 132.37, 132.39, 132.5, 136.8, 136.90, 136.94, 137.0, 137.7, 138.2, 165.37, 165.38, <sup>19</sup>F

NMR (565 MHz, CDCl<sub>3</sub>)  $\delta$  –129.3 (4F, s, br), –125.9 (4F, s, br), –125.1 (4F, s, br), –124.9 (4F, s, br), –124.5 (4F, s, br), –124.3 (4F, s, br), –114.2 (4F, t, J = 12.8 Hz), –84.1 (6F, t, J = 9.8 Hz).

## 7.3 Experimental Method for Chap. 4

Calculated CD and UV-Vis spectra of (M)-D-5/(P)-F-5 (general procedures). The concentration of a 1:1 mixture of solutions of (M)-D-5 and (P)-F-5 (2.5  $\times$  10<sup>-5</sup> M) is referred to as "total 2.5  $\times$  10<sup>-5</sup> M". The "calculated spectra" were obtained as follows: CD and UV-Vis spectra of (M)-D-5 and (P)-F-5 at the concentration of 1.25  $\times$  10<sup>-5</sup> M were obtained, and these were added in a 1:1 ratio assuming no interaction between (P)-D-5 and (P)-F-5 (Eq. 1).

The spectra of (*P*)-D-5 (1.25  $\times$  10<sup>-5</sup> M, 5 °C)  $\times$  1/2 + the spectra of (*P*)-F-5 (1.25  $\times$  10<sup>-5</sup> M, 5 °C)  $\times$  1/2 (Eq. 1).

Other calculated spectra were also obtained in the same manner.

Computational calculation of hetero-double-helix structure of (M)-tetramer/(P)-pentamer with methoxycarbonyl side chains. Energy-optimization of hetero-double-helix structure formed by the (M)-tetramer/(P)-pentamer complex with methoxycarbonyl side chains was implemented using MacroModel version 8.6 program [2] in the MMFFs force field [3–7]. The optimization protocol was carried out as follows: The structures of ethynylhelicene oligomers, (M)-tetramer and (P)pentamer with methoxycarbonyl side chains, were drawn, and were individually minimized using Polak-Ribiere Conjugate Gradient (PRCG) method until a final gradient below 0.05 kJ/Å mol was reached. Then, molecules were loosely twisted with each other in a right-handed manner. Starting from the twisted structure, conformational searching was carried out using the Monte Carlo multiple minimum (MCMM) method (50,000 steps), followed by minimization with PRCG method until a final gradient below 0.05 kJ/Å·mol was reached. Parameters used in the conformational search are as follows: Solvent (None), maximum number of steps (50000), maximum number of iterations (500), gradient (0.005), energy window for saving structure (50.0 kJ/Å·mol), and maximum distance between atoms in equal (0.8 Å). Parameters used in the multiple-minimization are as follows: Solvent (None), maximum number of iterations (20000), and maximum distance between atoms in equal (0.5 Å). The other settings were used as default.

Computational calculation of hetero-double-helix structure of (P)-tetramer/(P)-pentamer with methoxycarbonyl side chains. The structures of ethynylhelicene oligomers, (P)-tetramer and (P)-pentamer with methoxycarbonyl side chains, were drawn, and were individually minimized using Polak-Ribiere Conjugate Gradient (PRCG) method until a final gradient below 0.05 kJ/Å·mol was reached. Then, molecules were loosely twisted with each other in a right-handed manner. Starting from the twisted structure, conformational searching and minimization with PRCG method were carried out in the same manner as the calculation of (M)-tetramer/(P)-pentamer.

### 7.4 Experimental Method for Chap. 5

Sample preparation from toluene solution for TEM experiments. A 1:1 mixture of (M)-bD-4/(P)-bD-5 (toluene, total  $1.0 \times 10^{-4}$  M) was heated at 110 °C for 3 min in a glass vial and allowed to stand at room temperature for 24 h. A portion of the mixture was dropped on a 400 mesh carbon-coated copper grid. The samples were dried under ambient pressure for 6 h, and then dried under vacuum for 6 h.

Sample preparation from toluene solution for AFM experiments (General procedure). A 1:1 mixture of (M)-bD-4/(P)-bD-5 (toluene, total  $1.0 \times 10^{-4}$  M) was heated at 110 °C for 3 min in a glass vial and left at room temperature for 24 h. A portion of the mixture was dropped on a freshly cleaved mica surface, and the solvent was removed under ambient pressure. Samples of (M)-bD-4/(P)-D-5, (M)-D-4/(P)-D-5, and (M)-D-5/(P)-DF-4 systems (toluene, total  $1.0 \times 10^{-4}$  M) were prepared in the same manner as that of (M)-bD-4/(P)-bD-5 system.

**Determination of Minimum gel-forming concentration (MGC) of (***M***)-bD-4/**(*P***)-bD-5 in toluene (General procedure).** Toluene solutions of (*M*)-bD-4 and (*P*)-bD-5 ( $1.0 \times 10^{-2}$  M,  $5.0 \times 10^{-3}$  M,  $1.0 \times 10^{-3}$  M,  $5.0 \times 10^{-4}$  M,  $2.0 \times 10^{-3}$  M, and  $1.0 \times 10^{-4}$  M) were prepared, and sonicated to homogenize. Then, two solutions (0.15 mL) of (*M*)-bD-4 and (*P*)-bD-5 with the same concentrations were mixed in a capped glass tube (5 mm diameter). The mixture was heated at 110 °C for 3 min, and stood at room temperature for 24 h. A mixture of a  $1.0 \times 10^{-2}$  M solution of (*M*)-bD-4 and a  $1.0 \times 10^{-2}$  M solution of (*P*)-bD-5 is noted, for example,  $1.0 \times 10^{-2}$  M in the following experiments.

Gel formation was evaluated by upending the tube. When a homogeneous substance which exhibited no gravitational flow was obtained, it was concluded to be a gel. When a part of the substance exhibited gravitational flow, the substance was concluded not to be a gel. If crystals were formed, it was marked crystallization (C). When clear solution was retained even at  $1.0 \times 10^{-2}$  M, it was marked soluble (S). In case no gel was formed at  $1.0 \times 10^{-4}$  M, gel formation was examined at  $5.0 \times 10^{-5}$  M and  $2.0 \times 10^{-5}$  M in the same manner. For example, (M)-bD-4/(P)-bD-5 formed gels at  $1.0 \times 10^{-2}$  M,  $5.0 \times 10^{-3}$  M, and  $1.0 \times 10^{-3}$  M, but not at  $5.0 \times 10^{-4}$  M,  $2.0 \times 10^{-3}$  M, and  $1.0 \times 10^{-4}$  M. Therefore, the MGC of (M)-bD-4/(P)-bD-5 was determined to be  $1.0 \times 10^{-3}$  M (1 mM).

MGCs of (M)-bD- $\mathbf{n}/(P)$ -bD- $\mathbf{n}$ , (M)-bD- $\mathbf{n}/(P)$ -D- $\mathbf{n}$ , and (M)-D- $\mathbf{n}/(P)$ -D- $\mathbf{n}$  systems were determined in the same manner as that of (M)-bD- $\mathbf{4}/(P)$ -bD- $\mathbf{5}$  system.

**Dynamic light scattering (DLS) studies on (***M***)-bD-4/(***P***)-bD-5.** A 1:1 mixture of (*M*)-bD-4/(*P*)-bD-5 in diethyl ether (total  $1.0 \times 10^{-4}$  M) was put in a glass cell. After allowing to stand at 25 °C for 1 min, 30 min, 1 h, and 2 h, the mixture was gently stirred then stood for 5 min, and DLS measurements were carried out. Solvents were used after filtration through 0.2  $\mu$ m pore membrane filters.

Sample preparation from diethyl ether solution for TEM experiments. A 1:1 mixture of (M)-bD-4/(P)-bD-5 (diethyl ether, total  $1.0 \times 10^{-4}$  M) was allowed to stand in a glass vial at room temperature for 1 h. A portion of the mixture was

dropped on a 400 mesh carbon-coated copper grid. The samples were dried under ambient pressure for 6 h, and then dried under vacuum for 6 h.

Sample preparation from diethyl ether solution for AFM experiments (General procedure). A 1:1 mixture of (M)-bD-4/(P)-bD-5 (diethyl ether, total  $1.0 \times 10^{-4}$  M) was allowed to stand in a glass vial at room temperature for 1 h. A portion of the mixture was dropped on a freshly cleaved mica surface, and the solvent was removed under ambient pressure. Samples of (M)-bD-4/(P)-D-5, (M)-D-4/(P)-D-5, and (M)-D-5/(P)-DF-4 systems (diethyl ether, total  $1.0 \times 10^{-4}$  M) were prepared in the same manner as that of (M)-bD-4/(P)-bD-5 system.

Conversion of vesicles to fibers. A 1:1 mixture of (M)-bD-4/(P)-bD-5 in diethyl ether (total  $1.0 \times 10^{-4}$  M, 1.0 mL) was prepared and allowed to stand at room temperature for 1 h. Soft precipitates were centrifuged (6400 rpm, 10 min), and the supernatant was removed by decantation. Diethyl ether (1.0 mL) was poured to the residue, which was centrifuged again (6400 rpm, 10 min). After removal of the solvent by decantation, the precipitate was washed with toluene (1.0 mL) in a same manner. The residual soft precipitate was dissolved in toluene (1.0 mL) to obtain a solution with the concentration of ca.  $1.0 \times 10^{-4}$  M. The solution was heated at 80 °C for 1 h and allowed to stand at room temperature for 3 h. A portion of the resulted turbid solution was dropped on a freshly cleaved mica surface, and the solvent was removed under ambient pressure for AFM analysis.

Computational calculation of hetero-double-helix structure of (M)-bD-4/(P)-bD-5. To the lowest energy-minimum conformer of generated structures by the calculation of the (M)-tetramer/(P)-pentamer complex with methyloxycarbonyl side chains conducted in Chap. 4, 4-methyl-2-(2-methylpropyl)-1-pentyloxycarbonyl side chains were attached. Energy minimization of the whole structure was conducted again using the PRCG method until a final gradient below 0.05 kJ/ $\mathring{A}$ -mol was reached. Parameters used for calculation should be referred in the method for computational calculation of hetero-double-helix structure of (M)-tetramer/(P)-pentamer with methoxycarbonyl side chains (Sect. 6.2).

Computational calculation of hetero-double-helix structure of (P)-bD-4/(P)-bD-5. To the lowest energy-minimum conformer of generated structures by the calculation of the (P)-tetramer/(P)-pentamer complex with methyloxycarbonyl side chains conducted in Chap. 4, 4-methyl-2-(2-methylpropyl)-1-pentyloxycarbonyl side chains were attached, which was minimized in the same manner as the calculation of (M)-bD-4/(P)-bD-5.

#### References

- 1. Nakamura K, Okubo H, Yamaguchi M (2001) Org Lett 3:1097
- Mahamadi F, Richards NGJ, Guida WC, Liskamp R, Lipton CC, Chang G, Hendrickson T, Still WC (1990) J Compt Chem 11:440
- 3. Halgren TA (1996) J Compt Chem 17:490

References 87

- 4. Halgren TA (1996) J Compt Chem 17:520
- 5. Halgren TA (1996) J Compt Chem 17:553
- 6. Halgren TA, Nachbar RB (1996) J Compt Chem 17:587
- 7. Halgren TA (1996) J Compt Chem 17:616

## **Curriculum Vitae**

#### Nozomi Saito



Office Address: Graduate School of Pharmaceutical

Sciences, Tohoku University,

6-3 Aoba, Aramaki, Aoba, Sendai 980-8578, Japan

Phone: +81-22-795-6815 FAX: +81-22-795-6811

Email: nsaito@m.tohoku.ac.jp

Nationality: Japanese

#### WORK EXPERIENCE

Assistant professor, Tohoku University International	2012 Nov-Present
Advance Research and Education Organization	
Assistant professor, Graduate school of	2012 Apr-2012 Oct
Pharmaceutical Sciences, Tohoku University	
JSPS (Japan Society for the Promotion of Science)	2009 Apr-2012 Mar
Predoctoral Fellow	

#### **EDUCATION**

Tohoku University, Sendai, Japan	2009 Apr-2012 Mar
Ph.D. in Pharmaceutical Sciences	
Tohoku University, Sendai, Japan	2007 Apr-2009 Mar
M.S. in Pharmaceutical Sciences	
Tohoku University, Sendai, Japan	2003 Apr-2007 Mar
B.S. in Pharmaceutical Sciences	